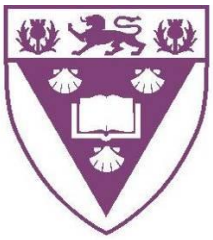

RHODES UNIVERSITY

Grahamstown • 6140 • South Africa

STRUCTURAL ASSESSMENT OF THE KOULEKOUN GOLD DEPOSIT, GUINEA, WEST AFRICA

By

JOSEPH SIBA DOPAVOGUI

A thesis submitted in partial fulfilment of the requirements for the degree of

MASTER OF SCIENCE

(Exploration Geology)

MSc Exploration Geology Programme

Geology Department

Rhodes University

P.O. Box 94

Grahamstown 6140

South Africa

2015

ACKNOWLEDGEMENTS

I would like to thank my employer Avocet Mining, particularly my wonderful Exploration Manager Guinea-Mali, Mr. Alexander Laurence MEYER; my General West Africa Exploration Manager Mr. Robert SEED; The Vice-President Exploration, Mr. Peter FLINDELL and Mr. Brett RICHARDS, the Chief Executive Officer for giving me this opportunity to study at Rhodes University.

My deepest gratitude to my supervisors Prof Yong YAO and Prof Steffen BÜTTNER, thank you for your advice, guidance, patience and for all the valuable comments that you demonstrated to me while writing this thesis. I would like to thank Mr. William POUNTNEY, Geology Manager, Mr. Jess Virador UMBAL, Senior Geologist and Mr. Patrick CHARLES, Exploration Manager for all the knowledge shared and orientation when preparing my study proposal and the synopsis writing.

To all the Wega mining/Avocet Mining colleagues, my exploration Geology class international students for their friendly attention and support. I wish you all the best; thank you for everything.

My special thanks to my lovely family: my wife (Monique), my daughters (Helene, Denise and Jeanne) and my Mom and my Dad as well as brothers and sisters. I love you all and thank you for all your love and sacrifices.

DECLARATION

I, Joseph Siba DOPAVOGUI, declare this thesis to be my own work. It is submitted in fulfilment of the Degree of Master of Science at the University of Rhodes. It has not been submitted before for any degree or examination in any other University or tertiary institution.

Signature of the candidate: …….

Date: ……

DEDICATION

The present work is dedicated to my lovely wife Monique and my wonderful daughters Helene, Denise and Jeanne.

ABSTRACT

The Koulekoun Gold project is the most important prospect of Avocet Mining plc. It is one of the projects within the TriK-block in Guinea (West Africa) for which an exploration permit has been granted. The Koulekoun deposit is located within the Siguiri basin of Birimian age in the Eastern Guinea region; where most Guinea's gold mines are situated.

The present study involves the investigation of structural elements (S_o, S_1, S_2, intrusive contacts, faults and veins) from selected drill cores from drill sections that intersect the Koulekoun orebody in four parts of the deposit; characterizes the principal orientations of measured structures and determines their relationships using stereonet; in order to predict important intersections to focus on in exploration programs within the TriK-block and suggests a possible structural model of the Koulekoun deposit.

Raw data used for the present research was collected from half-core samples due to the absence of surface outcrop from which direct measurements could have been made. Measured data were interpreted using stereographic projection. Often no preferred orientations of structural elements exist in the area, suggesting a complex structural situation, particularly with regard to hydrothermal vein attitudes.

Thus, it has been illustrated from structural data analysis and S_o data 3d interpolation of the four sub-structural domains (North-East, North-West, Central and South) that NE-SW structures (S_2, intrusive contact, fault and vein) have controlled the occurrency of gold mineralization in the Koulekoun deposit area.

Geometrical relationships between structure main cluster orientation from stereonet analysis show the majority of S_o moderately E-dipping; intrusive contacts dip at moderate angle to the SE in all zones, except in the North-East zone where they are sub-vertical and SE-dipping. Fault planes show variable orientation of NE-SW, NW-SE and E-W, and steeply SE-dipping. Vein planes correspond to fault systems and show high variability in their orientation with numerous orders of vein direction in each domain.

The cross-cutting relationships suggest two principal generations of faults: the NE-SW fault (F1) and the NW-SE fault (F2). These two fault systems and their associated vein intersection areas preferably define the ore shoot zones within the Koulekoun deposit.

The proposed structural model of the Koulekoun deposit suggests the intersection and interference of major NW-SE and minor NE-SW structures. The interference of folds formed basin-dome structures with oval shape geometries striking NW-SE and that dominantly occur in North-East, North-West and Central zones. The South Zone is characterized by NE-SW gently plunging and moderately inclined folds with NW-SE striking axial surface. Gold mineralization occurs at the edges of basin-dome structures in North-East, North-West and Central zones. Mineralized porphyry intrusions are likely located within the axial surface of the South zone folds and extend toward the Central zone.

The proposed model is compliant with the earlier model of the Koulekoun deposit presented by Tenova (2013); Fahey et al. (2013) describing the Koulekoun deposit as an auriferous NE-SW trending fault zone, intersecting a major NW-striking and steeply E-dipping porphyry units. The model also fits within the regional structural context suggested by Lahondere et al.

(1999a) related to the E-W vein structures attributed to NW-SE fractures and to the conjugated fault of NE-SW direction.

Comparatively to the three industrial gold deposits (Siguiri, Lero, Kiniero) being currently mined in the Siguiri Basin, and defined as mesothermal vein and lode mineralization hosted in Birimian meta-sedimentary rocks (Lalande, 2005), the Koulekoun gold deposit appears to be a porphyry hosted orogenic disseminated style mineralization system (Fahey et al., 2013). Although, similarities between the Koulekoun gold deposit and these three industrial deposits (Siguiri, Lero, Kiniero) constitute of the intensive extends of the weathering profile and at some stages, by the existence of numerous ring-shaped and curved lineaments enhanced by drag folding (Lero deposit for instance).

It is therefore recommended that targets selection around the Koulekoun deposit and within the TriK-block for further exploration programs be concentrated along NW-SE structures, in objective to determine possible intersection zones with NE-SW structures.

Key words: *Siguiri Basin, Trik-block, Koulekoun gold deposit, F1 & F2 faults, ore shoot zones, mesothermal vein, lode mineralization, meta-sedimentary rocks, porphyry hosted orogenic disseminated style mineralization, structural control of gold mineralization.*

TABLE OF CONTENTS

LIST OF FIGURES

LIST OF TABLES

CHAPTER 1 : INTRODUCTION

The Koulekoun Gold project is the most important prospect of Avocet Mining plc. It is one of the projects within the TriK-block in Guinea (West Africa) for which an exploration permit has been granted. The TriK-block is an assembly of five exploration properties including the three most advanced exploration projects which names start by K (Koulekoun-Kodieran-Kodiafaran) owned by Avocet Mining in Guinea. The Koulekoun project has now reached the feasibility stage, and active consultations are on-going with the Guinea government to grant the mining license for Avocet Mining to start project development.

Field exploration leading to the discovery of the Koulekoun deposit has recognized the possible presence of a strike-slip fault, which acted as a feeder channel for mineralized hydrothermal fluids (Wilson, 2008). This observation fits with the regional structural context of the project area, which is located within the Siguiri basin of Birimian age; in the Eastern Guinea region. Most Guinea's gold mines are located within the Siguiri basin. Gold mineralization found in the Birimian units is likely to be related to late tectonic plutonism and related hydrothermal events that remobilized gold along fractures and fault zones (Wilson, 2008).

This type of structural controls of gold mineralization may apply to large parts of the Siguiri basin. Besides the trends as defined by the mineralized bodies the structure of the deposits is poorly understood.

This study aims to investigate structural elements (S_o, S_1, S_2, intrusive contacts, faults and veins) in selected drill cores from drill sections that intersect the Koulekoun ore body in four parts of the deposit; characterize the principal orientations of measured structures and determine their relationships using the stereonet; understand the main order of structures that led to the deposition of gold mineralization in the Koulekoun area; predict important intersections to focus on in exploration programs within the TriK-block; and suggest a possible structural model of the Koulekoun deposit that fits within the regional structural context.

Although the raw data used for the present research was collected from half-core samples due to the absence of outcrop from which direct measurements could be made. Measured data were interpreted using stereographic projection with some extreme difficulty to establish any preferred orientations notably in veins data. Besides these limitations, the current study contributes information to decision making processes in the early-stage exploration initiative.

The report has been subdivided into five main chapters: An introductory section, which provides the study background including a brief overview of the project and the main questions addressed. The second chapter concentrates on the regional structural setting of the Siguiri basin with its main structure orientations associated with gold mineralization, and the related processes that have controlled gold genesis. The same chapter will provide an overview of the local geology of the project area. The third chapter qualitatively and quantitatively describes the measured structures in terms of; their orientations shown as stereonet plots. The discussion in chapter four puts the local observations into the regional structural context and proposes a possible structural model for the Koulekoun deposit.

The last section of this report draws conclusion and contains recommendations for further gold exploration in the TriK area.

1.1 Localization of the project area

The Koulekoun exploration license covered initially 162 km^2 (last renewal license of the 12th October 2010) and is located in the northern part of the TriK-block. The TriK-block comprises five exploration permits from DMS-01 to DMS-05 (according to the last re-application license of April 2013); the Koulekoun prospect is located within the DMS-01 license area (figure 1.1).

The TriK-block area is situated in north-eastern Guinea, approximately 535km east of the capital Conakry. The area is located in the Upper Guinea region, 85km of Kankan, the regional capital; and at 50km west of Mandiana.

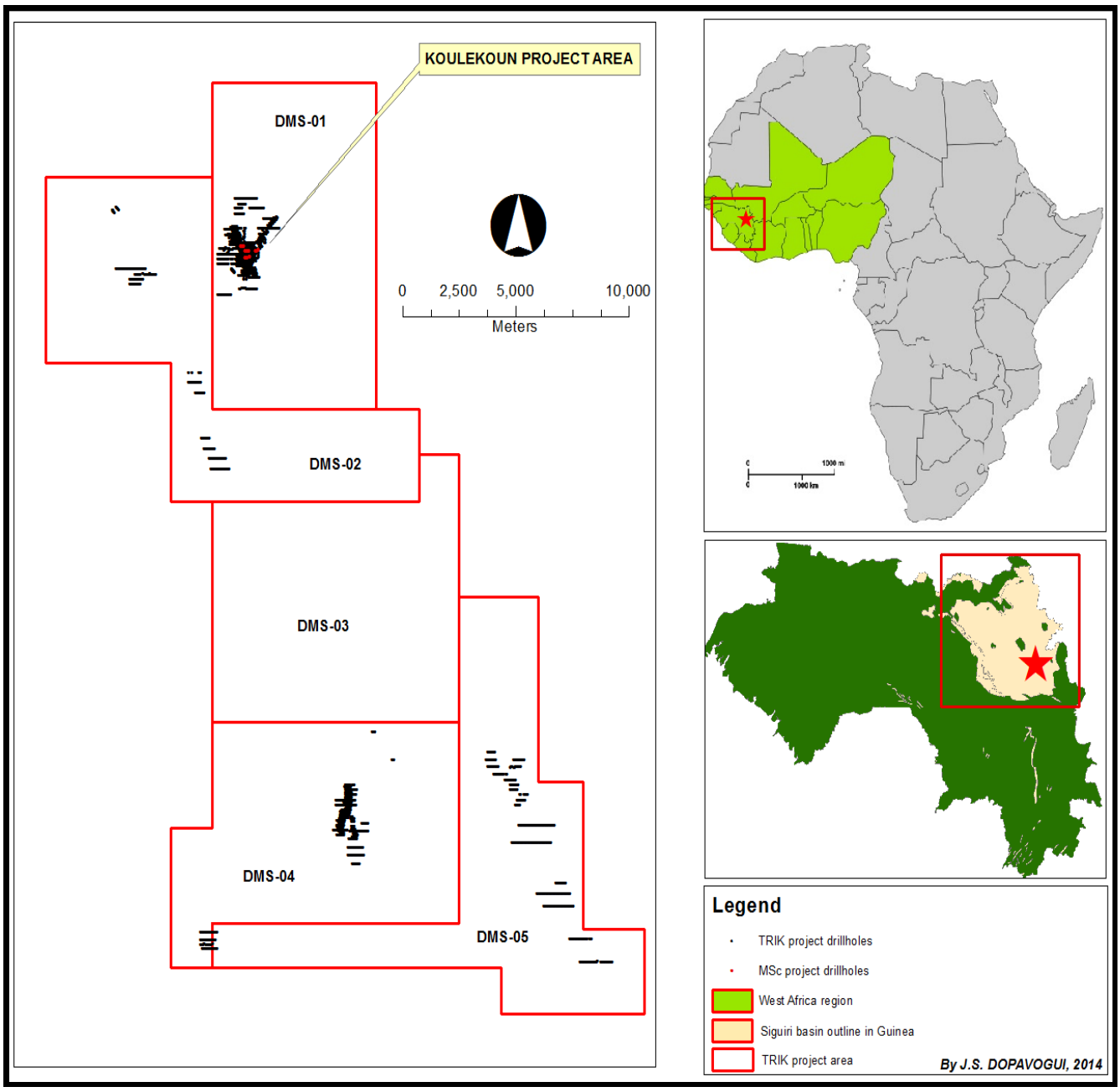

Figure 1.1: Localization map of the project area in West Africa, within the Eastern Guinea region and in the northern part of the TriK-block.

CHAPTER 2 : REGIONAL GEOLOGY AND TECTONIC SETTING

2.1 Tectonic setting

The Koulekoun area is located within the geological domain of the Siguiri basin of the Paleoproterozoic (Birimian age), which is an integral part of the West Africa Craton.

According to Attoh & Ekwmme (1997), the West Africa Craton (1.5 million km^2 Archaean and 3.0 million km^2 Paleoproterozoic terrain) is located in the north west of Africa and consists of the Reguibat Shield to the north and the Man Shield to the south (Figure 2.1.1). These two shields are separated by the Neoproterozoic to Palaeozoic Taoudeni basin.

Achaean rocks are exposed in the western parts and are separated from Paleoproterozoic rocks to the east by major shear zones, referred to as the Sassandra Fault in the Man Shield (Ivory Coast) and the Zednes Fault in the Reguibat Shield (Mauritania).

The area of interest is situated in the north-eastern part of the Man Shield and shows the Archaean or Birimian Kenema Man Domain in the west and the Proterozoic Baoule-Mossi domain in the east, which are separated by the Sassandra Fault.

Milési et al. (1992) established the evolution of the Birimian orogenic belt following four major phases:

(1) Deposition of the sedimentary Lower Birimian (B1) with minor tholeiitic volcano-sedimentary intercalations (with chert and/or Mn-formations), and with most of the detritus being derived from Early Proterozoic sources;

(2) Pre-Upper Birimian (B2) crustal thickening related to D1 thrusting;

(3) Formation, over about 40 Ma, of the Upper Birimian (B2) with numerous volcanic troughs of different composition (tholeiitic and rare komatiitic, bimodal tholeiitic to calc-alkaline, volcano-plutonic) and Tarkwaian clastic-infill basins;

(4) Major transcurrent (D2, D3) tectonic phase, typical of crustal contraction.

These deformation phases were responsible for the present configuration of the Paleoproterozoic basement and, to a certain extent, that of the Archaean basement. This is shown by D2- related N-S sinistral faulting, NE-SW thrusting and associated folding, and by the D3- related ENE-WSW dextral faulting and associated folding.

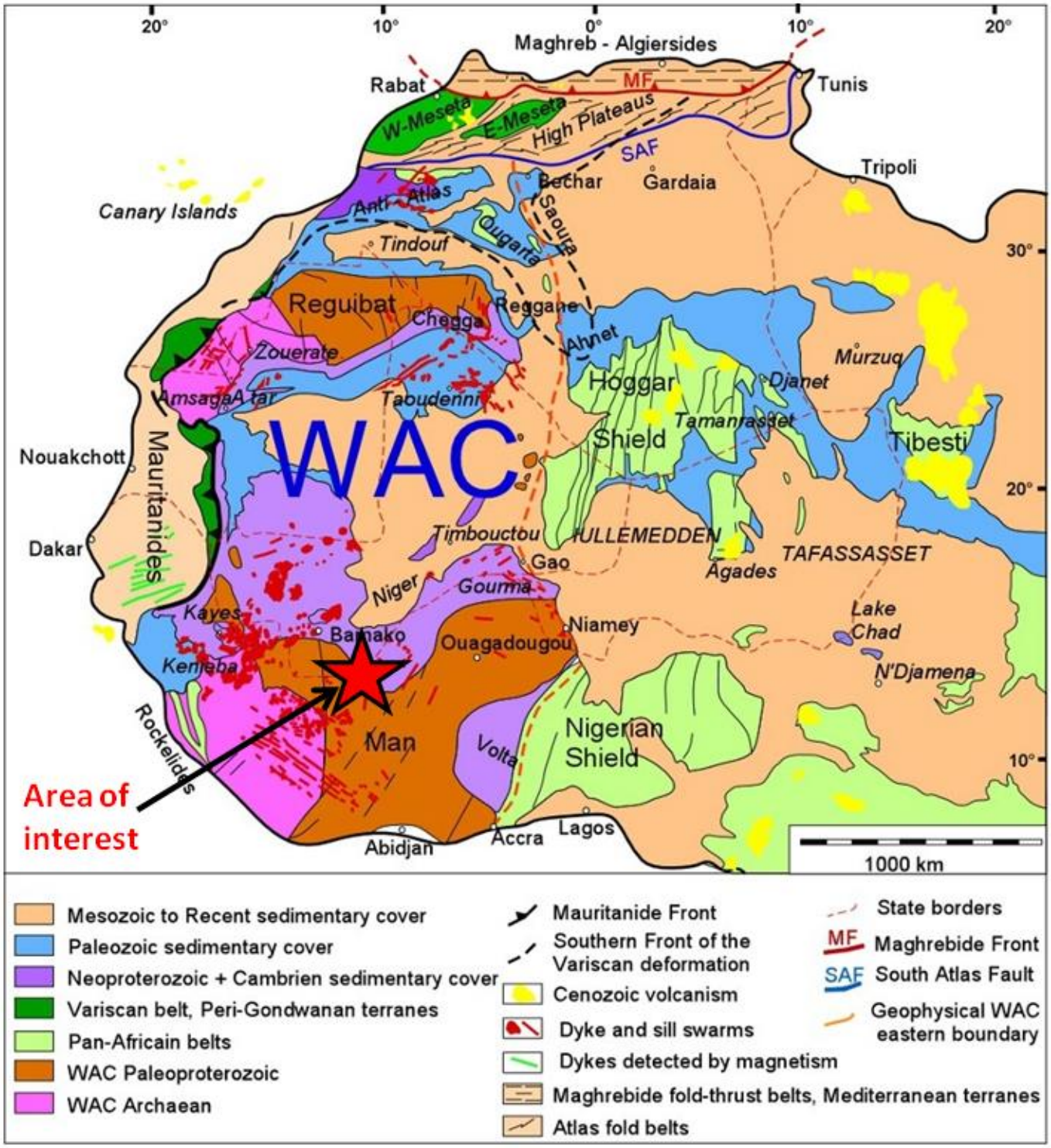

Figure 2.1.1: Geological map of the West Africa Craton showing the tectonic setting of the area of interest (Adopted from General Geology of the West Africa, Fabre, 2005; Liegeois et al., 2005; Ennih and Liegeois, 2008).

In the same paper, Milési et al. (1992) also established the metallogenic history of the Birimian including mineralization events related to three phases of the orogenic evolution, and extending over almost 150 Ma from the Perkoa massive (ZnAg) sulfides (2.12 Ga) with a clear mantle affinity to the late mesothermal Au quartz veins (~2 Ga) with (according to lead isotopes) a high crustal participation.

According to Milési et al. (1992) the economic mineralization of belt thus consists of:

(1) "Pre-orogenic" (pre-D1) deposits related to early extension zones. This was diverse with stratiform Au tourmalinite (type 1 Au: Loulo in Mali; Dorlin in Guyana), stratiform Fe (Cu) (Faleme in Senegal) and Mn (Nsuta in Ghana; Tambao in Burkina Faso), and a single massive ZnAg sulfide deposit (Perkoa in Burkina Faso) associated with regional volcanosedimentary (variably tholeiitic) stratigraphic marker beds;

(2) "Syn-orogenic" (post-D1 to syn-D2/D3) deposits with disseminated Au-sulfides (type 2 Au: Yaouré in the Ivory Coast) in extensional zones of the B2 followed by auriferous paleoplacers (type 3 Au) in B2 extensional zones (Tarkwaian Banket conglomerate) or syn-D2 transtensional zones (debris flow of Orapu in Guyana).

(3) "Late-orogenic" (post-peak D2/D3) deposits with mesothermal Au mineralization evolving from a "disseminated gold-bearing arsenopyrite and Au-quartz lode" type (type 4 Au: Ashanti in Ghana) to a "quartz-vein" type with free gold and CuPbZnAgBi paragenesis. Most of the gold in West Africa formed during this phase (Figure 2.1.2).

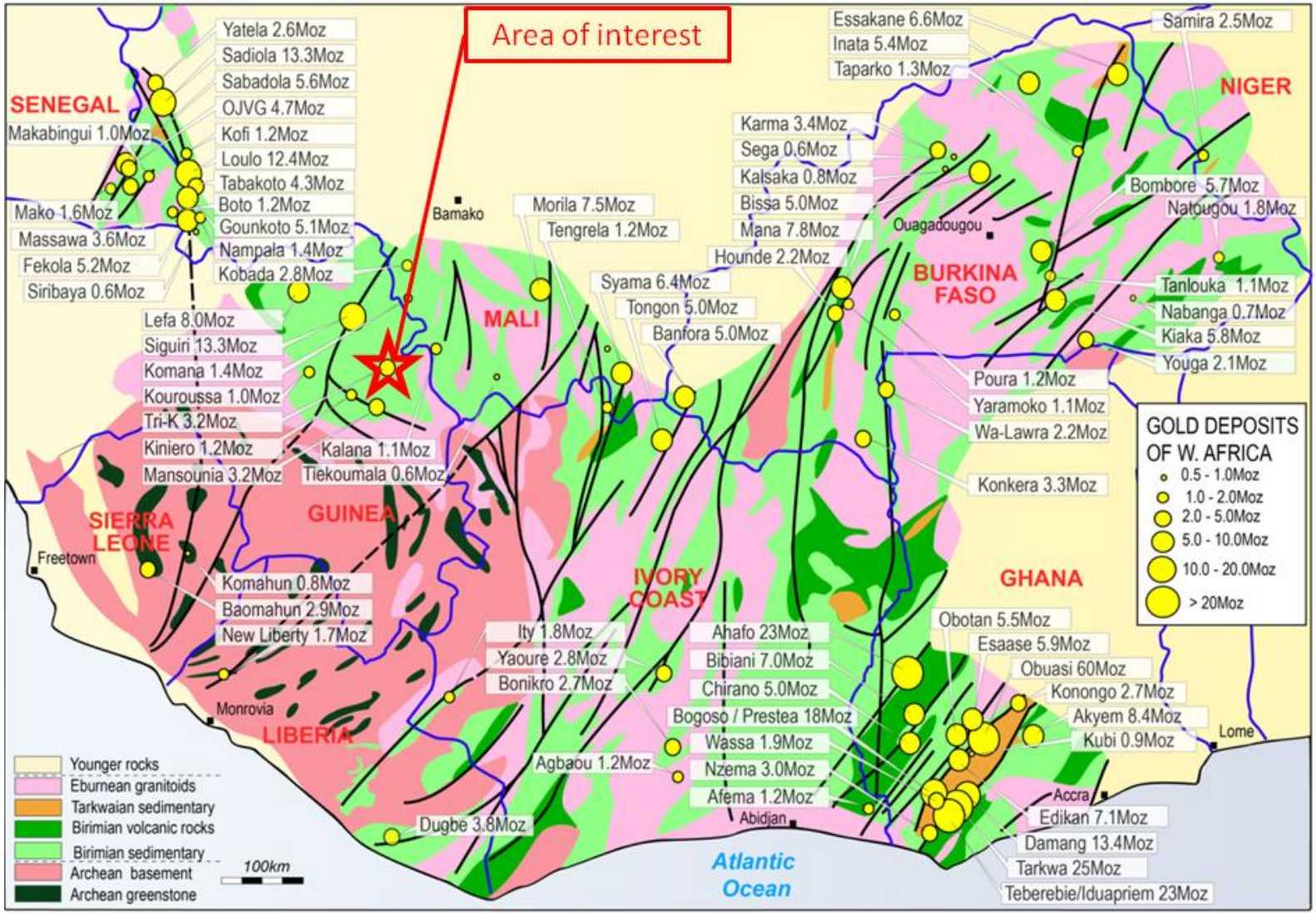

Figure 2.1.2: West Africa's major gold deposits and affiliation to geological domains (from Liberia, Aureus Mining INC. 2015).

2.2 Geology of the Siguiri basin

The Birimian Siguiri basin encompasses the north-eastern part of Guinea, so called "Upper Guinea". Mamedov et al. (2010) describe the basin as a large plain with lateritic crusts altered extensively developed over considerable widths, characterized by very poor exposure.

2.2.1 Limits

Natural limits of the Siguiri basin (Mamedov et al, 2010) to the west and southwest are the Niandan-Kiniero rift and the outcrop of the Archaean crystalline basement Bafing-Bone to the south-east. The basin is limited to the south by the Paleoproterozoic granitic belt and its northern part is covered by the Meso to Neoproterozoic sedimentary rocks. The Siguiri basin reappears in the territory of Mali and Senegal (Zones Faleme and Kedougou). The eastern portion of the Siguiri basin is limited by the Paleoproterozoic sedimentary larger basins of neighboring countries (Cote d'Ivoire, Mali) (see figure 2.2.1).

2.2.2 Lithology

Egal et al. (2002) present the lithology of the Siguiri basin as essentially composed of marine detrital sedimentary rocks (argilite to fine-grained sandstones) and, to a lesser degree, volcanic rocks (lava and pyroclastics) intercalated within these sediments, and subvolcanic dykes. All the rocks show irregular foliation and generally weak metamorphism. Locally, the sediments are transformed into mica schist, at least partially due to 'thermal' metamorphism at the contact of the neighboring plutons.

2.2.3 Volcanism and Plutonism

Several volcanic units of cartographic scale are distinguished in the Siguiri basin (Egal et al. (2002)).

Egal et al. (2002) research work published on the Precambrian granites of the Siguiri basin argue that the plutonism is marked by a belt forming a large batholith composed of various granitic rocks and extends along the edge of the Archaean craton, separating it from the Siguiri basin further to the northwest.
The belt, with an average width of 50–100 km, globally strikes SE–NW in the north, becoming E–W and N–S to the south. Some isolated plutons crop out within the Siguiri basin and the Archaean domain.
The most common rock type of the plutonic belt is granodiorite, which constitutes a vast batholith that cuts the small granite plutons and veins. Both granodiorite and small granite are sheared by regional major strike–slip faults (Egal et al. (2002)).

Even subject of ongoing discussions, the age of Birimian structures has gained more values after the geological data acquiring in Guinea and neighboring countries during the last century. The most important are the radiological dating of Birimian volcanic and various intrusions injected into these rocks (Mamedov et al, 2010).

According Mamedov et al, (2010); the lavas of dacite porphyry structure, identified in the region of Kiniero (Kouroussa) have an absolute age of 2093 ± 2 Ma and 2085 ± 2 Ma microjennites (U / Pb zircon method).

The volcanic complex porphyrite Niani (Mandiana) have an age of 2211 ± 3 Ma (Pb / Pb zircon method).

The gold sulphide mineralization around Poura, of 2001 ± 17 Ma (Pb207/Pb206). The absolute age of the epiclastic chain Niandan, is 2067 ± 12, 2127 ± 5 and 2153 ± 15 Ma. The absolute age of the establishment of granitoid intrusions injected into the birrimian deposits is characterized by several dating from 1920 ± 16 Ma (Pb / Sr isochron method) to 2030 ± 13 to 2077 ± 1.4 Ma (Ar40/Ar39 and U / Pb zircon).

Mamedov et al. (2010) propose dynamothermal metamorphism in the Siguiri basin which is indicated by the formation of thermal domes above the granitic intrusions in the Proterozoic rocks of the crystalline basement.

2.2.1 Structures

Egal et al. (2002) studied the Siguiri basin structures and established that the central part of the plutonic belt is extensively affected by major generally trending WNW-ESE (locally W-E or NW-SE) sinistral ductile strike shear zones. The same study observed in the south of the Siguiri basin, the continuation of strike shear zones converting to local thrust planes showing southward or, more rarely, northward dip directions. Feybesse et al. (1999) consider this thrusting to be associated with early regional thickening prior to sinistral tectonism.

Lahondere et al. (1999a) categorized lineaments in the Siguiri basin into three main types:

(1) WNW to ESE (to E-W) lineaments which form the main regional structural corridor. They form strike-slip faults that are steeply dipping to the south and form sinistral brittle shear zones developing mylonitic and ultramylonitic zones in places. Such lineaments crosscut granodioiritic and granitic rocks in the central part of the basin.

(2) *NW-SE lineaments* are found at the bordering parts of the basin and they form a dextral normal faults.

(3) *NE-SW lineaments* which are rare constitute the brittle sinistral deformation.

.

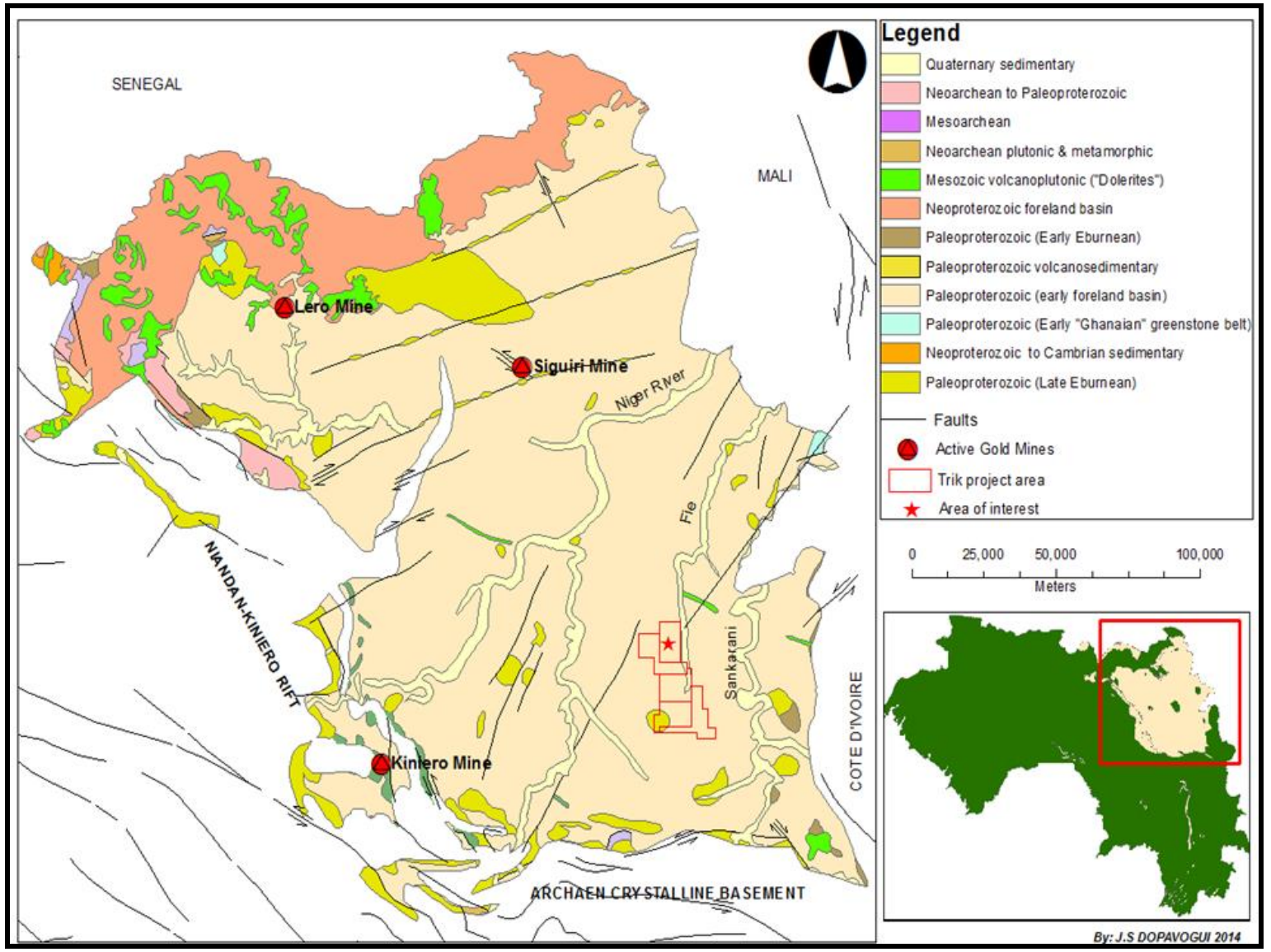

Figure 2.2.1: Geological map of the Siguiri basin adopted from WAXI Africa geology, 2010

Lahondere et al. (1999a) also described the Siguiri basin foliations as characteristic within the basin. At regional level four (4) types of foliation are defined but regrouped into three (3):

(a) S_1 Foliation or the earliest structure corresponding to the D1 deformation stage, mainly present in the northern part of the basin; oriented WNW-ESE to NW-SE and less dipping to the SW. These foliations affect micaschists and paragneiss located at the edges of the monzogranite intrusions.

(b) NNE-SSW oriented foliations are S_2 type of D2 deformation stage and highly penetrative, generally vertical. They represent the axial plan of N-S folds and are probably associated with the sinistral deformation corridor. The most important part of veins observed through the Siguiri basin is likely to be associated with S_2 structures.

(C) NE-SW foliations are of S_3 type of D3 deformation stage. They represent mylonitic plans oriented N45 or N80 and dip toward the SE (figure 2.2.2).

2.2.2 Mineralization

Gold mineralization in the Siguiri basin is either structurally controlled or associated with placer deposits. According to Lahondere et al. (1999a), two mineralized structure orientations are found:

(1) E-W structures represented by veins attributed to tensional sinistral fractures oriented NW-SE and to the conjugated faults of NE-SW direction;

(2) NNE-SSW structures which are developed within a dextral normal fault;

These structures may have controlled the distribution of magmatic fluids; which magma was responsible to the formation of the granitic and dioritic intrusions and their related volcanic equivalents and constitutes the source of gold mineralization (Lahondere et al., 1999a). Gold mineralization is characterized by complex veining and strings systems of white quartz often associated with pyrite and arsenopyrite**.** Map in figure 2.2.3 shows the potential for the presence of gold deposits ranking from zone 1 to zone 11 and the possible alluvial deposits localizations.

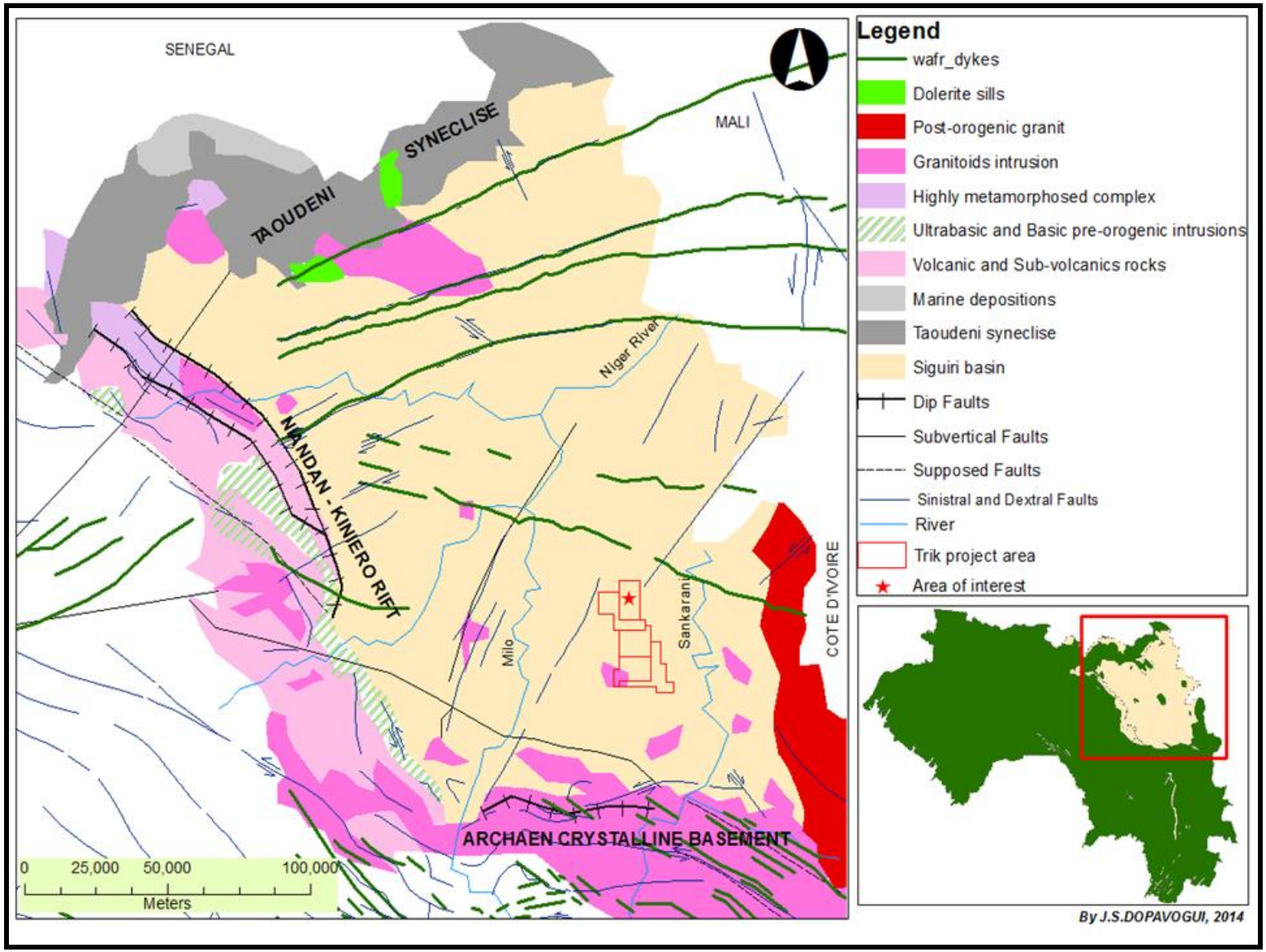

Figure 2.2.2: Tectonic and structural map of the Siguiri basin (adapted from Guinea tectonic map, Mamedov et al., 2010).

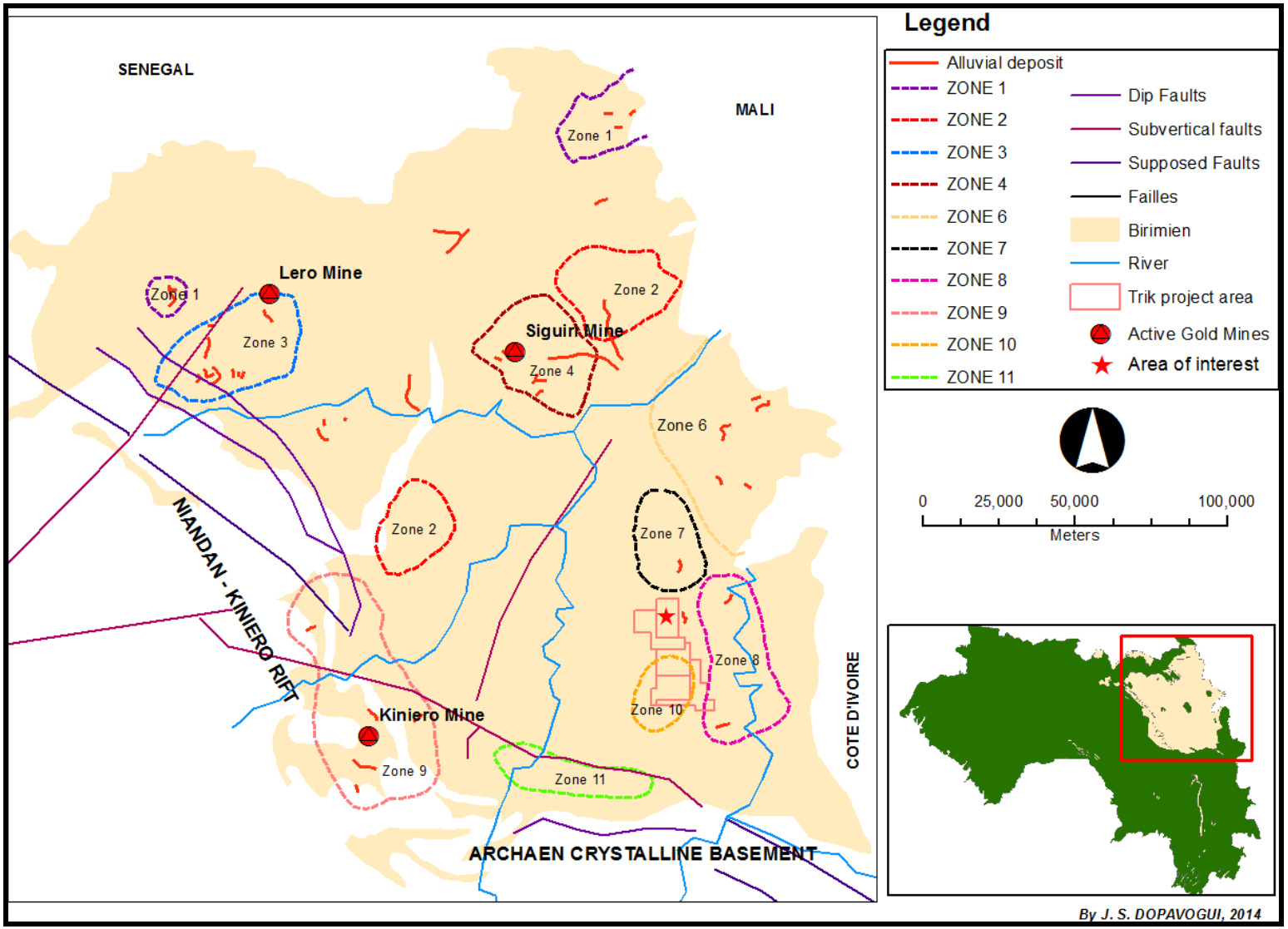

Figure 2.2.3: metallogeny and gold mineralization of the Siguiri basin showing the TriK project area located within the potential zones 7 and 10, respectively in north and south of the TriK-block (adapted from Guinea metallogeny map, Mamedov et al, 2010).

2.3 Geological setting of the TriK-block

2.3.1 Localization

The TriK-block area is located in the south to south-eastern part of the Birimian Siguiri basin. The landscape in the TriK-block permits is generally flat or a gently sloping hill terrain of moderate relief with very little exposure. The area is covered pervasively by laterites that are partly transported and *in-situ*. Underneath the lateritisation the lithologies are weathered to saprolites down to depths of 80m.

2.3.2 Lithology

Lahondere et al. (1999b) regional geological map of the Eastern Guinea region shows the area totally covered by the Paleoproterozoic sedimentary units (figure 2.3.1 left) of the Siguiri basin which consist of undifferentiated depositions of polymict and quartzitic sandstone, aleurolite, argillite, tuffitic sandstone, carbonaceous argillite, metamorphosed calcareous pyroclasts and epiclasts, carbonaceous shale and sandstone, and cherts.

The Tri-K magnetic and VTEM data (Core, 2011) have been interpreted to create lithology and structure maps (figure 2.3.1 right). The lithologies present in the area are a thick sequence of sediments intruded by several igneous bodies. The sedimentary units do not have a significant magnetic signature. The VTEM data interpretation distinguished the area lithologies into sandstone, silty sandstone, siltstone and shale, in order of increasing conductivity. The silty sandstone and siltstone could in fact be siltstone and mudstone respectively (Core, 2011).

2.3.3 Intrusions

Rare intrusive bodies were mapped by Lahondere et al. (1999b) around the TriK-block area; only one isolated granodiorite body is situated in the south-west (figure 2.3.1 left), but some felsic intrusions have been described during exploration drilling. The northern part of the block shows two younger Mesozoic dolerite dykes with NW-SE and E-W strike, post-dating the mineralization event.

Detailed airborne geophysical survey (Core, 2011) has also identified some granites and granodiorites within the block, intruding the interpreted four varieties of sedimentary rocks (sandstone, silty sandstone, siltstone and shale). The intrusive rocks are all low conductivity in the electromagnetic data.

Magnetic signature was used to discriminate between the different types of intrusions. The area is known to host granite, granodiorite, quartz-feldspar porphyry and diorite. However, there are only two different signatures apparent in the magnetic data: one set of strongly magnetic bodies, and another set of weakly magnetic bodies that are slightly more magnetic than the sedimentary units (figure 2.3.1 right). The strongly magnetic bodies are interpreted to be granodiorite and the more weakly magnetic bodies are interpreted to be granite (Core, 2011).

2.3.4 Structures

Several quartz veins (lode) were mapped by Lahondere et al. (1999b) within the TriK-block and are mainly situated in the east and in the south of the block. These veins have variable orientations ranging from primary NE-SW and secondary N-S.

Numerous tectonic events represented by lineaments are present within the block and show different senses of orientations: These include NE-SW, NW-SE, N-S and NWW-SEE.

Field observations (Avocet, 2013) indicate that fold axes within the TriK-block are typically oriented N-S, cut by NE and NW trending conjugated faults.

2.3.5 Gold mineralization

The primary gold mineralization in the TriK-block area is associated with quartz-carbonate-sulphide and quartz-sulphide veins and stockworks hosted within felsic intrusions, within sedimentary units marginal to these intrusions, and concordant within faults (Avocet, 2013).

(Lahondere et al., 1999b) mineralization mapping defined two promising gold potential terrains around the TriK-block (figure 2.3.1): the Kinieran circle or terrain 7 in the north and outside the Block; and the Kodieran circle or terrain 10 in the south. Gold mineralization in these terrains is interpreted to be associated with hydrothermal quartz lode system and quartz stringers type (stockworks).

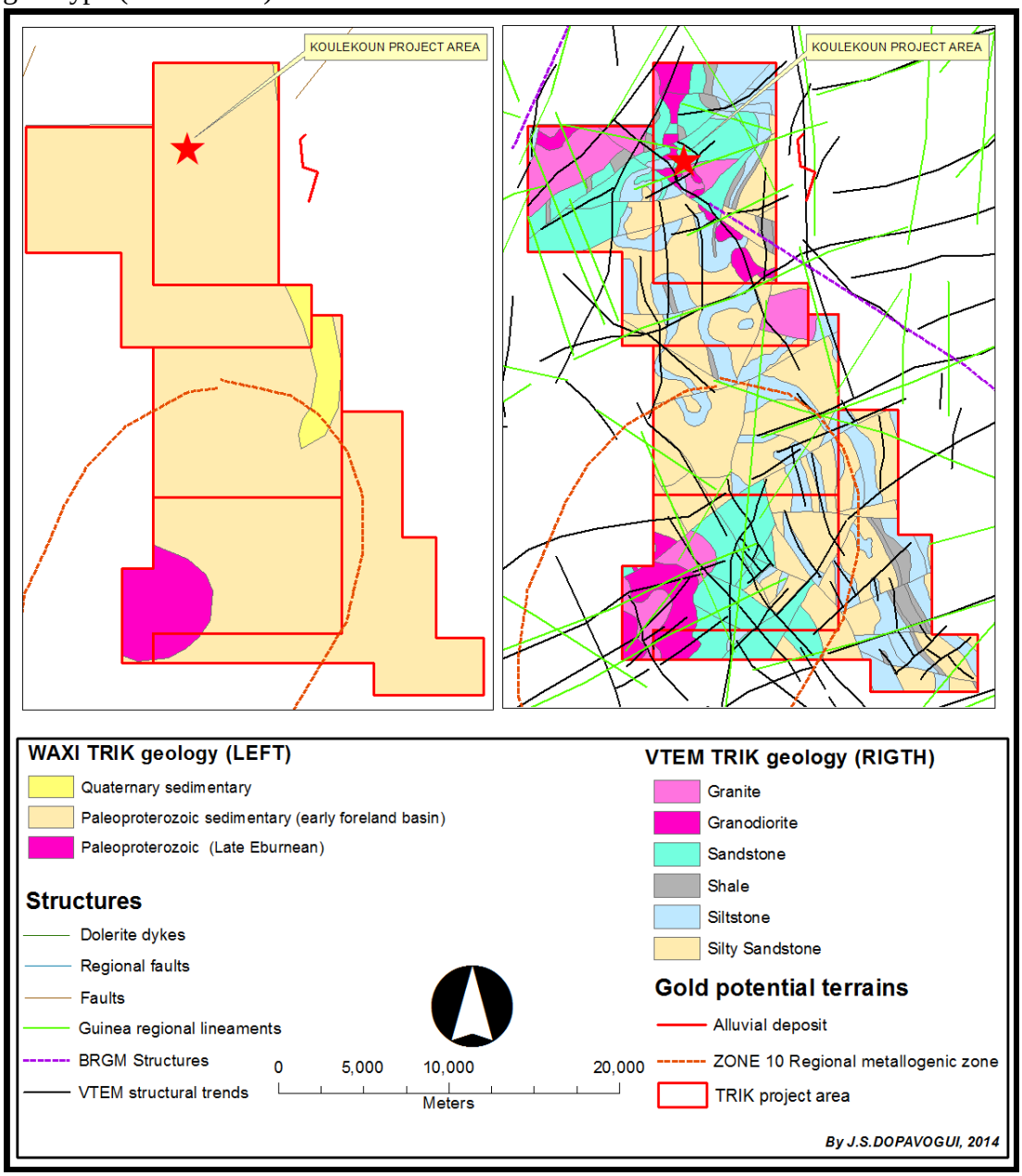

Figure 2.3.1: Geology, structure and metallogeny map of the TriK-block area (adapted from the WAXI (2010) and Core (2011)).

2.4 Petrography of rocks in the Koulekoun Deposit

The petrographic descriptions are based on the logging of twelve diamond drill holes on three selected drill sections of the Koulekoun deposit. The rock classification and terminology is based on the nomenclature used by Spectrum Petrographic (DePangher, 2011).

DePangher (2011) subdivided the Koulekoun rock types into Heterolithologic Multiple Cataclasite (sandstone?), Calcacerous Claystone (siltstone?), Dacite Microporphyry, Dacite Porphyry and the younger Mesozoic Dolerite. Petrographic descriptions of each rock type are presented and images are shown below (2.4A-F):

Heterolithologic Multiple Cataclasite unit possibly sandstone formations (figure 2.4A) are rock type probably formed by multiple cataclastic brecciation and hydrothermal alteration of claystone and dacite protoliths. The mineral assemblage consists of sericite (48%), quartz (20%), plagioclase (10%), chlorite (10%), ferroan dolomite (10%), rutile (1%), sphene (1%), pyrite (<1%) and either chalcopyrite or native Au (<1%). Textures are aphanitic, holocrystalline, multiple cataclastic brecciations.

Calcacerous Claystone unit possibly siltstone formations define rocks probably formed by low grade dynamothermal metamorphism and hydrothermal alteration of a calcareous claystone protolith (figure 2.4B). Mineralogy is dominated by quartz (40%), sericite (24%), dolomite (24%), weakly ferroan dolomite (10%), pyrite (1%), tetrahedrite (?) (1%), chalcopyrite (<1%) and bornite (<1%). Textures are aphanitic, holocrystalline, clastic sedimentary. The matrix is dominated by microcrystalline quartz and sericite with spherical concentrations spots of dolomite.

Dacite Microporphyry unit has an aphanitic, holocrystalline to microporphyritic texture (figure 2.4C). Fabrics associated to the matrix are not aligned. The Microporphyry Dacite is altered possibly by hydrothermal alteration (secondary quartz, sericite, ferroan dolomite, pyrite and arsenopyrite) and deformation of a dacite microporphyry flow or shallow intrusion. The mineralogy is represented by quartz (52%), plagioclase (17%), sericite (17%), ferroan dolomite (6%), arsenopyrite (6%), rutile (1%) and pyrite (1%).

Dacite Porphyry unit has an aphanitic, holocrystalline to porphyritic texture (figure 2.4D). The Porphyry Dacite probably formed by hydrothermal alteration (secondary chlorite, sericite, weakly ferroan calcite, epidote, rutile, quartz, apatite and pyrite) and deformation of a dacite porphyry flow or shallow intrusion. The mineralogy is characterized by plagioclase (58%), chlorite (20%), sericite (7%), weakly ferroan calcite (7%), epidote (3%), rutile (3%), quartz (1%), apatite (1%), biotite (<1%), zircon (<1%), pyrite (<1%).

Dacite cataclasite unit present a phaneritic, holocrystalline to cataclastic texture (figure 2.4E). The Dacite cataclasite probably formed by hydrothermal alteration (secondary quartz, ferroan dolomite, sericite, calcite and pyrite) and cataclasis of a dacite porphyry ash-flow tuff protolith. The matrix is composed of the comminuted equivalent of clasts, suggesting a dominantly cataclastic mechanism of brecciation. The mineralogy is represented by quartz (40%), plagioclase (32%), ferroan dolomite (15%), sericite (10%), calcite (2%), pyrite (1%) and zircon (<1%).

Dolerite dyke unit is dark green to black color (figure 2.4F). The Dolerite is mafic and composed by plagioclase, pyroxene, magnetite and chlorite, unaltered and magnetic. Within the dolerite there is no quartz veins; therefore no mineralization is associated. Dolerites cross-

cut all other lithologies at low-angle, sharp contacts. There are distinct chilled margins along contacts with country rock or the older felsic intrusions.

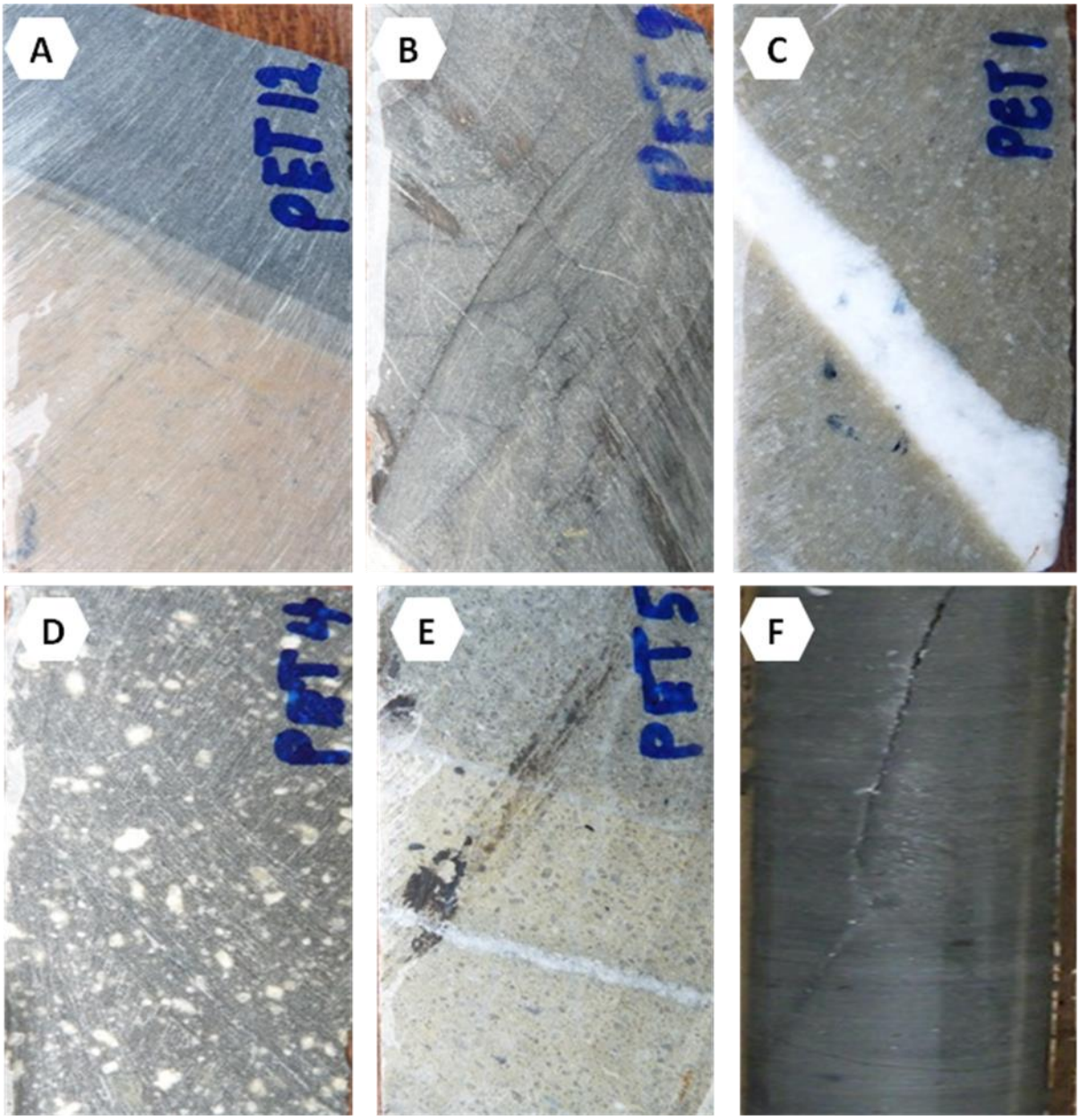

Figure 2.4A-F: Dominant rock types in the Koulekoun Deposit arranged according to their stratigraphic order; where oldest units are volcano-sedimentary sequence (i.e. interbedded sandstone, siltstone) that is cut by polyphase dacite microporphyry-porphyry intrusion, and later by a younger dolerite sill. Note (A) Heterolithologic Multiple Cataclasite unit or sandstone ; (B) Calcacerous Claystone unit or silstone; (C) Dacite Microporphyry unit; (D) Dacite Porphyry unit; (E) Dacite cataclasite unit and (F) Dolerite dyke. Field photographs: Avocet (2011).

CHAPTER 3 STRUCTURAL GEOLOGY OF THE KOULEKOUN GOLD DEPOSIT

The known geological and structural model of the Koulekoun deposit (Tenova, 2013) suggests an auriferous NE-SW trending fault zone, which crosscuts a major NW-striking and steeply E-dipping porphyry units. The most significant gold mineralization occurs at the intersection of this structure and the porphyry.

The intersection of NE-SW trending fault zone and the major NW-strinking porphyry units defines a sub-vertical dipping porphyry dyke (80m by 120m across); characterized by local higher gold grades, and dimish along strike (Tenova, 2013).

3.1 Structural domains definition and project holes selection

In order to test and to add value to the existing structural model of the Koulekoun gold deposit; this study investigated structural elements in selected drill cores from four parts of the deposit. The project area was subdivided into four structural domains (figure 3.1.1) informally described here as the North-East, North-West, Central and South Zones and described as follow:

i. The North-East zone (NE_Zone) describes the NE-SW structure trend in the project area (exposing the NE continuity of the auriferous fault zone);

ii. The North-West zone (NW_Zone) corresponds to the NW trend of the main NW-SE fault following the north western set of the main gold-bearing porphyry body);

iii. The Central zone (C_Zone) located at the main intersection of the NW-SE and NE-SW structures where the most prolific Koulekoun high grade intercepts are centered; and

iv. The South zone (S_Zone) which consists of the southern extension of the same NW-SE fault trend.

The main reason for the selection of these structural domains is to cover representative domains of the ore body. The orientation of S_o, S_1, S_2, intrusive contacts, faults, and vein will allow to determine similarities and differences of attitude of the same structure types amongst these zones. In a similar way, internal relationships between two or more structure types will help in predicting their possible relation with gold accumulation.

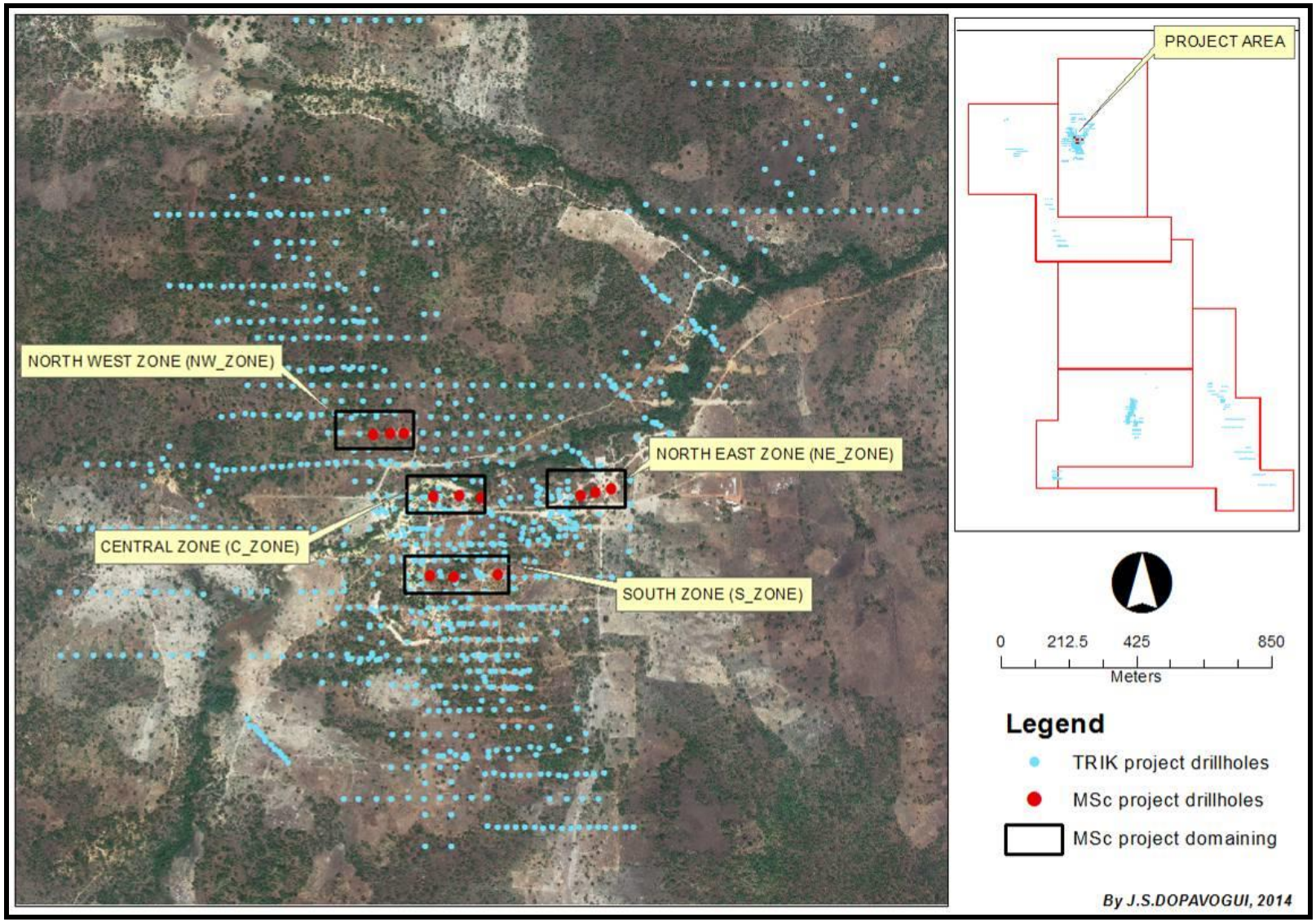

Figure 3.1.1: Localization of the four selected section (structural domains) of the Koulekoun deposit area over the 2011 regional QuickBird satellite photograph.

Within each structural domain, three drill holes were selected on a particular section for structural measurements (figure 3.1.2). The drilling lines that were chosen are likely to be the most representative sections across the mineralized zone (N1190900 and N1190650) or representing a sporadic gold grade (N1191100). The hole selection has considered the presence of mineralized porphyry intrusions, evidence of alteration and mineralization (especially sulphides dissemination), intensive veining, deformations and gold grade.

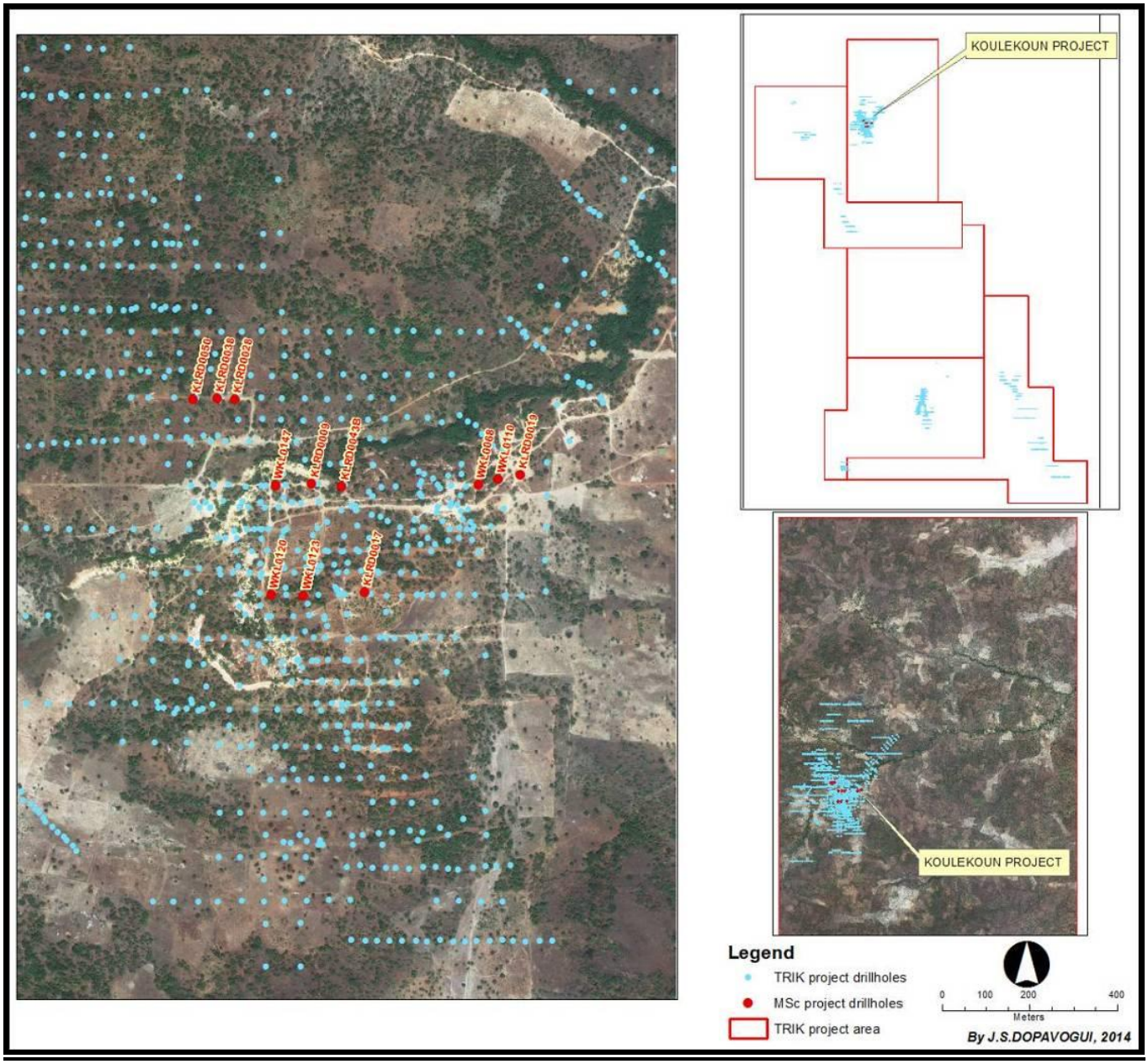

Figure 3.1.2: Localization of selected drill holes within the Koulekoun deposit area over the 2011 regional QuickBird satellite photograph.

In total, 12 drill holes with 3.368.45 meters of core were re-logged and 689 structural measurements were obtained to carry out this study. Table 3.1.1 indicates parameters of drill holes (Hole_ID, depth, azimuth and dip), drilling sections and the identification of proposed structural domains. All holes were drilled at an azimuth of 270° and -55° plunge; meaning that holes were drilled from east to west.

Table 3.1.1: Project drill holes parameters.

STRUCTURAL DOMAIN	DRILL SECTION	HOLE ID	DEPTH (m)	AZIMUTH	PLUNGE	HOLE TYPE
NORTH-EAST	1190900N	WKL0068	152	270	-55	DD
		WKL0110	199.9	270	-55	DD
		KLRD0019	381.4	270	-55	RD
NORTH-WEST	1191100N	KLRD0050	267.4	264	-57	RD
		KLRD0028	210.25	270	-55	RD
		KLRD0038	184	270	-55	RD
CENTRAL	1190900N	KLRD0043B	426.4	270	-55	RD
		WKL0147	218	270	-55	RD
		KLRD0009	357.6	270	-55	RD
SOUTH	1190650N	WKL0123	300	270	-55	RD
		WKL0120	174.4	270	-55	RD
		KLRD0017	497.1	270	-55	RD

DD = Diamond Drill hole; RD = Precollared Drill hole

Sections of representative drill holes are shown on figures 3.1.3; 3.1.4; 3.1.5 and 3.1.6 below. These sections show high gold grade (0.3g/t to >0.57g/t) associated with felsic porphyry intrusions and locally at the intrusive contacts and/or with sedimentary country rocks units that show multiple intrusion phases. All the selected holes were precollared with reverse circulation drilling in the oxide/saprolite zone (~0-80m) and extended in the fresh as diamond tails (were the structural measurements were taken). Sections were generated using the montaj drillhole plotting function in Oasis montaj version 6.3.

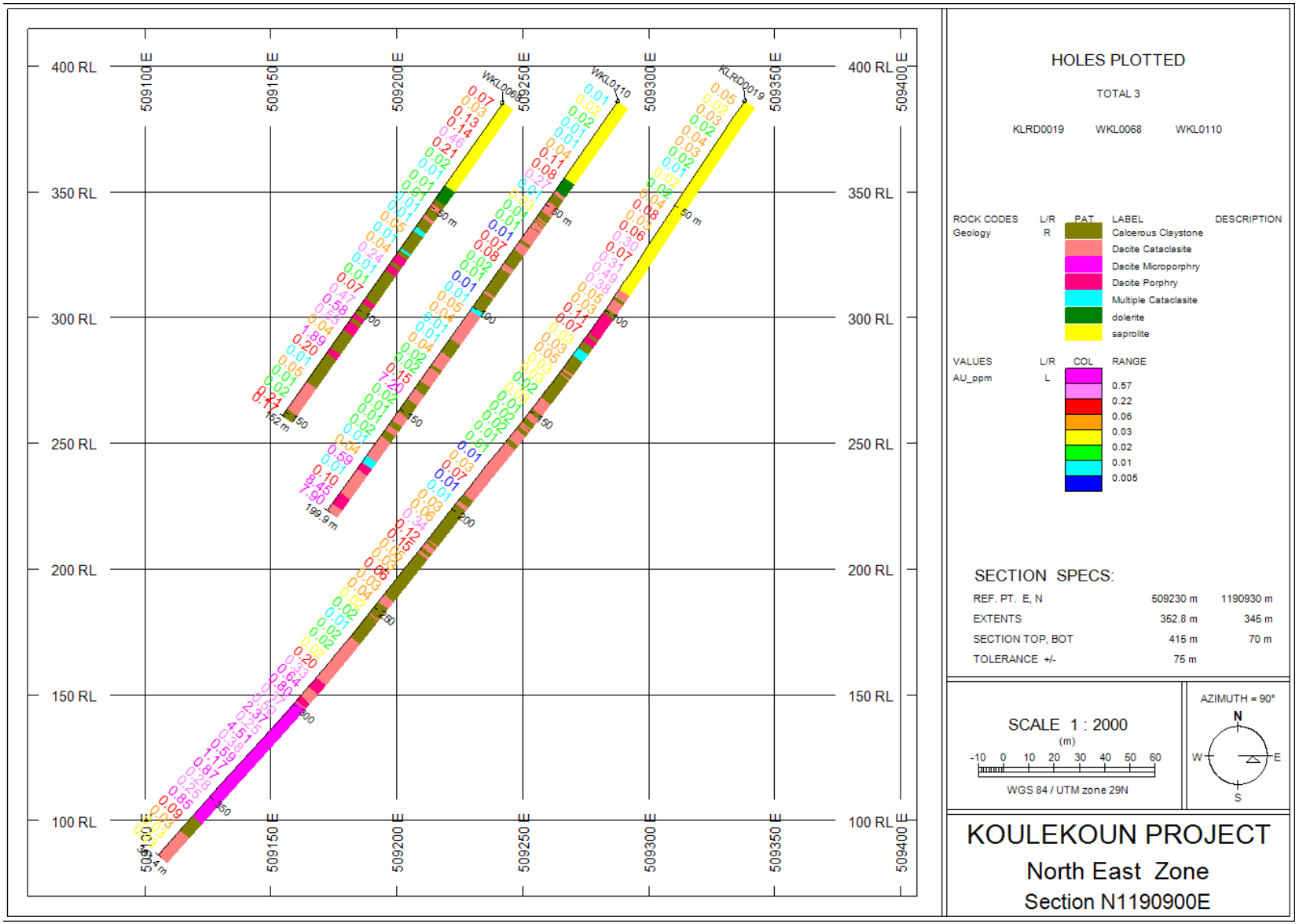

Figure 3.1.3: North-East Zone lithology and gold mineralization shown on section N1190900E.

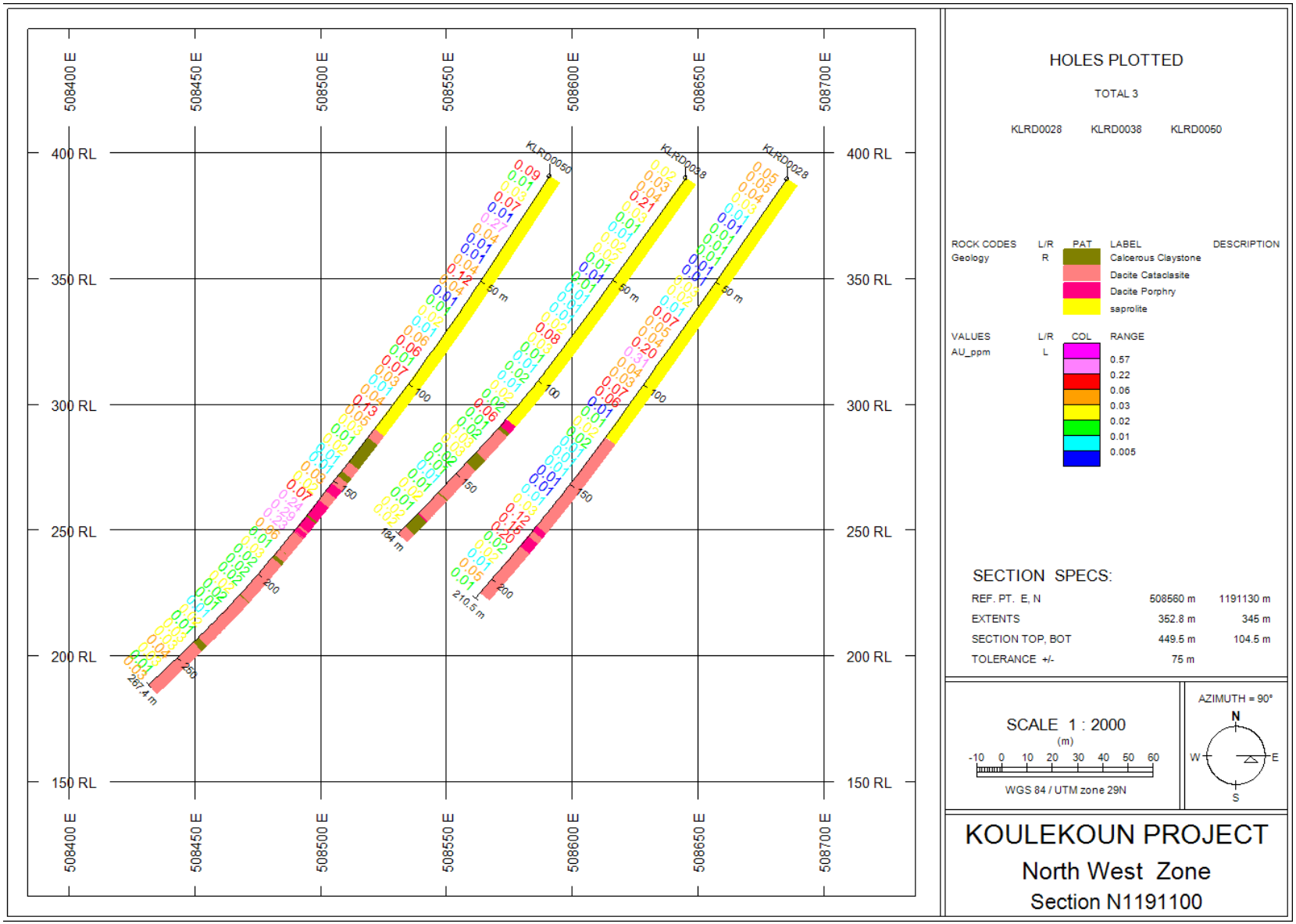

Figure 3.1.4: North-West Zone lithology and gold mineralization shown on section N1191100.

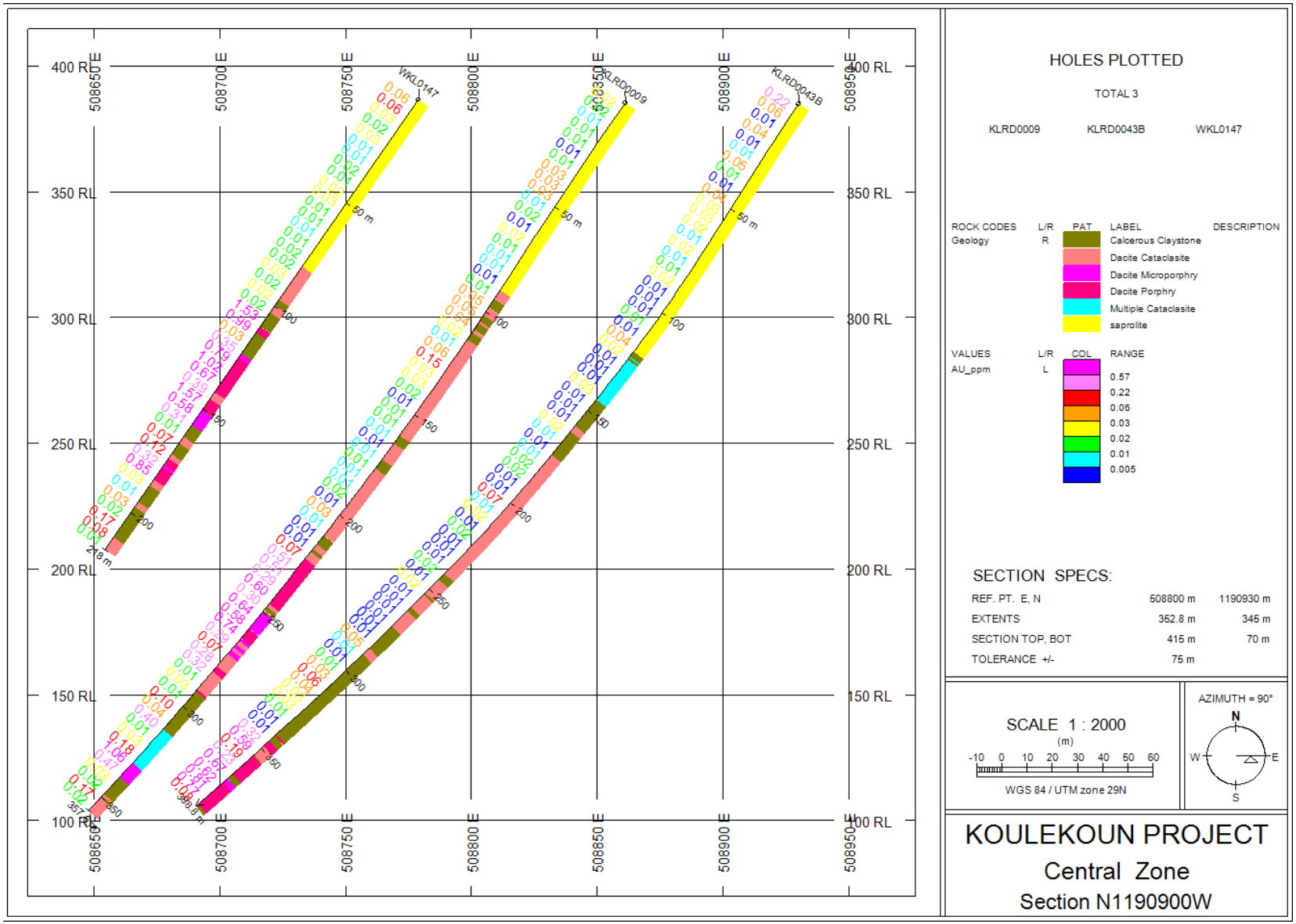

Figure 3.1.5: Central Zone lithology and gold mineralization shown on section N1190900W.

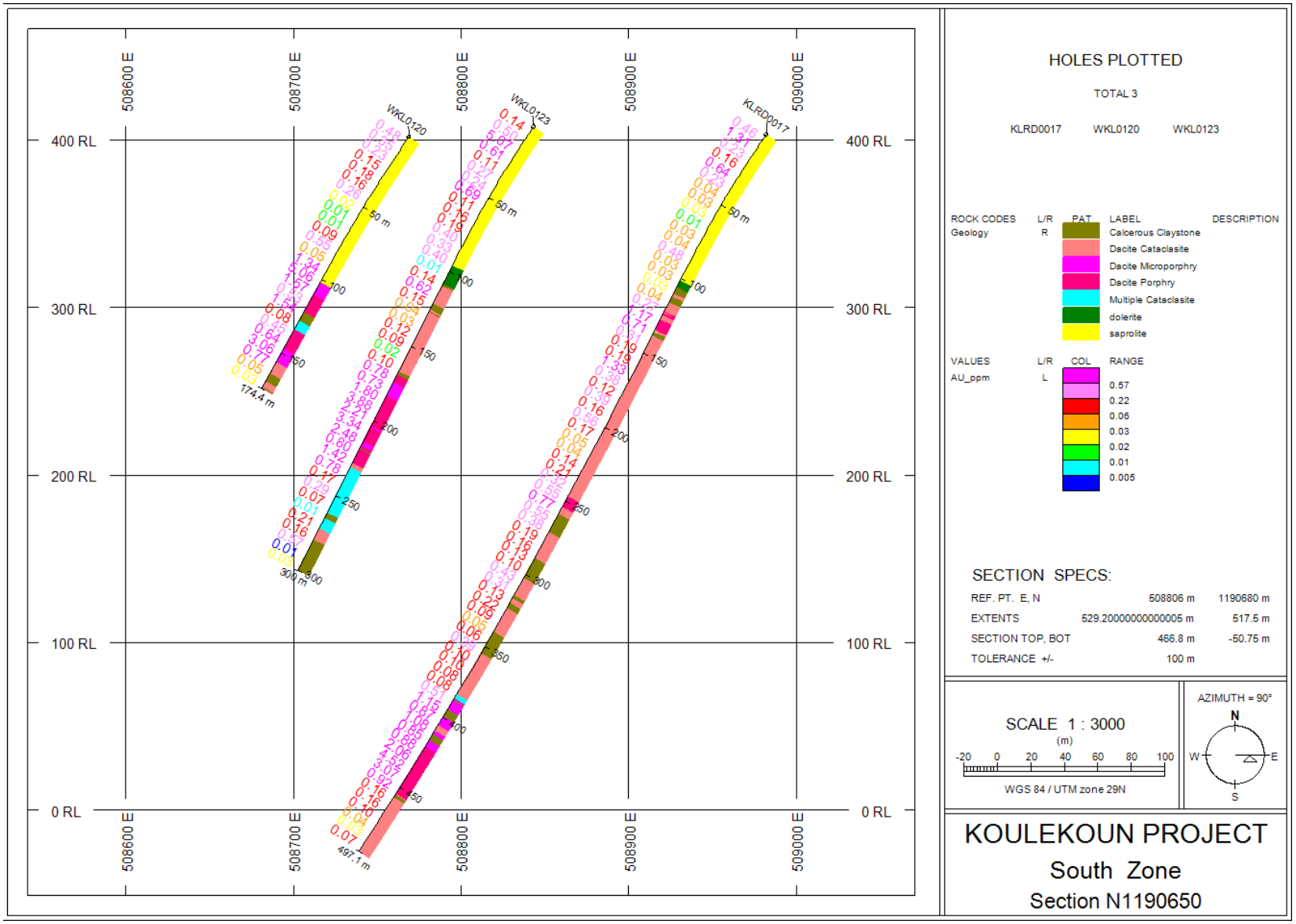

Figure 3.1.6: South Zone lithology and gold mineralization shown on section N1190650.

3.2 Data collection and processing methodology

The dataset comprises planar structures (S_o, S_1, S_2, intrusive contacts, faults and vein). Readings of α and β angles in order to reconstruct true orientation from non-vertical core were done on half-core. Linear structures could not be determined with sufficient accuracy from half-core. An α angle was measured using the Douglas ruler where possible; but in most of the cases, the goniometer device was used to measure both α and β angles. Measuring of planar features on entire core aims to define α and β angles. Before attempting to measure α and β the elliptical shape of the structural feature is traced with a chinagraph wax pencil, and the downhole apex of the structure is marked. The figure 3.2.1 below illustrates the measurement of internal angles of a specific structural element; where:

α (alpha) is the minimum angle between plane and core axis;

β (beta) is the angle between the bottom-of-core line and the down hole end of the elliptical trace of the plane in core. Measured clockwise (looking down-hole) around core circumference;

ɣ (gamma) is the angle between a lineation on a plane and the long axis of the ellipse formed by the plane in core. Note that no linear elements were measured during the data collection of the present project work; therefore ɣ (gamma) angles were not measured.

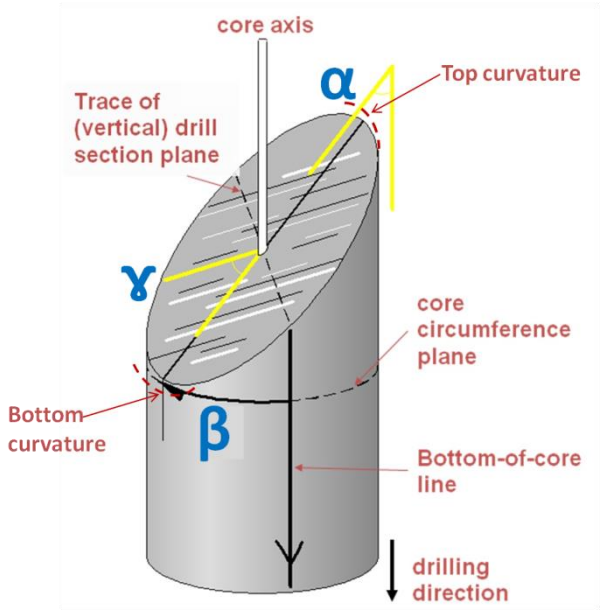

Figure 3.2.1: α, β and ɤ measurement procedure when using a Goniometer device on drill core; measured data are then converted to real-space orientations using a computer program which is GEOrient in this case (Avocet, 2009).

For the purpose of the present project, only measurements on a half-core referred to the orientation line (Bottom-of-core line, cf. fig. 3.2.1) which was preserved during the cutting of the core would be considered.
When measuring the β angle on half-core (where the bottom curvature had been sampled), the angle of the top curvature was measured and the value was subtracted from 180^0 (designating

the diameter of a half of cylinder) and the resultant angle will represent the correct β angle (that represents the angle β if the core was entire).

Structural readings were logged and encoded into a standard Microsoft Excel spreadsheet. Parameters measured are: depth, structure type, α and β angles, lithology, alteration, mineralization, paragenesis and comments.

For the computer program processing of the recorded structural data, the GeoCalculator and the GEOrient software were used. GEOrient and GeoCalculator software are one of a number of structural geology packages developed by Rod Holcombe in 1985 from the University of Queensland, Australia. The packages (unregistered) are free to academic users (teachers and students) for teaching and noncommercial research purposes (Holcombe, 2010).

GeoCalculator software version 4.9.3 was used to convert α and β readings into dip angles and dip directions. For a specific depth, this conversion was in relation with the corresponding drill holes survey azimuth and plunge, initially measured during drilling to control drill hole deviation.

For graphical display, GEOrient software version 9.4.4 was used to plot structures as stereographic net projections in the form of pole points.

The structures database was organized and formatted according to each structural domain (zone) and structure types. For each zone, individual structure types (S_o, S_1, S_2, intrusive contacts, faults and veins) are plotted and described separately. This has permitted to characterize the structural setting of respective structure type in individual zones and to undertake a comparative interpretation of the attitude of either the same structure in different zones or the attitude of multiple structure types in the same zone.

3.3 Structures of the Koulekoun Gold Deposit

The structures of the Koulekoun deposit have been established based on three-dimensional orientation of drill core using downhole survey data.
Observations made during core logging have identified primary S_o in sedimentary rocks and very limited S_1 foliations corresponding to the D1 deformation event.
S_2 foliations related to the D2 deformation phase are abundant, penetrative and dominantly vertical. S_2 foliations are regionally associated to sinistral shearing and mark the axial plane of folds.
The majority of veins are parallel to S_2 foliations (Lahondere et al., 1999b). Detailed observations of S_o, S_1 and S_2 foliations, intrusive contacts, faults and veins show S_o often parallel to S_1 and S_2 foliations or veins.

Locally, the S_o is either intersected perpendicularly by folded quartz veins or is parallel to them (figure 3.3.1). Some black shale layers are present within siltstone units and are characterized by their dark coloring (figure 3.3.2) and cubic pyritic crystals deposition in places. Some measurements of black shale indicate their widths varying from 0.5 to 6.3cm.

The definition of the stratigraphic younging direction on half-core was considered inaccurate, therefore was not tackled in the present study.

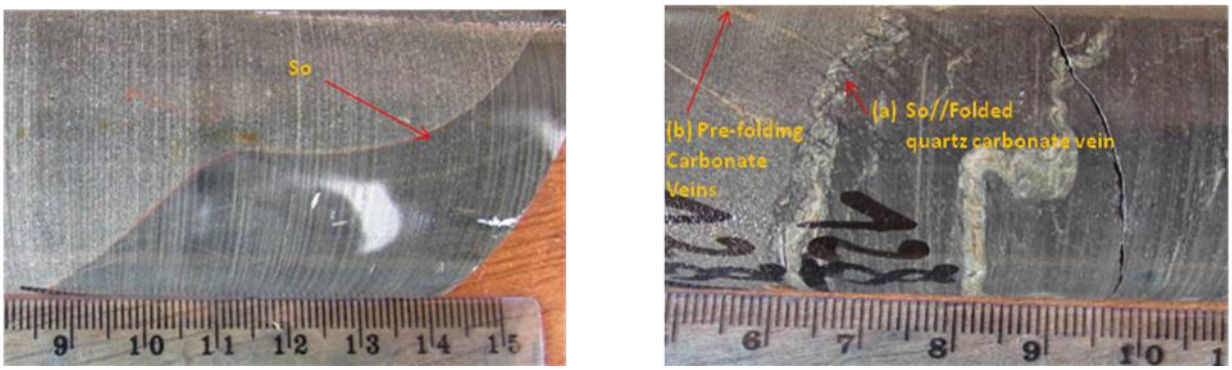

Figure 3.3.1: showing S_o (left) and typical folded quartz-carbonate vein (a) parallel to S_o (right); note early carbonate veins (b) within the coarse grained sandstone limited at the S_o are perpendicular to folded quartz-carbonate vein which is parallel to S_o.

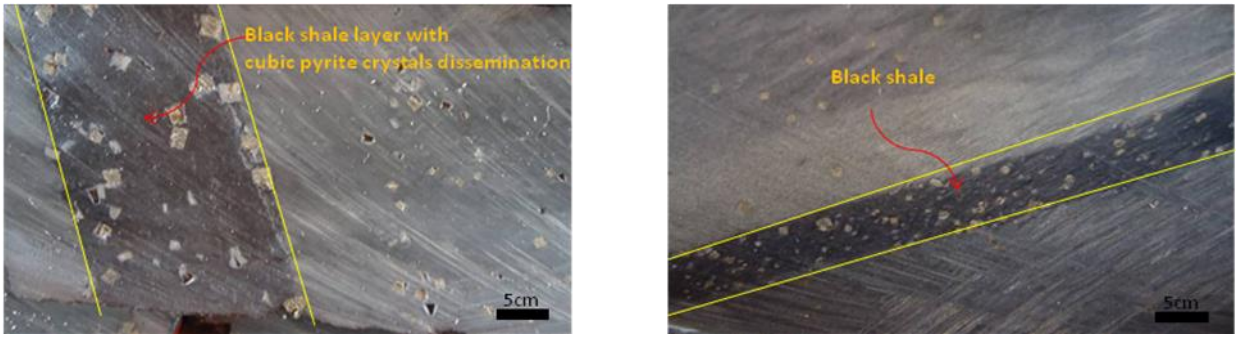

Figure 3.3.2: very fine-grained black shale interbedded with medium to fine-grained siltstone with cubic pyrite crystals; note these types of pyrite crystals are not associated to gold mineralization.

Contacts between felsic intrusions and country rocks are often characterized by the remobilization of pyrite and arsenopyrite, and in places native gold; the intensity of sulphides minerals diminishes from the contact zone towards the host rock (figure 3.3.3). Intrusive contacts are sharp, irregular, gradational or tectonic (when faults are present at contact).

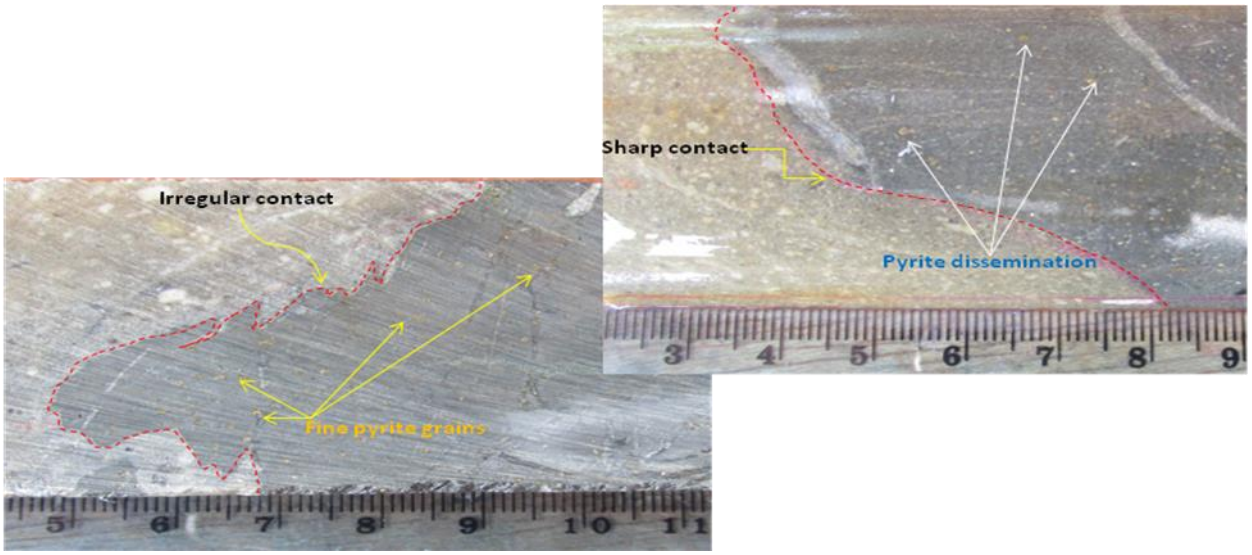

Figure 3.3.3: irregular contact between dark grey metasedimentary country rock and silicified intrusive dacite porphyry showing the dissemination of pyrite in the country rock from the contact zone. The intensity decreases as progressing toward the sedimentary country rock.

Fault systems in the project area are related to D1, D2 or D3 deformations events and represented by small scale faults, graphitic fault, brittle or shear zone and breccia zone. Commonly seen fragmentation (figure 3.3.4B or cohesive breccias (figure 3.3.4C) may be related to the regional strike-slip faulting. Fault zones are 0.8 -1.5m in width.

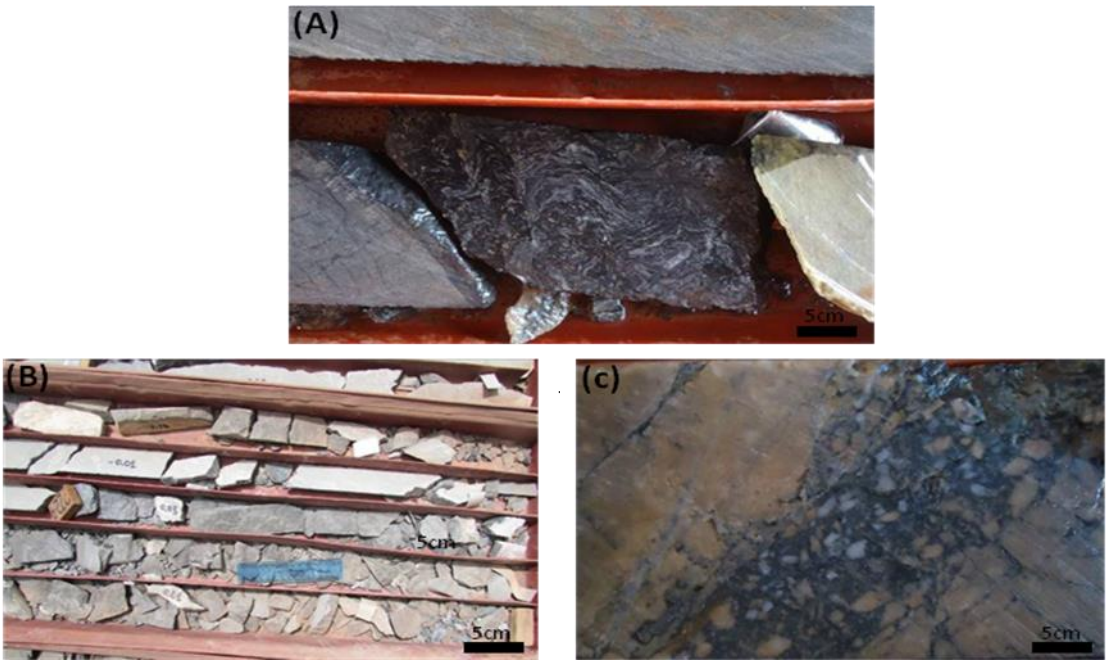

Figure 3.3.4: showing some fault features observed on Koulekoun drill cores: (A) represents a dark rock (possible graphitic schist) intensively deformed located at the contact of the intrusive microporphyry and the country rock. Some bright folded segregation quartz veins are associated to the graphitic schist. Possible graphitic fault? (B) indicates the fragmentation of grey materials (siltstone) within strongly jointed zones (possible brittle deformation). (C) Typical cohesive breccia observed in porphyry intrusions at some places.

D1 structures related to S_1 foliations are rare and when present are sometimes parallel to S_o. S_1 foliations can also be parallel to folded veins and intrusive contacts (figure 3.3.5). S_2 foliations are abundant and mark the D2 deformation stage in the study area. S_2 foliations overprint all the rocks units and mostly affect competent porphyry intrusions forming very thin structures where they occur with abundant veins systems. S_3 foliations are rare, but some late veins and small scale-faults observed are interpreted as D3 deformations structures and are associated with S_3 foliations.

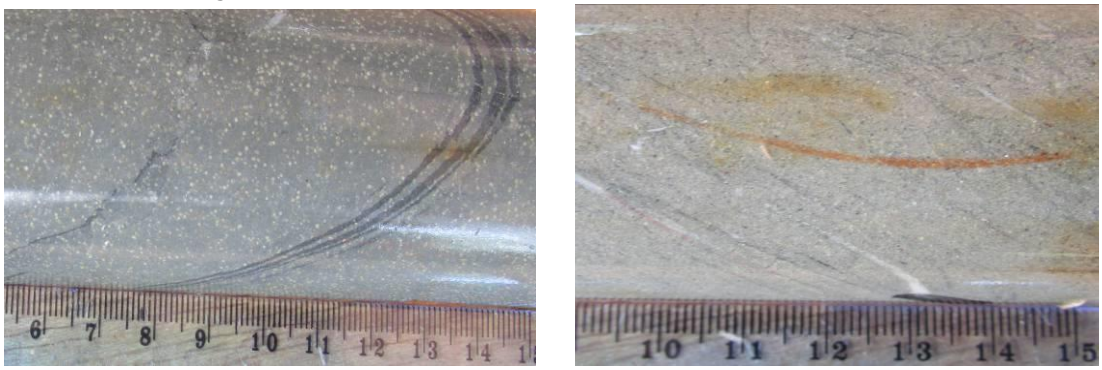

Figure 3.3.5: Left photograph shows local foliation associated to sedimentary country rocks. Image on right shows remarkable S2 foliations associated to dacite cataclasite justifying a post intrusive D2 deformation event.

Veins are abundant in the mineralized zone (porphyry dikes and intrusive contacts zones), where main alterations (silicification, chloritization, carbonatization and potassic) are dominant; and pyrite and arsenopyrite are disseminated in host rocks or occur along veins.

In places, veins are weakly to strongly folded, and follow the direction of elongated feldspar minerals within the porphyry rocks.

Morphologically, veins can be boundinaged (Figure 3.3.6), laminated or undifferentiated. Inter-crosscutting relationships between different veins types or between veins and others structures (S_o, S_1 and S_2 foliations, intrusive contacts, etc.) are present. Veins thicknesses vary from 0.3 to 4cm; some rare types are 10cm thick.

Vein assemblages (vein arrays) are frequent and occur as sheeted veins or stockworks (figure 3.3.7) of 1-50cm thick, with <2-4mm spacing. Veins are associated with shear zones and breccia zones (figure 3.3.8) and are regularly observed and vary from 0.1-1.5m in thickness.

Sulphide minerals are usually precipitated along quartz veins (figure 3.3.9). Native gold associated to quartz veins has been identified during core logging (figure 3.3.10).

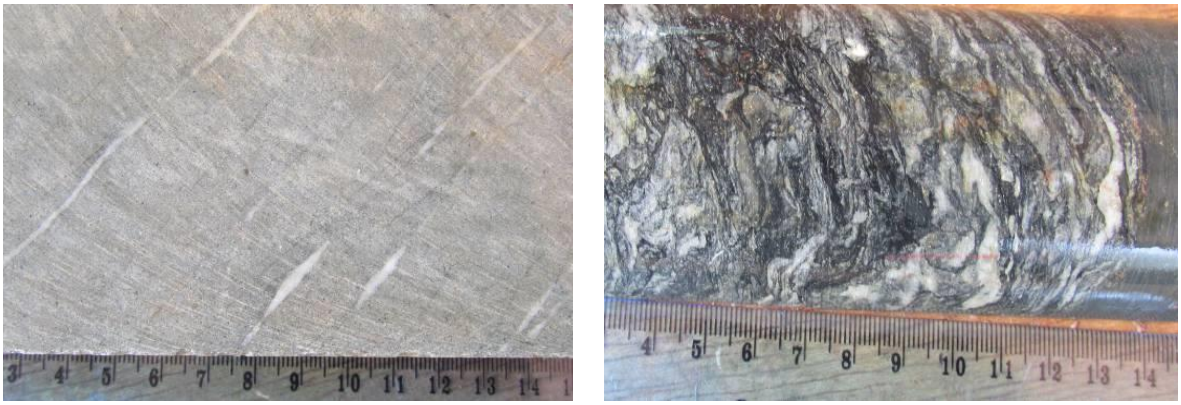

Figure 3.3.6: Boundinaged quartz veins (left) and typical shear-zone associated veins.

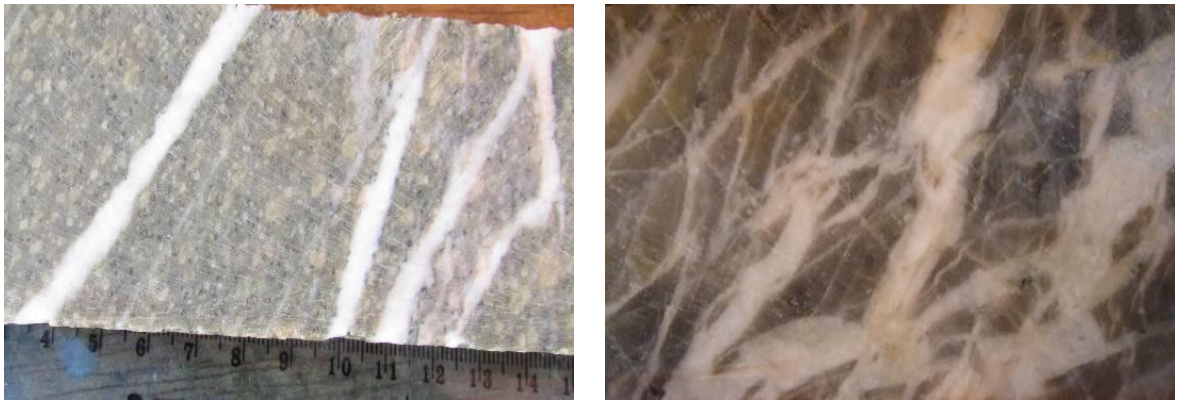

Figure 3.3.7: Vein assemblages showing sheeted veins (veins rays) and stockworks within dacitic intrusion.

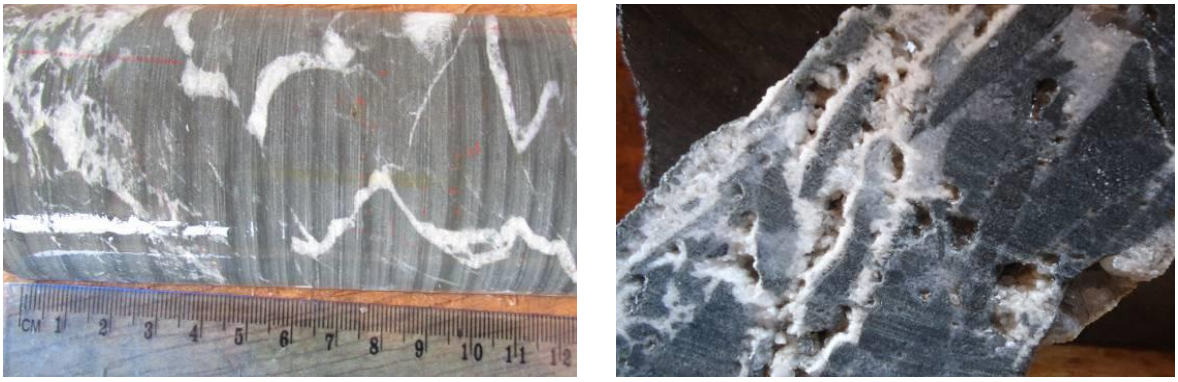

Figure 3.3.8: Quartz vein breccia (left) and quartz carbonate vuggy within country rock.

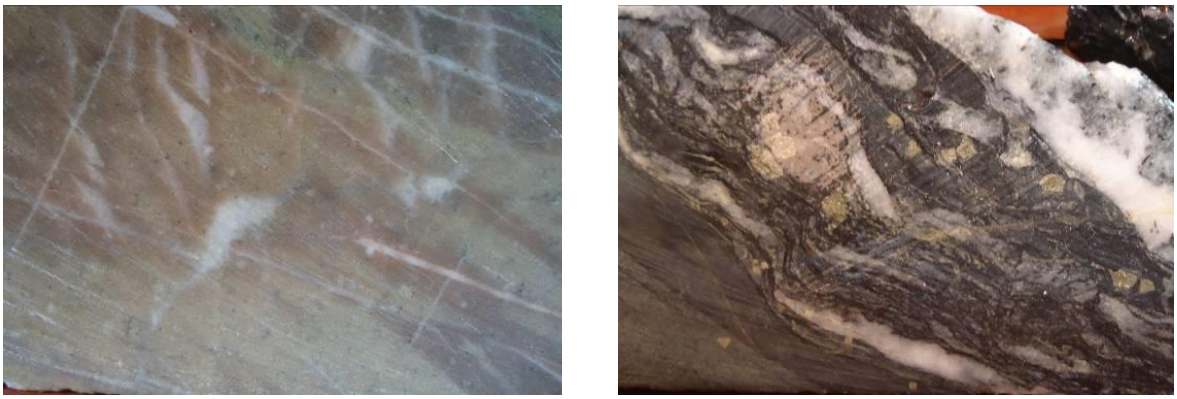

Figure 3.3.9: Competent microporphyry with intensive veining, showing an intensive albitisation (left) and shear-zone with pyrite deposition along quartz veins.

Figure 3.3.10: Inclusions of native gold in quartz veins.

3.4 Stereonet analysis and domain structure orientation

The present structural analysis was undertaken using the GeOrient version 9.4.4 program by plotting the dip direction and dip angle of planar structures on stereonet in respect with the following three mains steps:

(1) Create scatter plot for each planar structural elements of each zone;
(2) Create the corresponding contour plot;
(3) Interpret each plot as fully as possible;

Although, where structural readings account more than 15-20 records such as S_o, intrusive contacts and veins, data were plotted on a Schmidt net as poles to create a scatter plot, because when planar data in considerable amount are contoured as great circles; they do not allow to extract meaningful information. In contrast, all structural readings of up to 15 data points were plotted as great circles or scatter plot when meaningfully readable. These include faults, foliations and contacts.

In order to guide interpretation of planar data scatter plots, the orientation data contouring method was applied. The resulting contours show data density patterns. Contouring the values of the density distribution of plotted points provides a measure of the degree of preferred orientation. Perhaps, minor sub-populations and subtle patterns hidden by the noise will often be brought out or highlighted by countering scatter plots on stereonet (Allison, 2004).
To evaluate density distribution, the equal-area net is subdivided into a gridwork of many overlapping circular areas, each of which corresponds to 1% of the area of the stereographic projection.

Density is described in terms of percentage of total data points falling within a given 1% area of the stereographic projection. Density distribution is thus calculated as follows:

$$\textit{Density \%} = \frac{\textit{Number of points within 1\% area of net}}{\textit{Total number of data points}} \textit{ x 100}$$

The produced stereograms are actually pole-density diagrams, as planar structures have been plotted as pole points, which are useful in summarizing large quantities of geometric data.

Each pole-density diagrams as well as great circles have been labeled in respect of indication of the structural domain, structural element, number of measurements and the indication of the high density pole orientation. To make the diagrams more understandable, the white background was applied for all stereograms and different symbols to distinguish plotted elements. The statistically highest density orientation is indicated in red color as great circle. Where significant sub-populations are present, further great circles highlight their orientations as red dashed great circles.

So, S_1, S_2, intrusive contact, faults and vein orientations were plotted separately in different stereonets in order to identify orientation patterns and to compare such patterns of different structures and between different zones of the deposit.
At the end of each individual stereonet description, a brief evaluation is presented; which interprets the meaning of the data (clusters, random, several clusters, indication or evidence of folding, and if there is any, the presumed hinge line orientation, etc.). Then the geometrical relationship of structures in each zone supported by an additional stereonet and by referring to observations made in the core concludes the interpretation.

Detailed stereonet description of individual structural element plot regarding individual zone is presented in the following sections:

3.4.1 North-East Zone (NE_Z)

A total of 246 structural data were recorded from the three drill holes in the North-East Zone. According to the total structural data recorded, two types of plots are produced for data analysis of this zone. (i) Scatter plot for the most representative dataset grouping S_o planes (n=44) and veins (n=181); which are plotted as poles. (ii) Great circles structures with data records <15 comprising intrusive contacts (n=5), S_1 and S_2 foliations (n=5) and faults (n=11).

3.4.1.1 NE_Z Bedding:

North-East domain beddings scatter plot (figure 3.4.1a) shows the main density cluster area encompassing both 12% and 24% contour lines. This high pole density point is located in the western portion of the stereonet (figure 3.4.1b).

The main data density corresponds to moderately E-dipping bedding in the NE_Z of **090/36**.

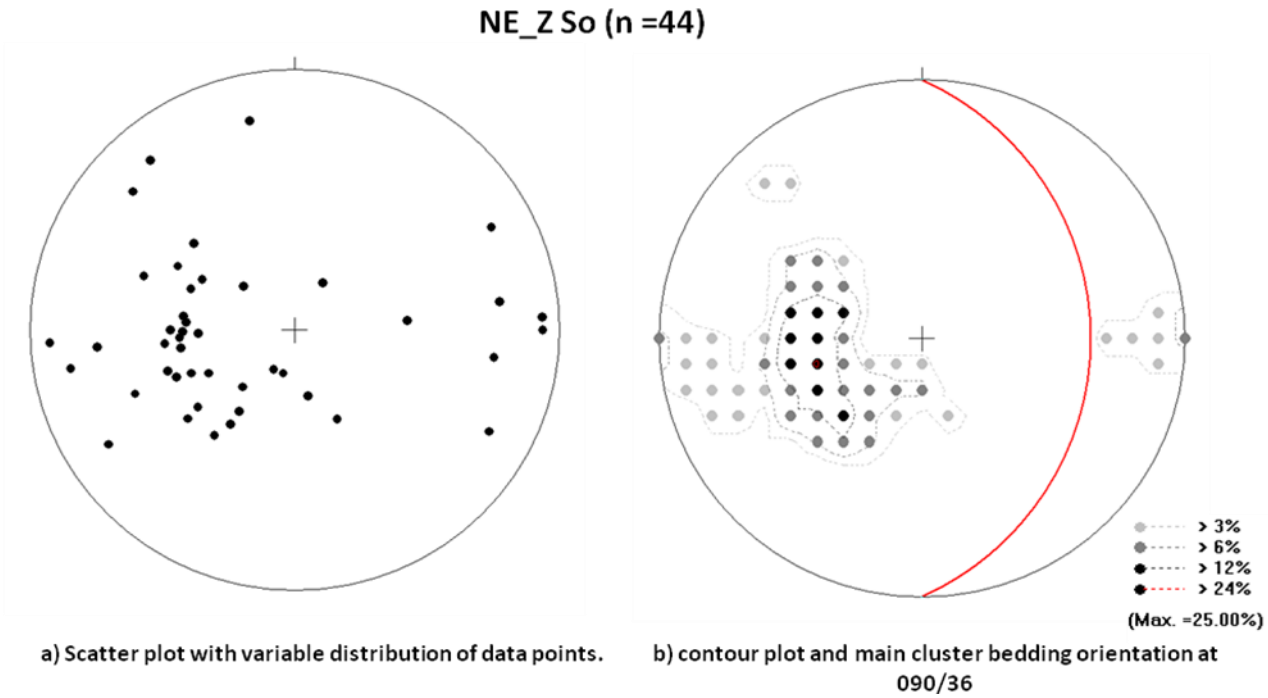

Figure 3.4.1: NE_Z S_o stereonet plots indicating a variable distribution with the main cluster point located in the western portion of the stereonet and extended from the south-west toward the north-west quadrant.

3.4.1.2 NE_Z Intrusive contacts

Due to the limited contacts records (only five) as shown on figure 3.4.2a, the NE_Z contacts between intrusions and country rocks are plotted as great circles (figure 3.4.2b). Contacts mainly strike N-S to NE-SW and dip steeply to the east and west. The north-east to south-west dipping contact shows the same orientation as the mean contact orientation. On average, the contacts dip steeply to the ESE at **105/79.**

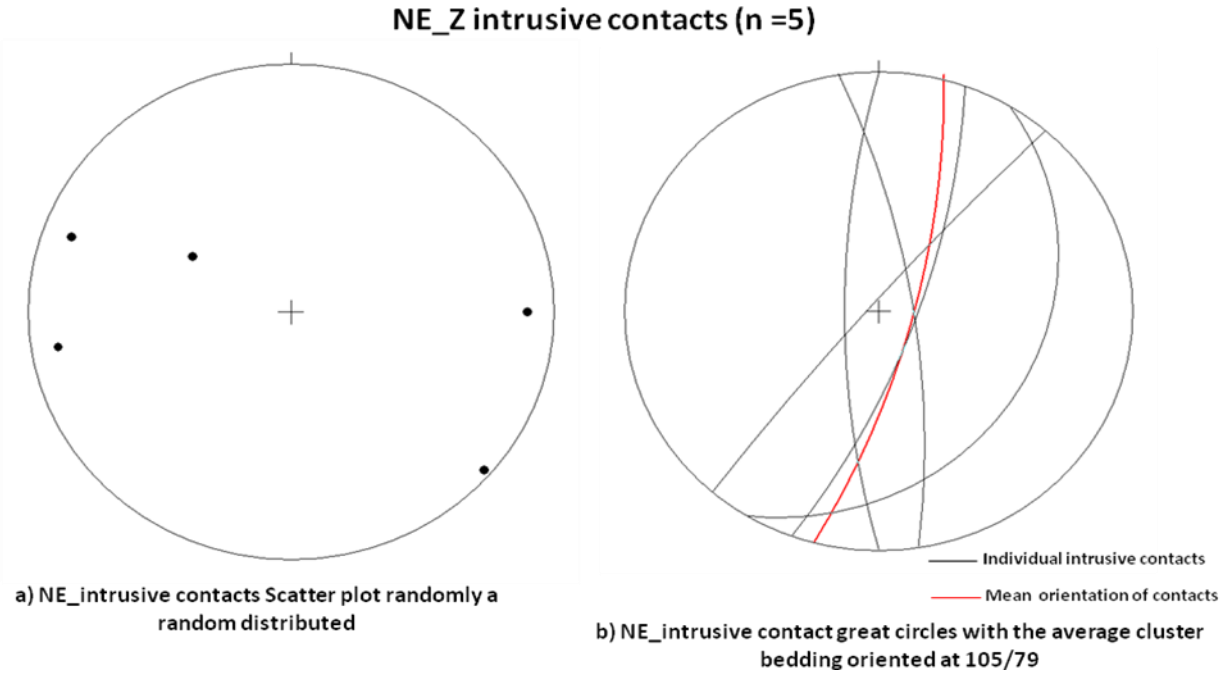

Figure 3.4.2: NE_Z intrusive contacts plot as great circles showing the average orientation of contacts is the same direction like north-east to south-west great circles, which steeply dip to the east.

3.4.1.3 NE_Z Foliations (S_1, S_2)

Foliations readings of NE_Z were subdivided into S_1 and S_2 foliations. The S_1 type is represented by one reading at 102m from KLRD0019. S_2 records comprise four (4) readings. Due to the limited total foliation readings; the NE Zone foliations were also plotted as great circles.

Here, the single S_1 plane is oriented from north to south and shallowly dips to the east at **089/27** (figure 3.4.3). Note S_1 orientation in this zone is likely parallel to the orientation of S_o; but the S_1 is shallower than S_o (see figure 3.4.3).

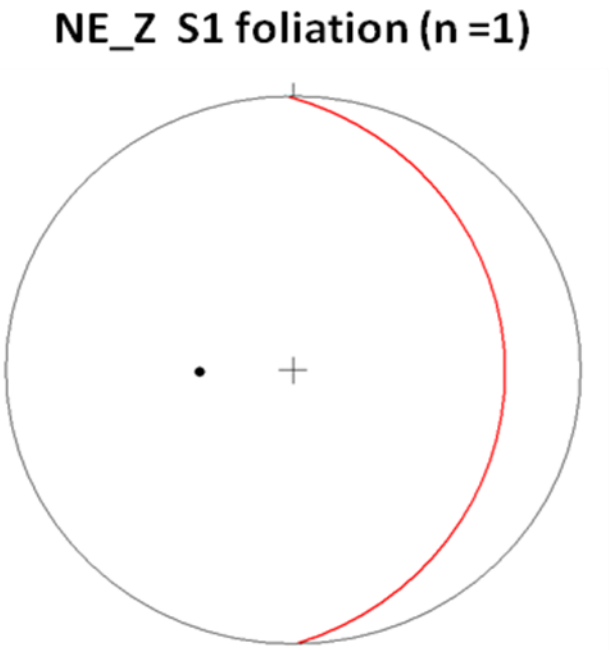

Figure 3.4.3: NE_Z S_1 plot showing a single pole point with N-S strike and ENE-dipping at **089/27.**

Contrarily to the S_1 records in the NE_Z, S_2 type accounts four (4) readings and show a variable girdle circles orientation (figure 3.4.4a). Here again, the majority of S_2 planes strike N-S and moderately dip to the east (figure 3.4.4b). The mean principal orientation of S_2 planes will moderately dip to the east at **095/39**.

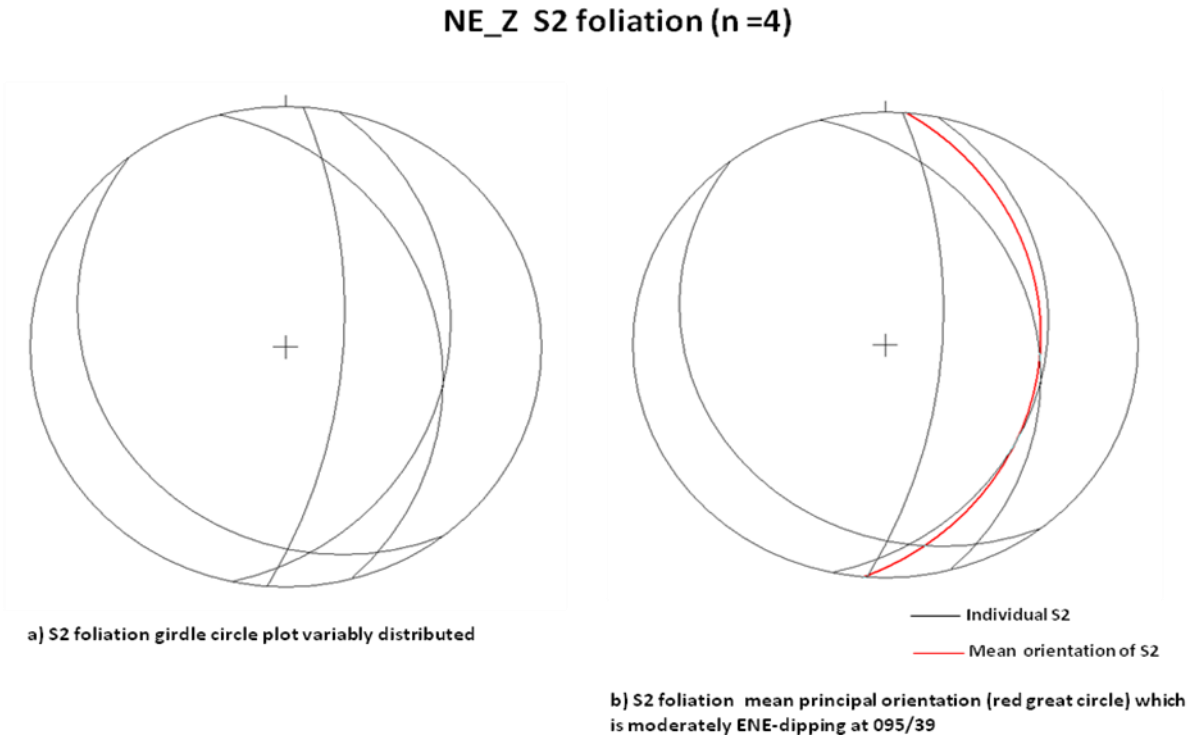

Figure 3.4.4: NE_Z S_2 girdle circles variably distributed and the mean principal orientation of S_2 which will moderately dip to the east.

3.4.1.4 NE_Z Faults

The stereonet presenting fault planes shows a high variability in their orientation (figure 3.4.5a). In general, two major oriented population sets are distinguished when looking at the contour plot (figure 3.4.5b). (i) The more abundantly oriented fault group is located in the northern portion of the stereonet and shows an E-W strike, which will steeply dip to the south. (ii) The secondary and single oriented fault group situated in the eastern part of the stereonet shows N-S strike and also steeply dips but to the west.

Although, fault planes principal orientation in the NE Zone dips steeply to the south at **179/66**; a secondary plane orientation is present dipping variably but mainly steep to the west, on average at **270/59** (figure 3.4.5b).

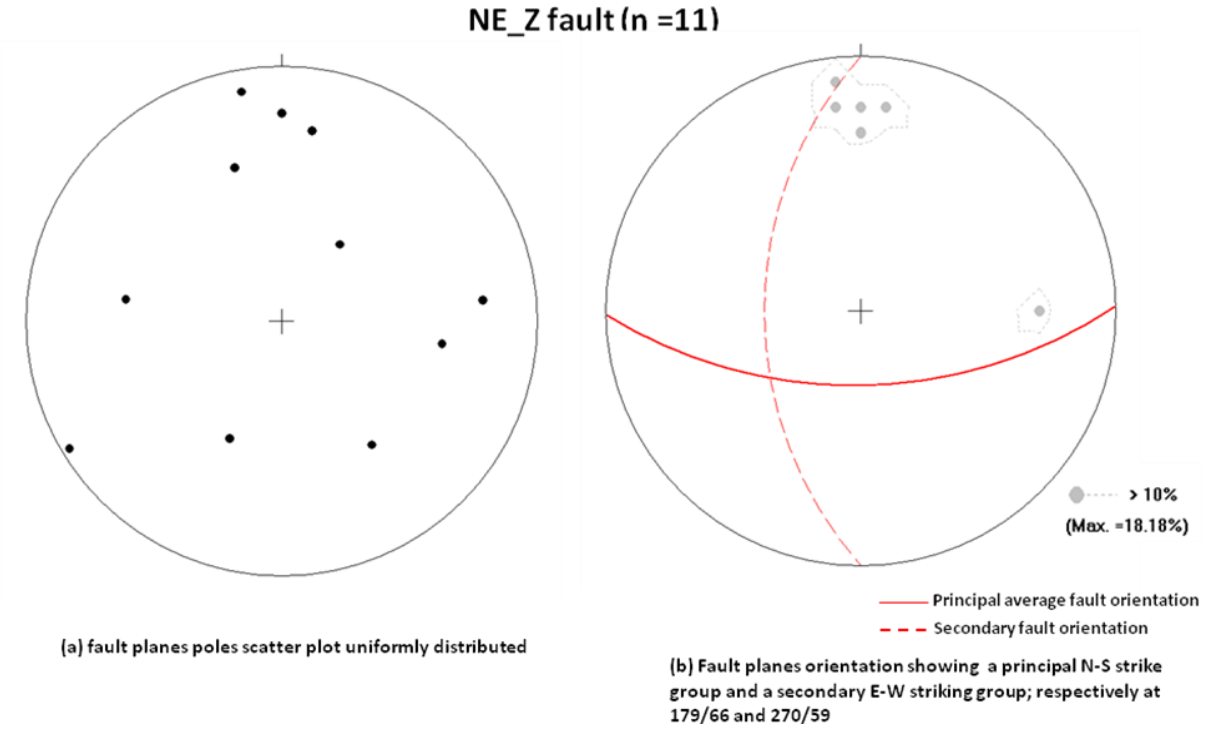

Figure 3.4.5: NE_Z fault planes scatter and contour plots. (a) Showing pole point random distribution with no preferred orientation. (b) Defining the two principal orientations of faults groups with a perpendicular relationship.

3.4.1.5 NE_Z Veins

Vein records in North-East Zone account 181 data. The scatter plot of NE domain vein planes shows variably oriented planes with certain domains where they are more abundantly oriented than others (figure 3.4.6a). When carefully looking at the contour plot of veins planes (figure 3.4.6b), the most representative oriented population sets are located within the 4% to 8% contour lines.

An accurate definition of NE Zone vein orientation allows prioritizing the abundantly oriented vein domains, for which five orders of orientation (figure 3.4.6b) can, in decreasing abundance of data points, be defined as follows:

(i) The first order (most commonly seen) vein orientation will fall in the north-western portion of the net with an average SSE-dip direction at a steeply dip angle of **135/64**;

(ii) The second order vein orientation group falls within the centre northern part of the net and represent the majority population domain. The statistical mean orientation of this group shows a SSW-dip direction with a shallow dip angle of **195/21**;

(iii) The third order vein orientation group represents the minority population domain adjacent to the second order vein orientation set in the centre northern portion of the net. Here in contrarily, the average orientation shows WSW-dip direction at moderate dip angle of **242/30;**

(iv) The forth order vein orientation group is located in the south-eastern portion of the stereonet and show a NNW-dip direction with moderate dip angle of **330/33**;

(v) The fifth and last order vein orientation group is situated in the western part of the stereonet and an average ENE-dip direction at steep dip angle of **075/82**.

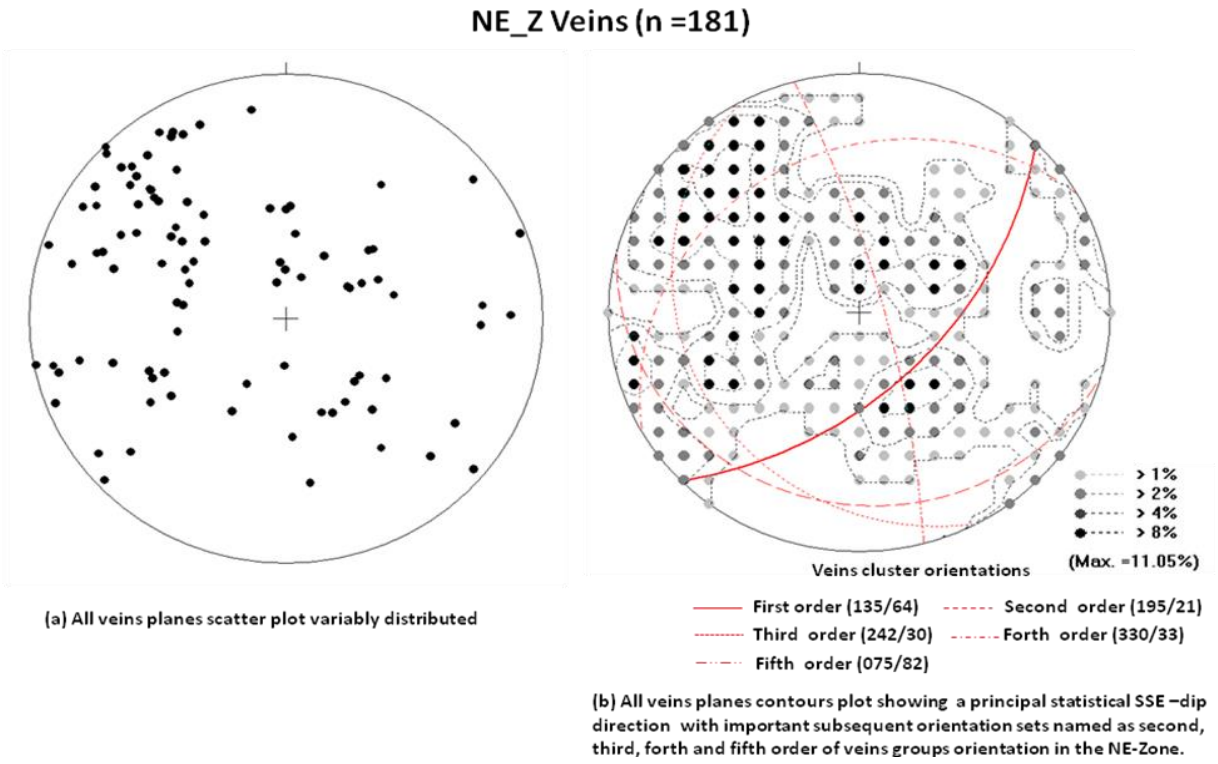

Figure 3.4.6: NE_Z veins scatter and contour plots showing a variable distribution and five major orientation groups. (a) Variably oriented vein planes orientation with certain domains more populated than others; (b) First to fifth order vein orientations shown as great circles.

The highly variable orientation of veins in the NE domain render average values calculated from the whole data set not fully representative for the vein orientations. However, the great circles shown on figure 3.4.6b can be interpreted as approximate directions where vein orientations may be more commonly intersected.

3.4.1.6 Structural relationships in the North-East Zone

The geometrical relationship of S_o, S_1, S_2 intrusive contacts, fault and veins in the North-East Zone was established statistically and is shown in detail on the figure 3.4.7. The following fundamental observations can be noticed:

(i) S_o and S_1 great circles are parallel, but sub-parallel to S_2, all dipping moderately to the E (figure 3.4.7).

(ii) Intrusive contact great circles, showing steep ESE-dip direction, intersect both fault and vein mean great circles at high angle. Contacts also crosscut S_o, S_1 and S_2 great circles at 40° (figure 3.4.7).

(iii) Vein and fault mean orientation great circles (figure 3.4.7) respectively show SW and SSW-dip direction and horizontally intersect S_o, S_1, S_2 and contact.

(iv) Detailed analysis of fault data has identified two perpendicular fault planes orientation (figure 3.4.5b). Fault major great circles intersect the fault minor great circle at high angle (figure 3.4.7).

(v) Detailed vein clusters analysis has identified five main orientations (figure 3.4.6). Vein order 1 and vein order 4 crosscut, respectively at steep and shallow angle all other fabrics (figure 3.4.7), but they dip in different directions. Vein order 2 and vein order 3 (figure 3.4.7) are sub-parallel and intersect fault minor and intrusive contact great circles at the same point and dip to the same WSW dip direction (figure 3.4.7). It should be noticed that vein order 5 intersect all other vein orders at low angle (figure 3.4.7).

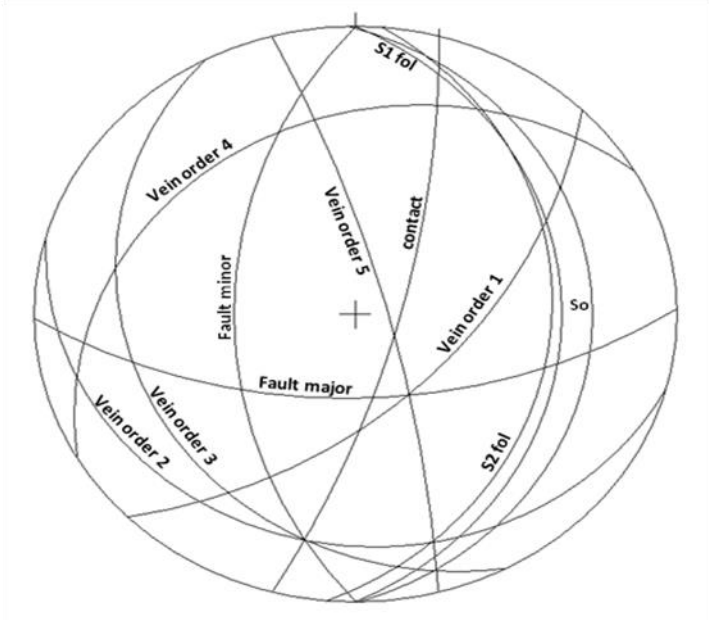

Figure 3.4.7: NE_Z structures geometrical relationship as described in the section 3.4.1.6

In summary, NE Zone detailed structures analysis and geometrical relationship have shown so much variation in the major structures type orientation. It appears in general that:

a) S_o and S_1 represent N-S structures group and dip to the east; while S_2 is sub-parallel to them and dips to the same direction.

b) Intrusive contacts dip steeply to the SE;

c) Faults are E-W in majority and dip to the south; but some minor N-S and W-dipping faults are observed:

d) Veins are variably oriented with more common populations dipping SE or SW.

3.4.2 North-West Zone (NW_Z)

175 structure surfaces have been recorded in the North-West Zone. They respectively comprise: S_o (29), S_2 (7), intrusive contacts (12), fault (8) and veins (119).

3.4.2.1 NW_Z Bedding

The North-West Zone S_o stereonet plot shows variable pole distribution (figure 3.4.8a). The contour plot (figure 3.4.8b) shows four clusters. However, none of these clusters consists of more than 6 data points. Overall the data points do not show any systematic geometric patterns.

Three clusters lie in the NW part of the stereonet with the two shallower-dipping clusters being connected by the 8% density contour (figure 3.4.8b).

The dominant S_o orientation (red great circle) is the first order S_o direction and shallowly dips to the SE at **125/26**. The second order dominant direction (red dashed great circle) shows an E-dip direction at moderate dip angle of **097/45**. The single secondary S_o orientation group within this principal cluster area corresponds to the fifth order of S_o orientation and shows a steeply SSE-dipping at **142/71**.

The secondary S_o cluster area is located in the central most east portion of the stereonet (figure 3.4.8b) and shows two groups. The first group represents the third order S_o orientation and shallowly dips to W at **272/21**. The second S_o orientation group of this cluster area forms the forth order S_o orientation group that is shallow WSW-dipping at **230/25**.

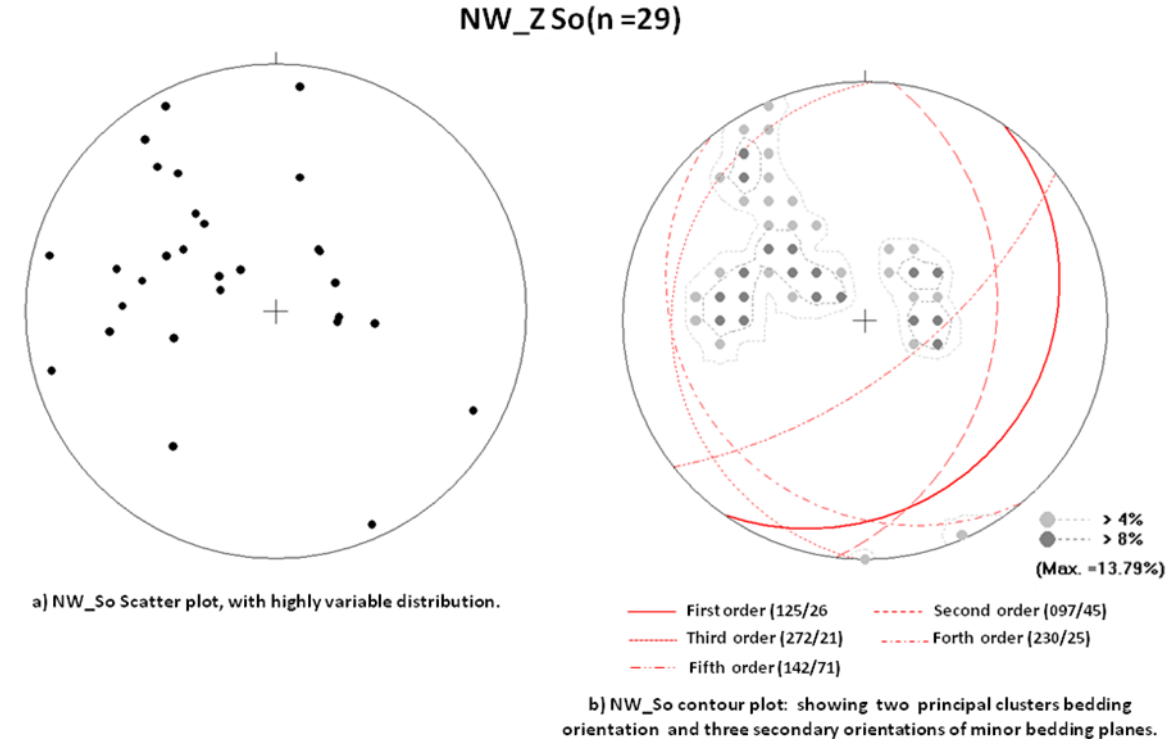

Figure 3.4.8: NW_Z S_o stereonet plots. (a) Scatter plot showing highly variable poles distribution. (b) Contour plot with two main clusters data density with internal oriented S_o groups. The primary pole cluster orientation shows shallow to moderate ESE dip; while the secondary pole cluster corresponding to the two minor oriented S_o group (third and forth order) are moderate WSW-dipping.

3.4.2.2 NW_Z Intrusive contacts

Stereonet plot of intrusive contact poles in NW zone shows a highly variable distribution pattern with four poles concentration points (figure 3.4.9a). The main contact cluster is connected to the 18% contour and shows moderate SE-dipping at **136/45** (figure 3.4.9b). Two others secondary contact clusters falling within the 9% contour represent respectively the second order contact orientation and steeply W-dipping at **274/80**; and the third order contact orientation which is also steeper, but NNW-dipping at **334/81**(figure 3.4.9b).

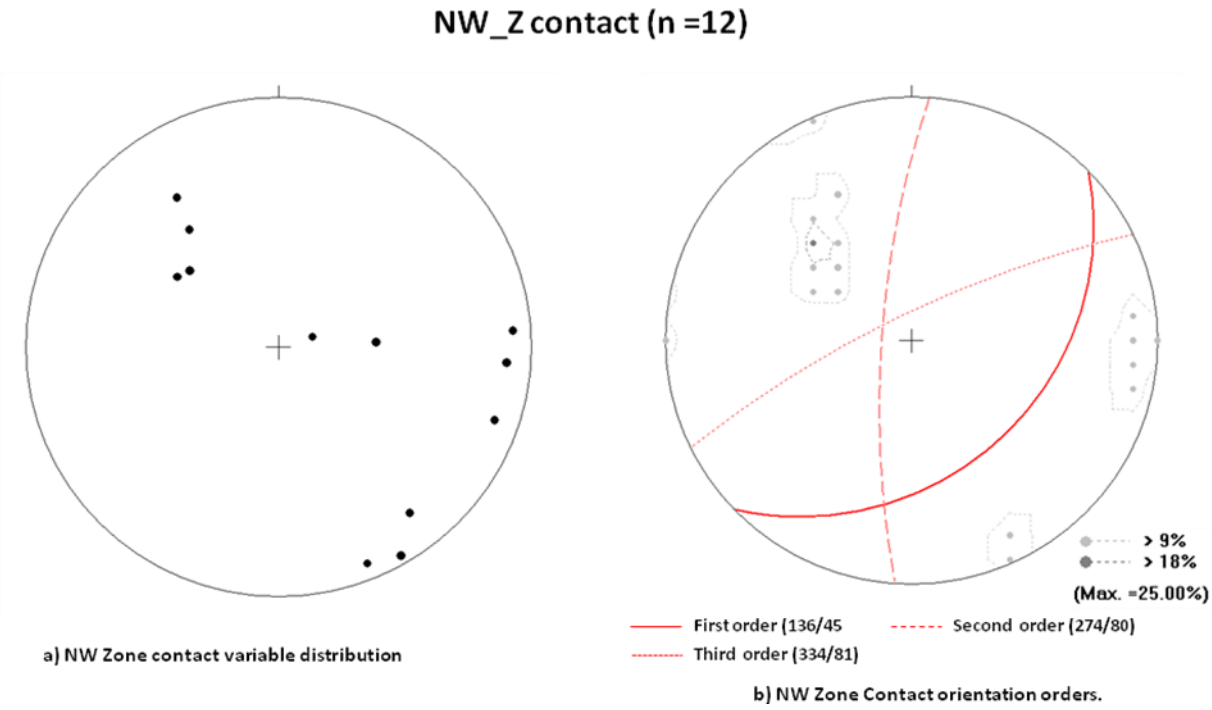

Figure 3.4.9: NW_Z intrusive contact stereonet plot (a) showing a variable poles distribution pattern. (b) Showing that most contacts have approximately NE-SW strike and dip variably to SE, W and NNW.

3.4.2.3 NW_Z Foliations (S_1, S_2)

S_1 orientation readings is NW Zone were not sufficient (only 2 data) to be represented in this section.

S_2 poles point diagram shows 7 data variably distributed (figure 3.4.10a). In this case, the red great circle does not represent all the 7 S_2 data. However, the red great circle indicates that 5 of the 7 data points lie on a steeply SE-dipping great circle of **135/41** (figure 3.4.10b).

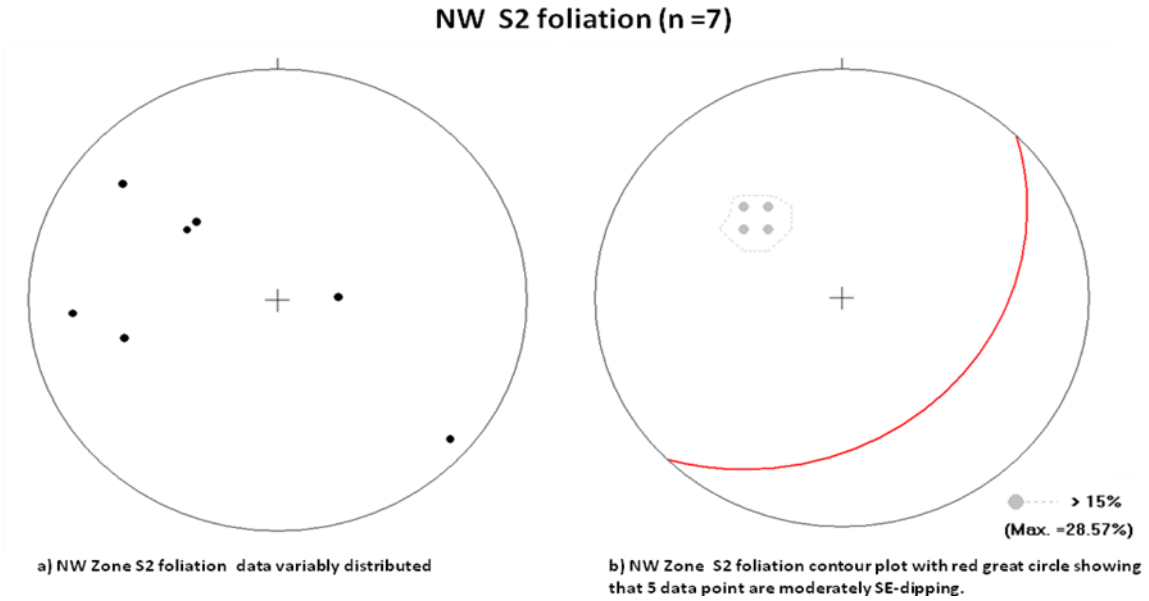

Figure 3.4.10: NW_Z S_2 stereonet plot (a) showing a variable distribution pattern; (b) suggesting that 5 of the 7 data points are moderately SE-dipping.

3.4.2.4 NW_Z Fault

Faults in the North-West Zone are variably oriented with some pole points plotting close to the centre, close to the SE margin, or at various places in the western sector of the stereonet (Figure 3.4.11a). When looking at the fault orientation contour plot (figure 3.4.11b), two small clusters pole are observed and fall within the 13% contour lines.

The dominant density cluster shows NNW steep dipping angle of **320/68,** representing the three data points in the SE sector. The secondary density cluster, which is located in the centre of the stereonet, may be described by shallow WSW dipping orientation of **223/17** (figure 3.4.11b).

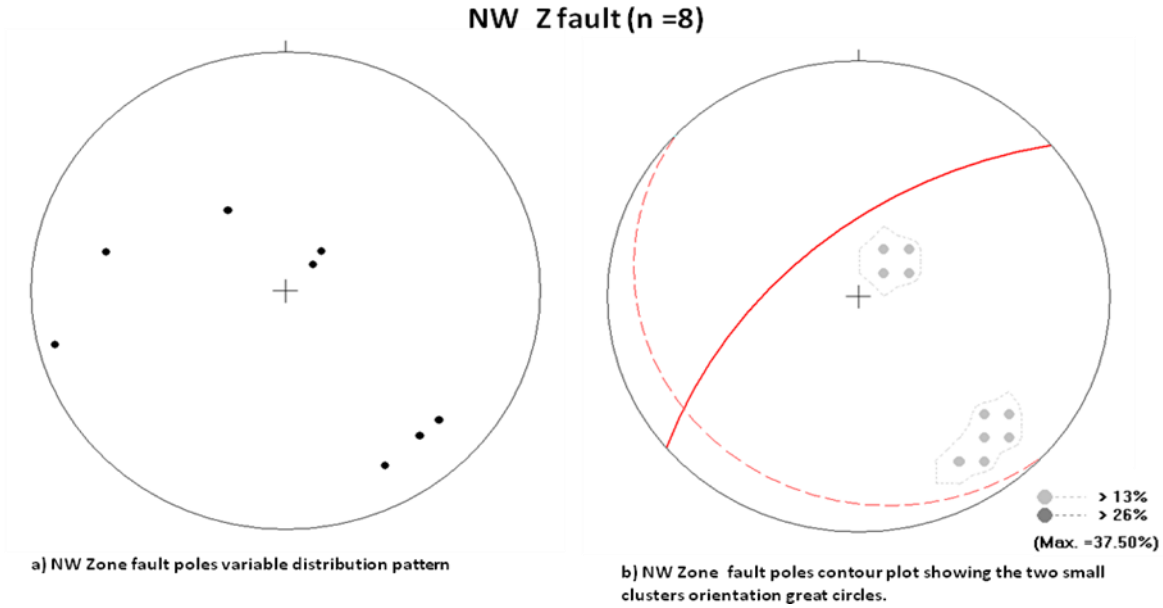

Figure 3.4.11: NW_Z fault poles points diagram and contour plot. (a) Showing the variable fault poles distribution. (b) Showing the two small clusters orientation, respectively NNW-dipping and WSW-dipping.

3.4.2.5 NW_Z Veins

Vein data also encompasses all types (extensional, shear, oblique, quartz carbonate and quartz chlorite) as previously described (sub-chapter 3.3).

The stereonet showing NW vein orientation (figure 3.4.12a) suggests variably distributed poles with high density concentration domains in the north-west, centre-east and south-east of the stereonet.

In general, North-West Zone vein orientations were determined from poles concentrated within the 8% contour line (figure 3.4.12b). Here again, three main oriented domains corresponding to the high density domains are observed and they are as follows:

(i) the north-west high density area which forms the principal NW veins direction (first order orientation group) and moderately dips to the SE at **135/47**;

(ii) the central most east high density area (or the second order orientation group), which also shows a moderate W-dipping at **274/33**;

(iii) the further east to south high density oriented group (third order orientation set) which is steeper and W-dipping at **281/75**.

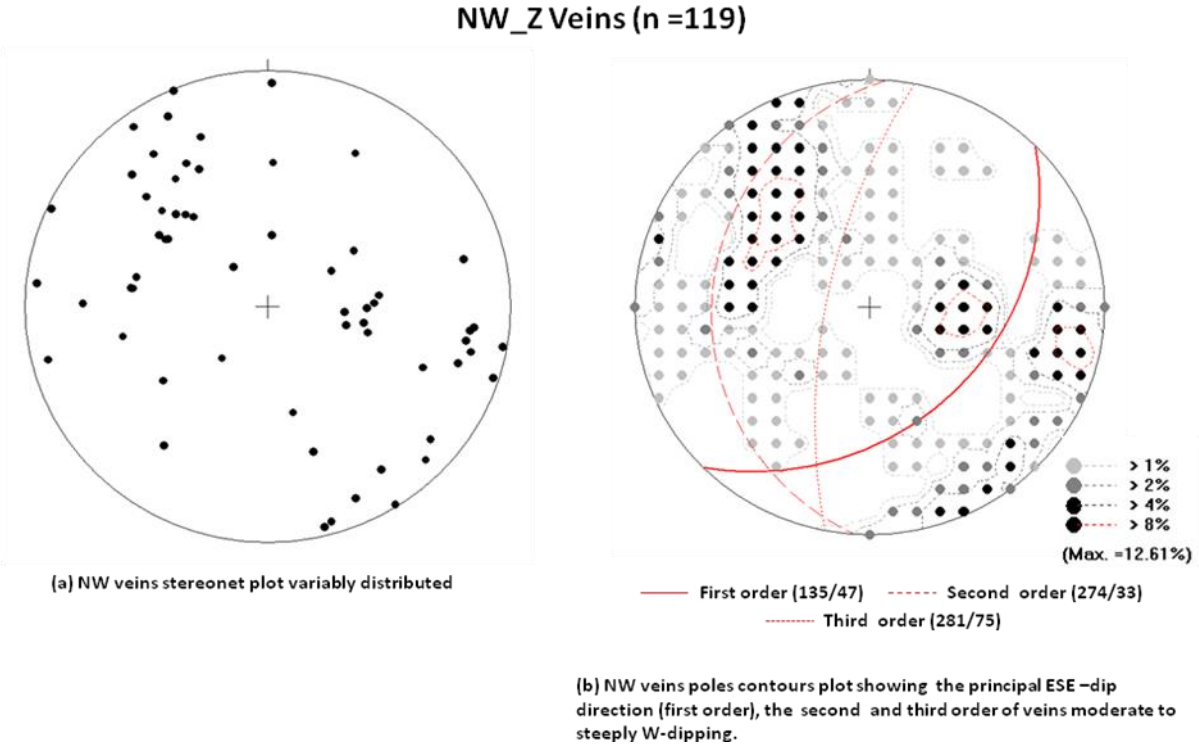

(a) NW veins stereonet plot variably distributed

(b) NW veins poles contours plot showing the principal ESE –dip direction (first order), the second and third order of veins moderate to steeply W-dipping.

Figure 3.4.12: NW_Z veins stereographic plots: (a) widespread data distribution with three high density domains. (b) Density contour diagram showing three oriented domains: the red great circle corresponds to the principal high density area or the first order oriented group; the red dashed great circle defines the second order orientation group, and the steeper dotted great circle shows the direction of the third order oriented group.

3.4.2.6 Structural relationships in the North-West Zone

Geometrical relationship of structures in the North-West Zone suggests three main strikes corresponding to NE-SW, N-S and NW-SE (figure 3.4.13). Thorough, the crosscutting relationships of measured structures (figure 3.4.13) shows that:

(i) Principal orientation of S_o, S_2, intrusive contact and vein great circles are parallel to sub-parallel and NE-SW strike and dipping to the SE; but S_o is shallower than other features.

(ii) Fault dominant orientation great circle is also NE-SW, but steeply dips to the NNW.

(iii) Secondary orientations of structures show N-S, NW-SE or NE-SW strike, and respectively dip to W; E or SE. Their corresponding principal orientations intersect in the SW and NE sectors of the stereonet.

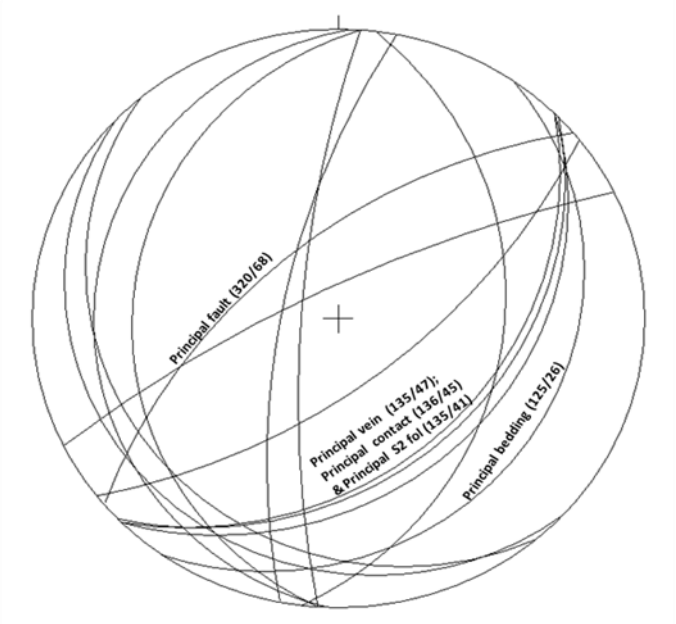

Figure 3.4.13: NW_Z structures geometrical relationship showing statistical averages or means orientations, in general falling within each structure dominant direction.

In conclusion of the stereonet description of NW Zone, it should be noticed that geometrical relationship between measured features has also shown number of variation of great circles directions (figure 3.4.13). Although, three main oriented groups can be considered for this zone:

i. NE-SW structures group represented by principal orientations of S_o, S_2, intrusive contact, fault and veins. Also the fifth order S_o orientation is lie to this strike.

ii. N-S structures group accounts the second and third orders S_o, the second order contact, and second and third orders vein orientations.

iii. NW-SE structures group encompasses mainly secondary directions of S_o (third and forth orders), second order fault.

3.4.3 Central Zone (CZ)

278 data were recorded in drill holes from the Central Zone: 40 S_o planes, 23 intrusive contact, and 200 vein readings. Structural readings of these planes are plotted as poles. Small data sets are three S_1, five S_2 and seven fault readings.

3.4.3.1 CZ Bedding

Like in the NW Zone, Central Zone S_o readings show a highly variable pole distribution (figure 3.4.14a). The contour plot stereonet of the CZ S_o (figure 3.4.14b) shows two data concentration zones with internal high density domains that form the dominant orientation cluster area all falling within the 6% contour line.

Two pole clusters in the southwestern quadrant may be interpreted as defining a vague great circle (figure 3.4.14b): (i) the major cluster area which represents the first order S_o orientation cluster moderately dips to NNE direction at **015/34**. (ii) The minor cluster zone that forms the second order S_o orientation cluster of the Central structural domain also dip moderately, but to the East at **081/51**.

Three pole clusters in the northwestern sector extended to the northeastern quadrant may also describe vague great circles (figure 3.4.14b): (i) the principal cluster area corresponds with the third order S_o orientation of the Central zone; which is steeply SE-dipping at **130/62**. (ii) The secondary poles concentration zone represents the forth order S_o orientation of this structural domain and moderately dips to SW at **238/29**. (iii) Finally, fifth order S_o orientation group shallowly dip to the south at **177/24**.

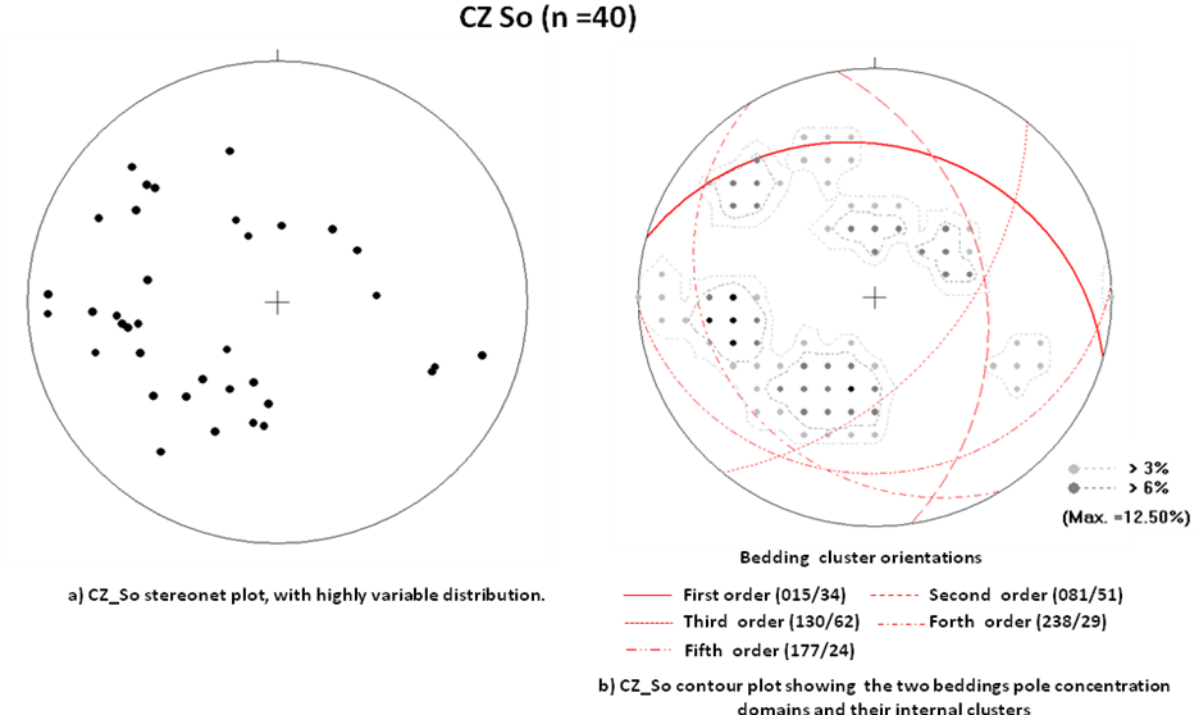

Figure 3.4.14: C_Zone So stereonet plot: (a) scatter plot with highly variable distribution pattern. (b) Contour plot with internal cluster domains that correspond to the bedding orientation orders in the central structural domain.

3.4.3.2 CZ Intrusive contact

A total of 23 readings of intrusive contacts in the Central Zone show variable orientation (figure 3.4.15a) with limited high density domains. The resulting contour plot (figure 3.4.15b) shows three clusters within the 10% contour line. An orientation that might be representative of the main cluster delineated by the 20% contour line is moderately ESE-dipping at **122/53**. However, a variety of other contact orientations exists in the Central Zone.

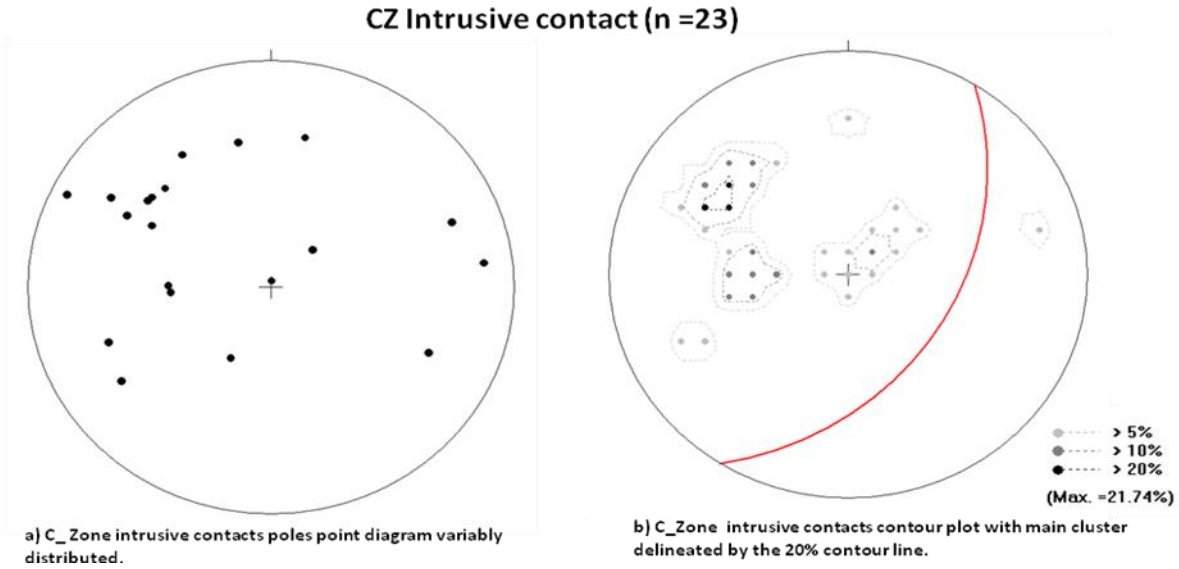

Figure 3.4.15: C_Zone stereonet plot: (a) variable pole points distribution pattern; (b) contour plot showing three cluster domains with an ESE dip direction great circle representing the principal orientation of contact in this zone.

3.4.3.3 CZ Foliations (S_1, S_2)

S_1 orientation readings in Central Zone were not sufficient (only 2 data) to be presented in this section.

Three S_2 readings show moderate dip towards the east or southeast with an average orientation of **119/33** (3.4.16 a, b).

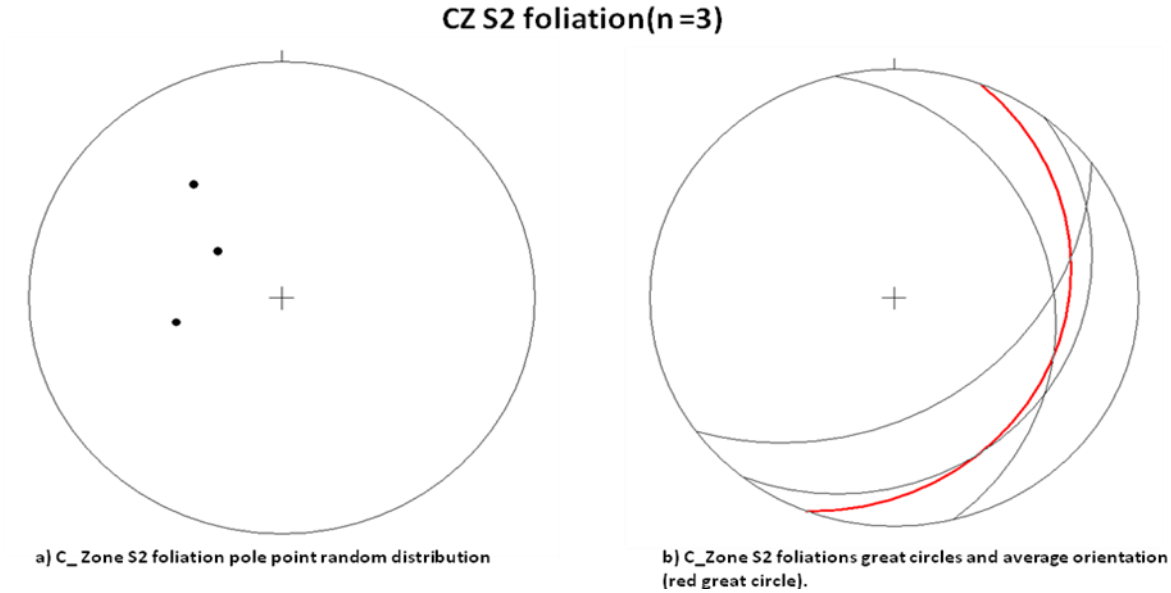

Figure 3.4.16: C_Zone S_2: (a) pole point diagram; (b) great circles with average S_2 orientation (red).

3.4.3.4 CZ Faults

Fault data records count 7 readings in the C-Zone and show the pole point diagram with variable distribution pattern (figure 3.4.17a). The great circle plot (figure 3.4.17b) shows in majority N-S to NE-SW strikes from fault readings. The strike directions vary by more than 90° and consequently the mean orientation with SE-dip direction of **109/78** is associated with large standard deviation and therefore not particularly meaningful.

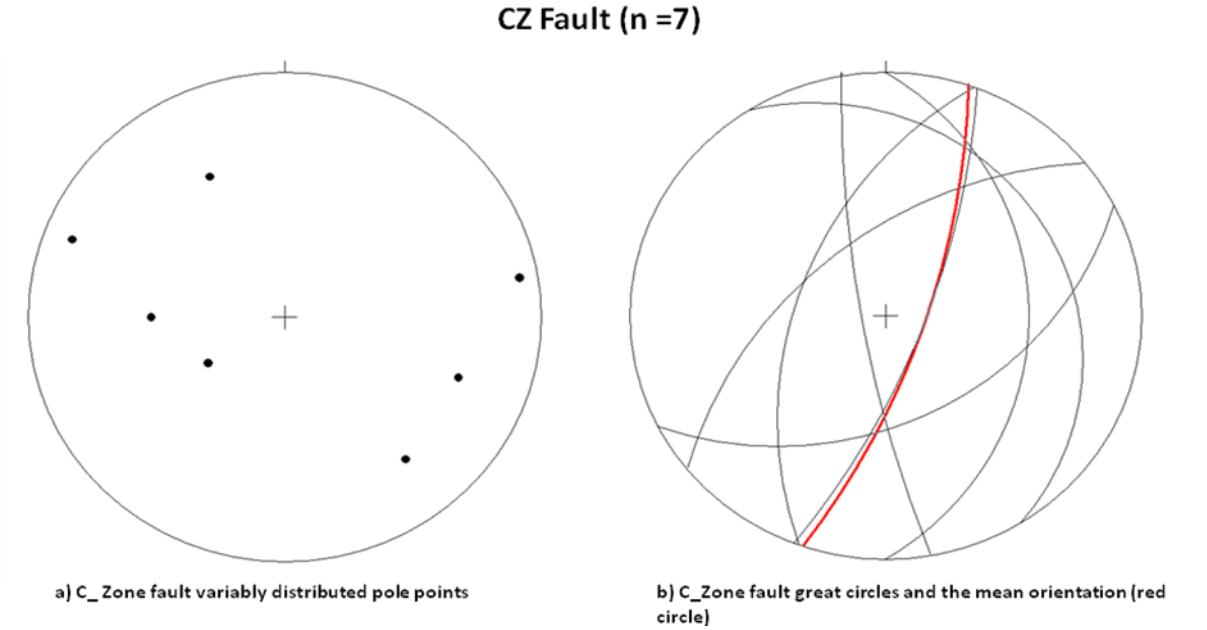

Figure 3.4.17: C_Zone fault (a) pole point diagram with variable distribution pattern; (b) mean orientation of fault individual direction.

3.4.3.5 CZ Veins

Veins readings of C_zone comprise records of extensional veins, shear-veins, oblique veins as well as quartz-carbonate and quartz-chlorite veins. Vein data accounts 200 readings and plot in majority in the north-west of the stereonet (figure 3.4.18a, b) and stereonet shows numerous high density domains.

The most significant clusters fall within the 8% contour line (figure 3.4.18b). As two significant clusters points of 8% contour line are observed, they may define two principal directions of dominant vein features in this zone. Thus, major orientations will moderately dip to SE at respectively **130/49** (first order) and **142/55** (second order).

The absence of principal cluster point in the remained high density points located in the south-east portion of the stereonet may justify the less significant influence of these veins to the general trend of C_zone veins features.

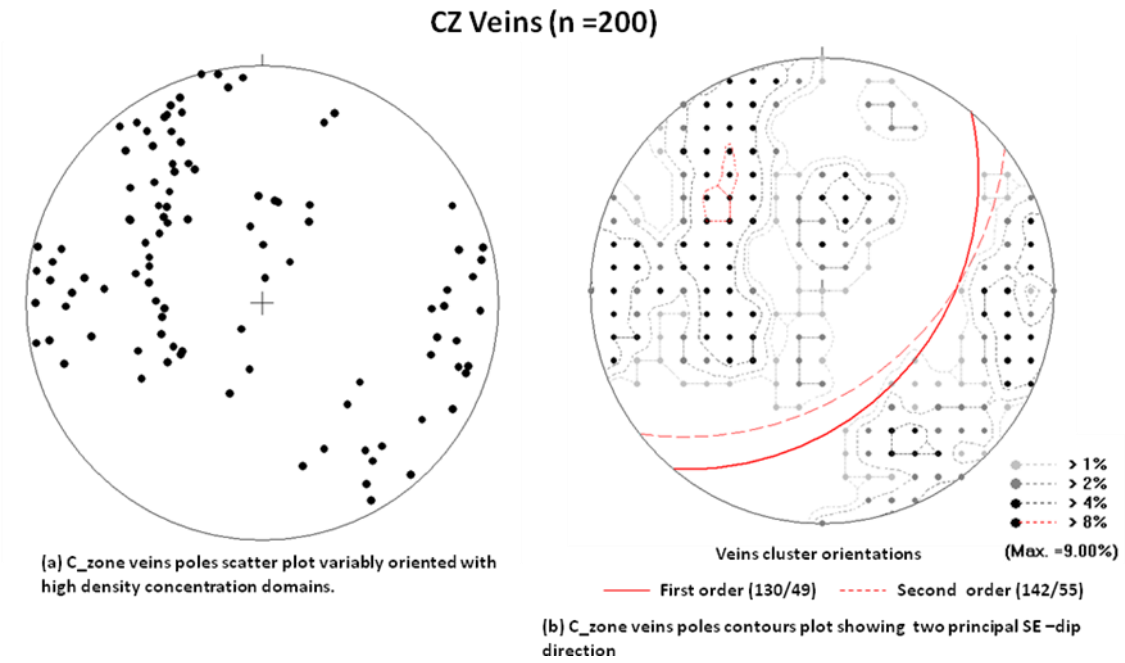

Figure 3.4.18: C_Zone vein (a) scatter plot variably oriented poles with numerous high density domains; (b) showing the two significant vein features average orientation in the same direction.

3.4.3.6 Structural relationships in the Central Zone

Geometrical relationship of C_Zone structures has permitted to establish two dominant directions NE-SW and WNW-ESE of principal structures orientations (figure 3.4.19).

It appears in general that the first order vein, the average S_2 and the principal contact orientations are parallel to sub-parallel in orientation and perpendicular to the first order S_o orientation.

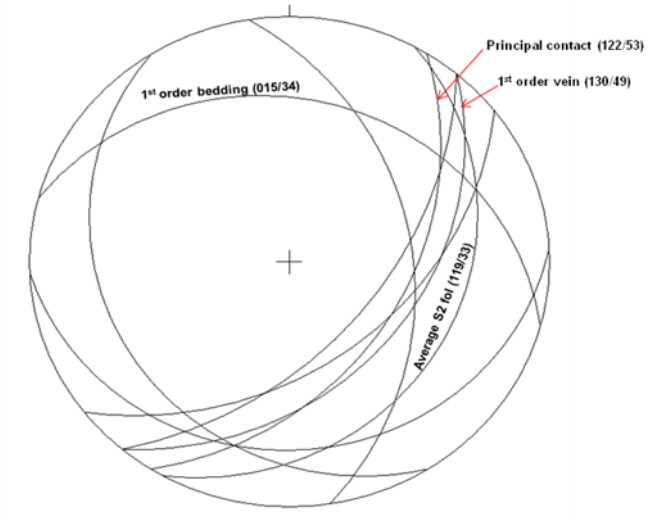

Figure 3.4.19: C_Zone structures geometrical relationship showing the two dominant NE-SW and WNW-ESE strikes of major structures orientations.

Briefly, stereonet analysis of structural measurements of the C-Zone has identified two dominant directions:

(i) NE-SW structure type represented by intrusive contact principal orientation, average orientation of S_2 and first order orientation of veins.

(ii) WNW-ESE structure type formed by the first order S_o orientation.

3.4.4 South Zone (SZ)

Structures recorded in SZ accounts 364 data which comprise S_o (42), S_1 (7), S_2 (17), intrusive contact (17), fault (7) and veins (271).

3.4.4.1 SZ_Bedding

S_o records in S_Zone basically shows a high density concentration pattern (figure 3.4.20a), with some insignificant isolated readings. Contour plot (figure 3.4.20b) also shows high density zone falling within the 12% contour line, which represents the average orientation of S_o in this zone. Thus, the average S_o orientation shows moderate ENE-dip direction at **059/31**.

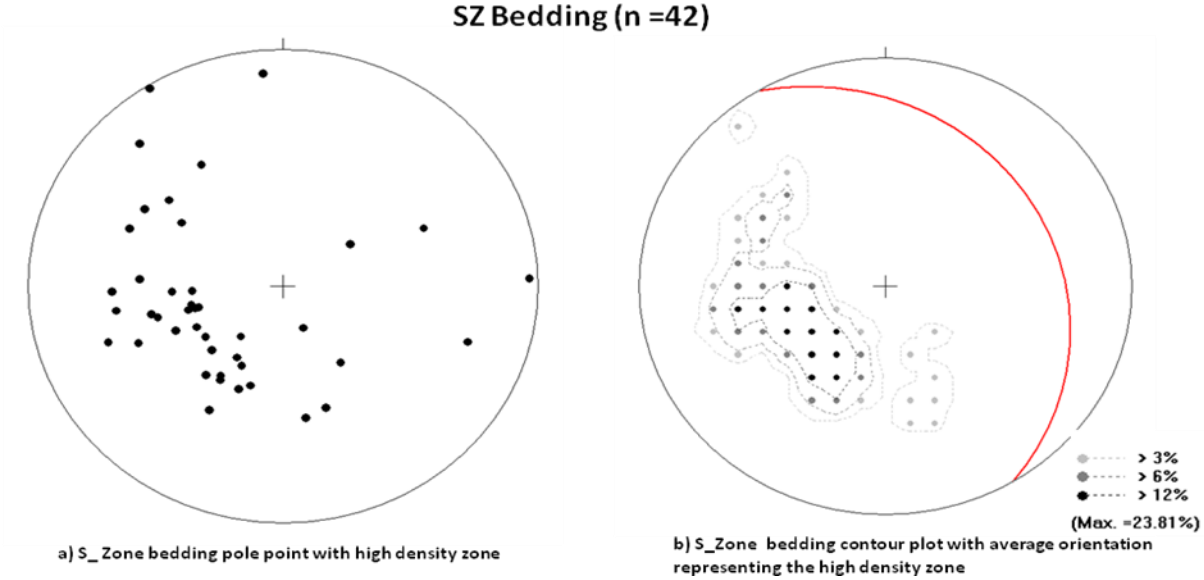

Figure 3.4.20: S_Zone S_o stereonet plot: (a) poles distribution with high density zone; (b) great circle representing the average orientation related to the high density area of ENE-dip direction

3.4.4.2 SZ_Intrusive contact

Like on S_o stereonet plot, intrusive contact plot shows high density distribution pattern with the dominant concentration point located in the western portion of the stereonet (figure 3.4.21a). The average contact orientation corresponding to those data falling within the 24% contour line shows eastern dip direction of **082/36** (figure 3.4.21b).

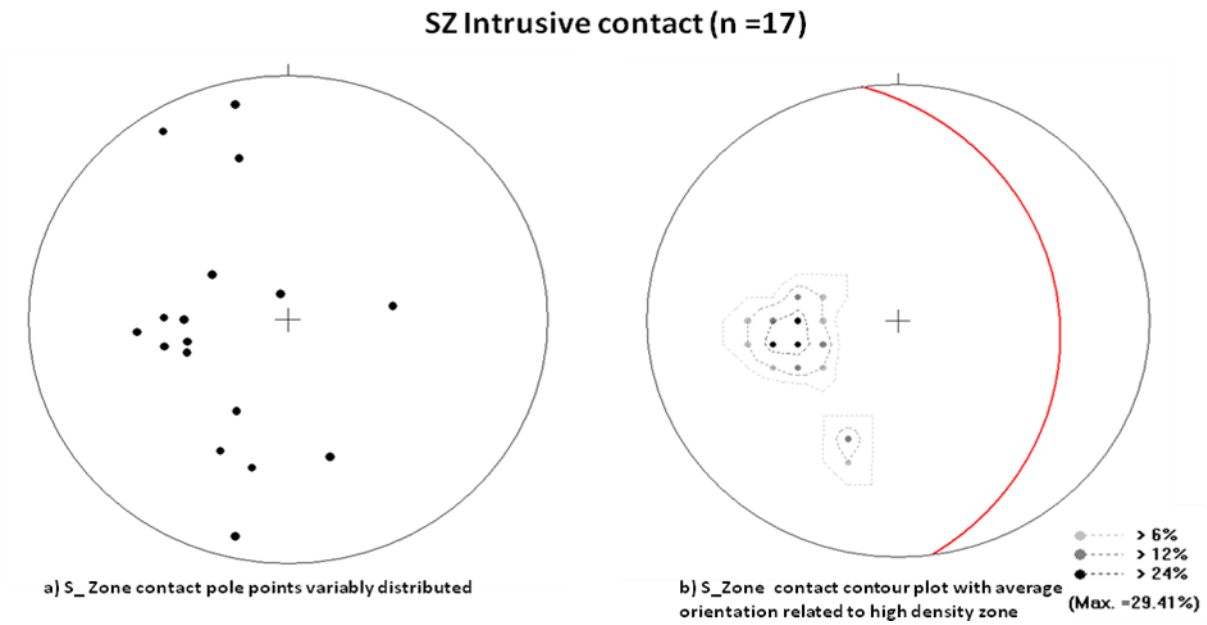

Figure 3.4.21: S_Zone intrusive contact: (a) pole points diagram with variable distribution pattern; (b) contour plot with red great circle representing the average orientation of contact in this zone.

3.4.4.3 SZ_Foliation (S1, S2)

Stereonets presenting foliations readings of S_zone show different pole point diagram for S_1 and S_2.

The S_1 distribution pattern (figure 3.4.22a) and the corresponding contour plot (figure 3.4.22b) shows moderate with NNE-dip direction of **025/39** as a best representation of S_1.

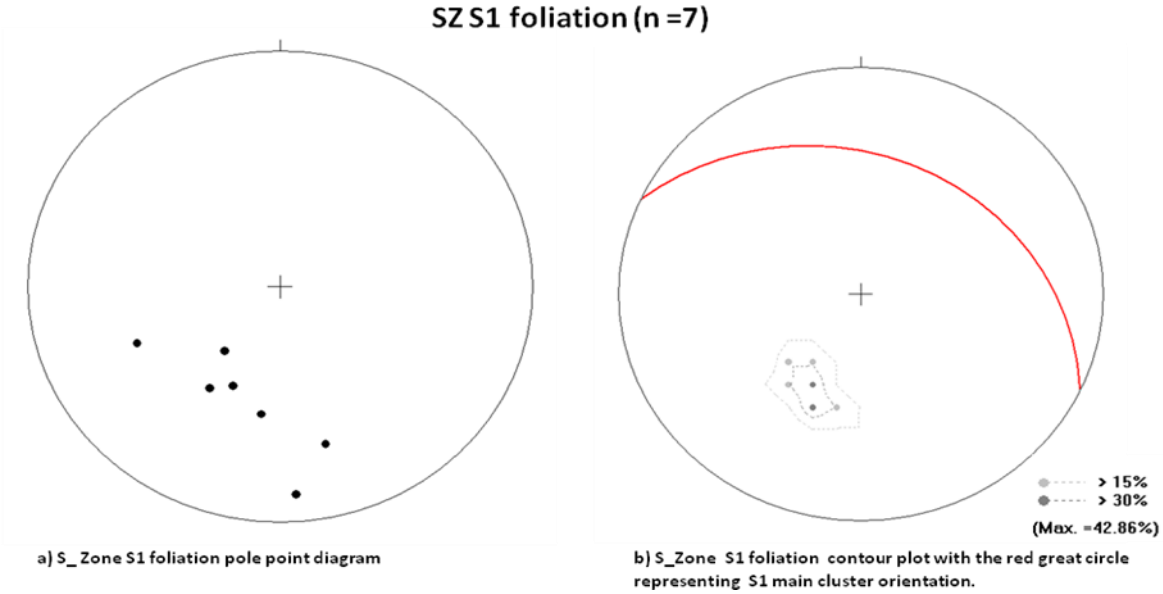

Figure 3.4.22: S_Zone S_1: (a) scatter plot with poles locally concentrated; (b) contour plot corresponding to the high density area which also represents the average orientation of S_1 in this zone.

S_2 are variably distributed (figure 3.4.23a) and the resulting contour plot shows two main clusters delineating poles points fitting within the 14% contour line (figure 3.4.23b). The principal S_2 orientation is moderate and dips to East at **107/30** and represents the cluster area

located in the centre west sector. The secondary cluster zone situated in the Northwestern part of the stereonet shows SSE-dip direction of **152/79**.

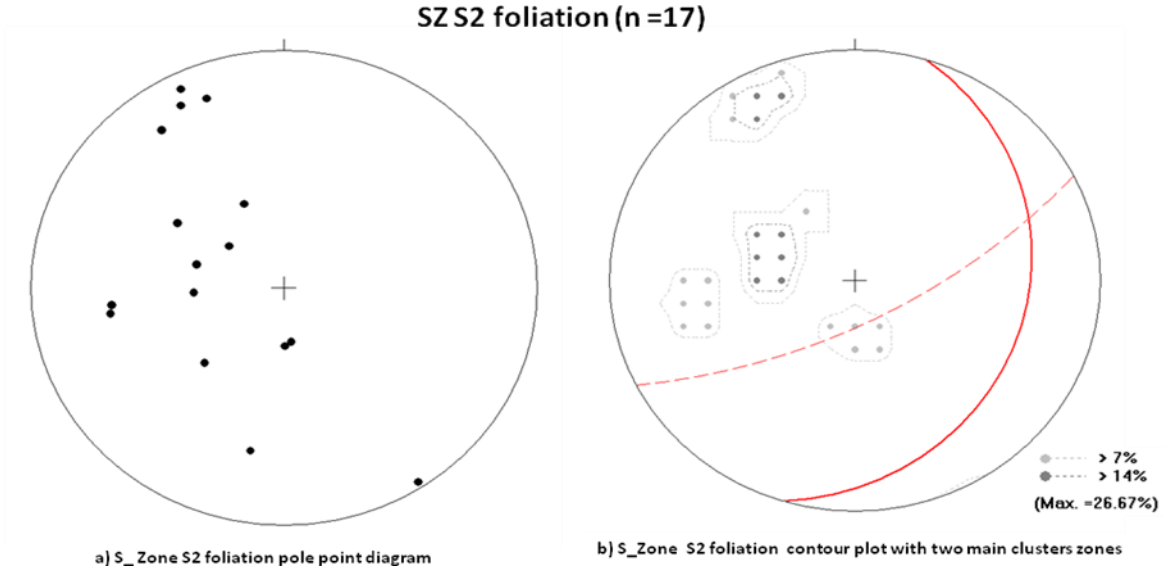

Figure 3.4.23: S_Zone S_2: (a) pole points diagram with variable distribution pattern and possible best fit girdle circle of NNW-SSE strike; (b) contour plot with two main clusters orientation of S_2 data.

3.4.4.4 SZ_Fault

Fault poles point diagram shows variable distribution in S_Zone (figure 3.4.24a). The great circle plot (figure 3.4.24b) shows five of seven faults strike NW-SE and dip steeply either NE or SW. Two other faults are oriented at high angle to them, either striking ENE-WSW or dipping moderately SE.

Principal orientation of SZ fault represents the average orientation calculated from the five NW-SE striking faults, which is steeper with NE-dip direction of **049/89** (figure 3.4.24b).

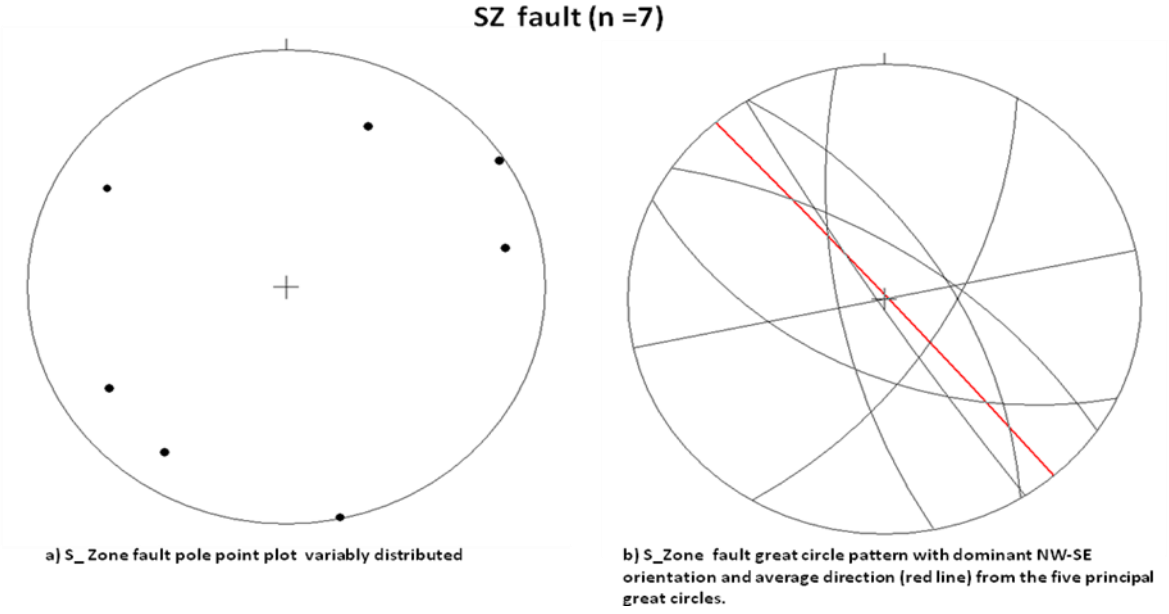

Figure 3.4.24: S_Zone fault: (a) pole point diagram variably distributed; (b) dominant NW-SE great circles indicating the preferred direction in average.

3.4.4.5 SZ_Veins

Veins readings of S_Zone combine all vein types (extensional, shear, oblique, quartz-carbonate and quartz-chlorite veins).

Here again, the stereonet shows poles to veins randomly distributed with high density area clearly distinguished and located in the northwestern sector (figure 3.4.25a). On the contour plot (figure 3.4.25b) the majority vein data fall within the 16% contour line. The average orientation of vein in the S-Zone corresponds to the average orientation for the >16% cluster in the NW; which steeply dips to the south-east at **147/74**.

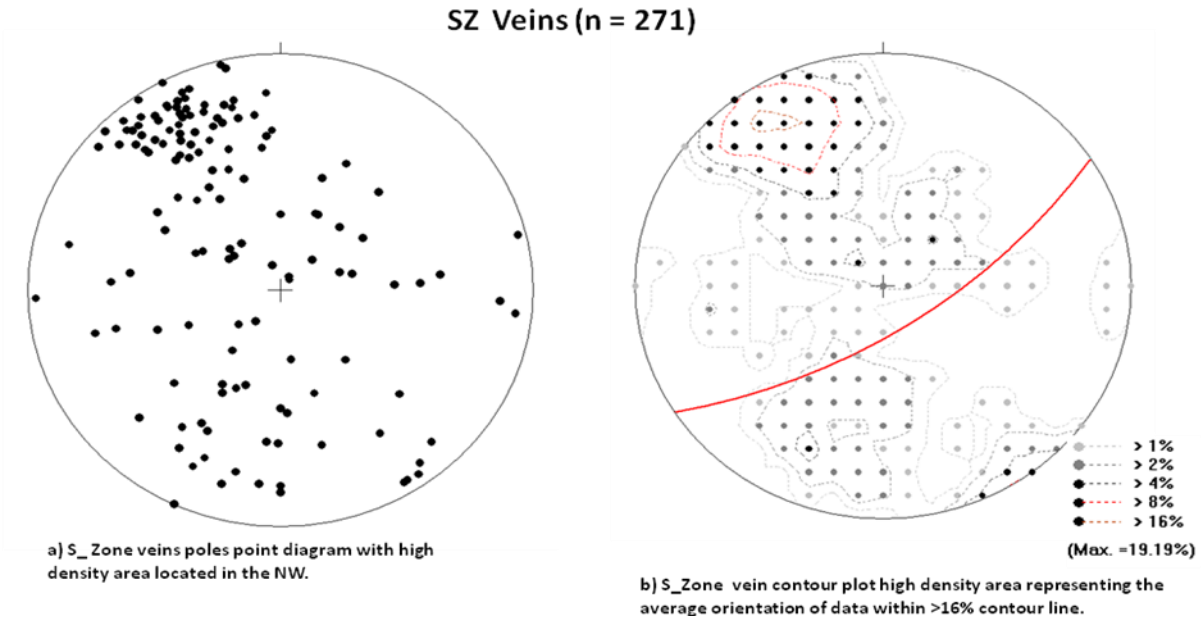

Figure 3.4.25: S_Zone veins: (a) vein poles diagram randomly distributed with high density area in the NW; (b) contour plot showing the average orientation of data located within the high density area (>16% contour line).

3.4.4.6 Structural relationships in the South Zone

Geometrical relationship of structures in S_Zone (figure 3.4.26) was established from the detailed stereonet analysis and base on the principal and average orientations of maximum data clusters. Thus, it can be concluded that:

(i) Average orientations of S_o, S_2 and intrusive contact are parallel to sub-parallel and dip at moderate angle to ENE or to ESE;

(ii) Average S_1 intersects S_o, S_2 and contact at slightly oblique angle and strike WNW to ESE;

(iii) Average vein main cluster orientation and secondary S_2 are all steeper and perpendicular to other features, and SE-dipping;

(iv) Fault main cluster average orientation is vertical and intersects all other features at high angle;

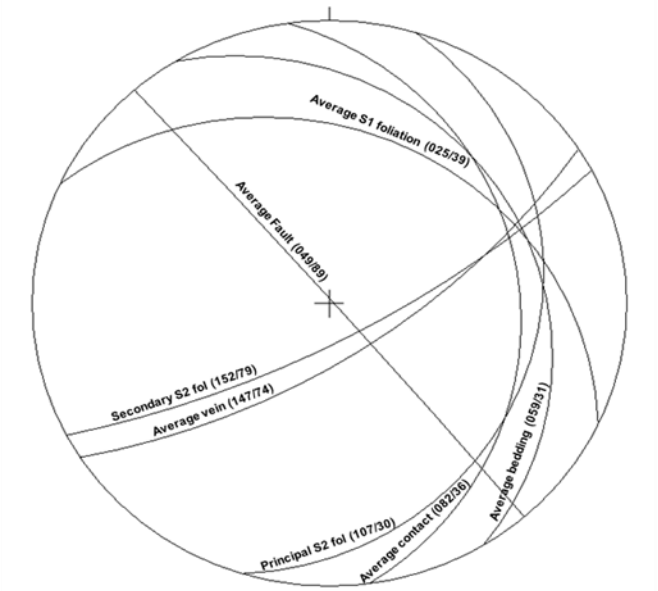

Figure 3.4.26: S_Zone structures relationship showing the two dominant NW-SE and NE-SW strikes of major structures orientations.

In summary, stereonet analysis of S_Zone structures data has identified two major directions:

(i) NE-SW structures group composed of average vein and secondary S_2;

(ii) NW-SE structures comprising average S_o, average S_1, average intrusive contact and average fault.

3.5 Bedding data assessment and 3d interpolation

Software-based 3d analysis of S_o orientations contextualized S_o orientations along individual bore holes and associates such interpretations with corresponding analyses from neighboring drill holes. This allows the interpretation and identification of macro-structures in a particular zone.

S_o dip angles were projected across drill sections using the Leapfrog 3d software trial version 2.0.2. The 3d model was adjusted in reference to the plane that is parallel to the mineralized body. This technique has permitted to confirm if there is any fold, whether, the mineralized zone corresponds to the axial plane of the presumed fold.

In the North-East Zone, no best fitted great circle was identified during stereonet analysis (cf. figure 3.4.1). S_o dip projection on drill section (figure 3.5.1) shows dominant moderate dip angle around 30°.

The software interprets the S_o orientation as associated with complex convoluted folds with large thin-shaped limbs (figure 3.5.2), which do not appear to be compatible with commonly seen fold geometries. The programmed algorithms cause such interpretations but these do not necessarily reflect the true structural geometry. However, besides the artefacts that may be contained in Figure 3.5.2 the complexity of convoluted folds and fold interference may qualitatively describe the nature of the structures in the NEZ.

S_o dip interpolation (figure 3.5.2) shows two principal basin structures (light-blue and orange surfaces) and some dome structures (small green and orange surfaces). Basin-dome structures present an oval shape and mainly strike NW-SE, parallel to the projection plane and the mineralized body. Mineralization occurs in general at the edge of basin-dome features.

S_o dip projection on section does not show a preferred direction (figure 3.5.3). This corresponds to the stereonet showing the North-West Zone S_o data (cf. figure 3.4.8) with five orientation orders.

Like in the North-East Zone, stereonet showing S_o pole point distribution of North-West Zone does not show any best fitted great circle.

Despites, the 3d interpolation of S_o orientations interprets synformal and open antiformal structures (figure 3.5.4) with SE plunging hinge lines and steeply SE dipping axial surfaces. This interpretation is not obviously in the stereonet (figure 3.4.8), possibly due to the variability of orientation data that the software did not use for interpretation. Here, some spread mineralized intervals occurs along the axial plane of the presumed folds.

S_o data projection on section in the Central zone (figure 3.5.5) also shows variable orientation.

The 3d interpolation of S_o dip data of Central Zone (figure 3.5.6) presents dome structures (small green and orange forms). The general trend of the modelled shape describes a possible antiform or lenses. Like in the North-West Zone, Central Zone might suggest an interference of two or more fold generations with some local dome structures.

The stereonet analysis of South Zone S_o data recognized a best fitting great circle pattern, which suggests the presence of more or less cylindrical folds. Projection of S_o dip data shows regular orientations (figure 3.5.7). The 3d projection plane is parallel to mineralized body.

The interpolation of S_o data in 3d shows complex NE-SW trending folds possibly formed by two generations (?) with few and isolated basin-dome features (figure 3.5.8). The 3d model of S_o dip angle also shows that mineralization occurs in the axial plane of the presumed fold.

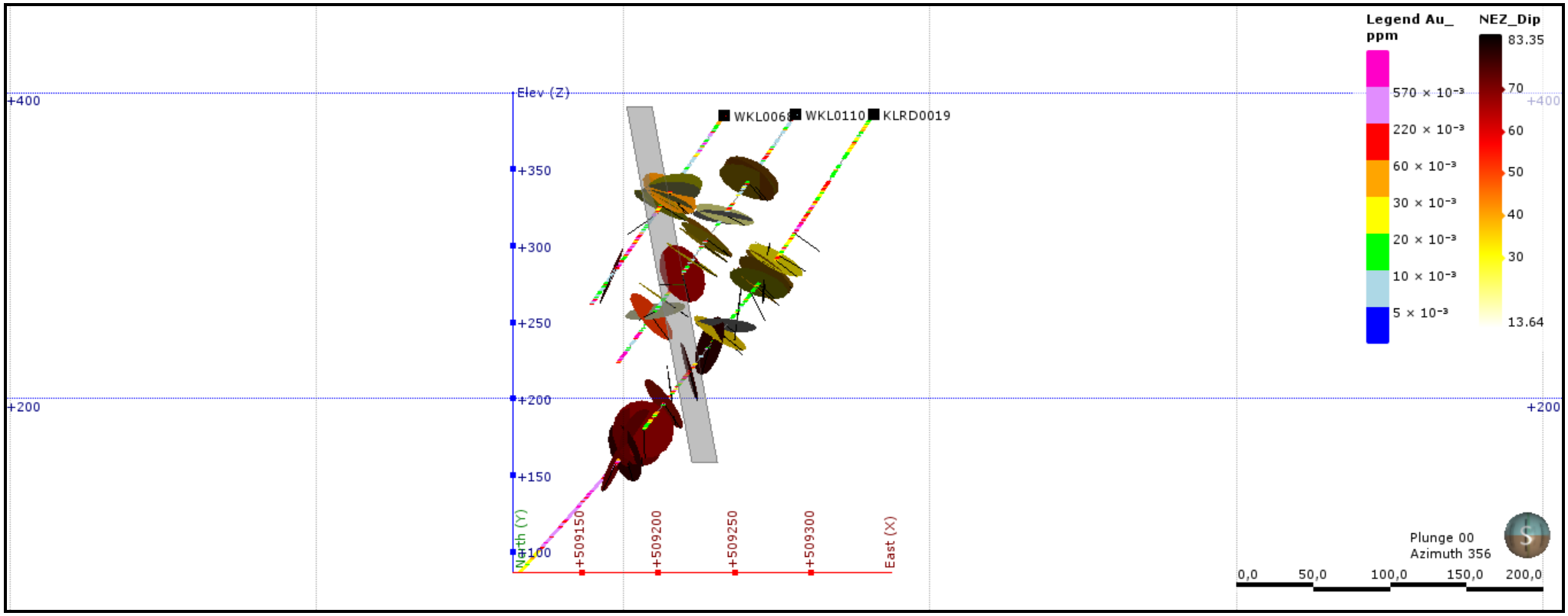

Figure 3.5.1: Dip of So across NEZ drill line, showing the majority of So moderately dipping to the SE.

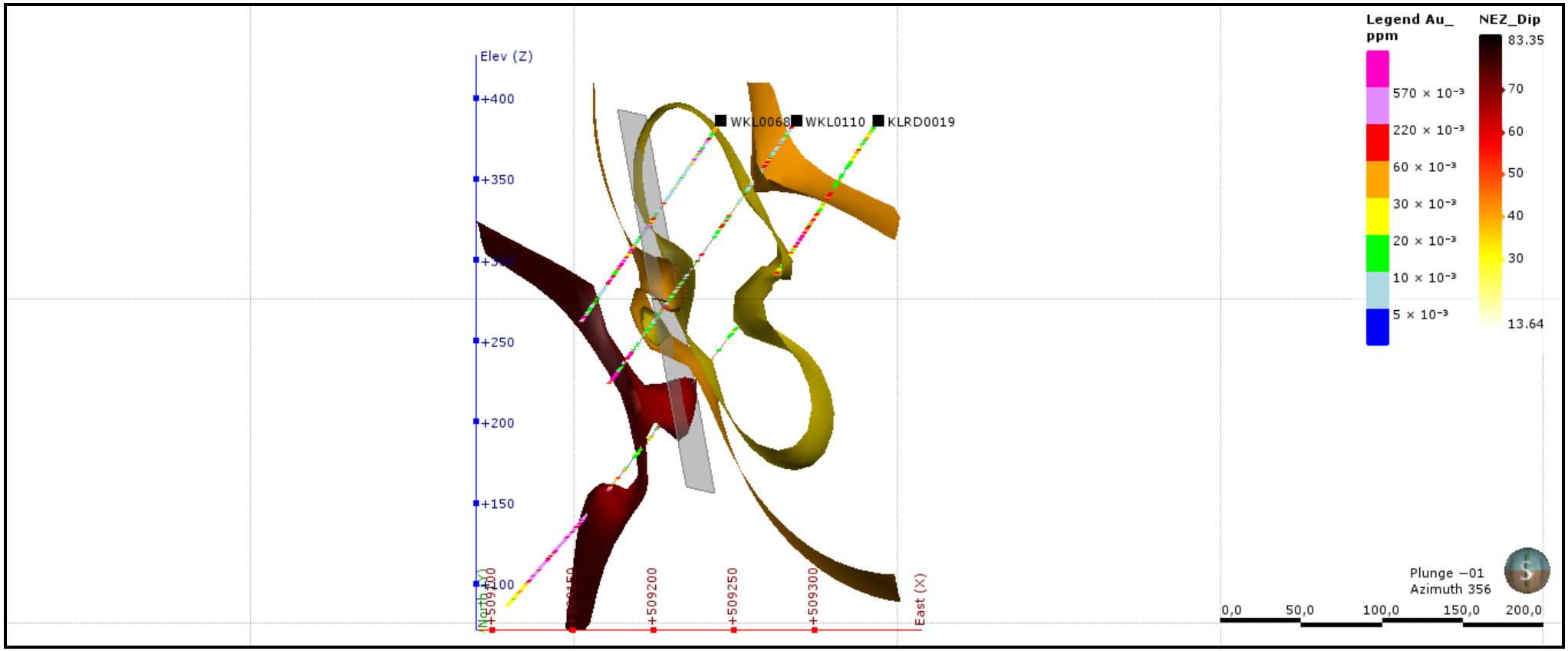

Figure 3.5.2: NEZ S_o dip 3d interpolation showing basin-dome features (interference of fold) with oval shape mainly striking NW-SE.

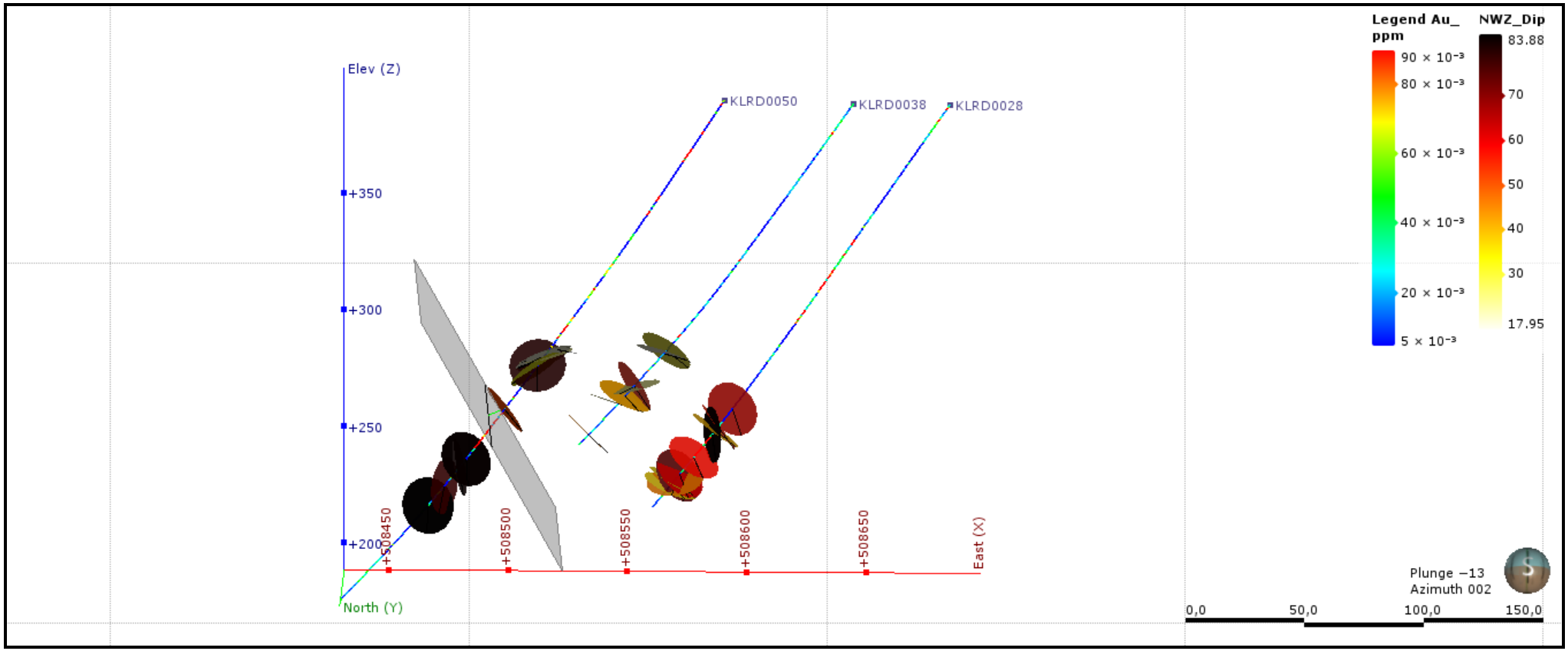

Figure 3.5.3: NWZ S_o dip data with variable directions as shown on the corresponding pole points diagram.

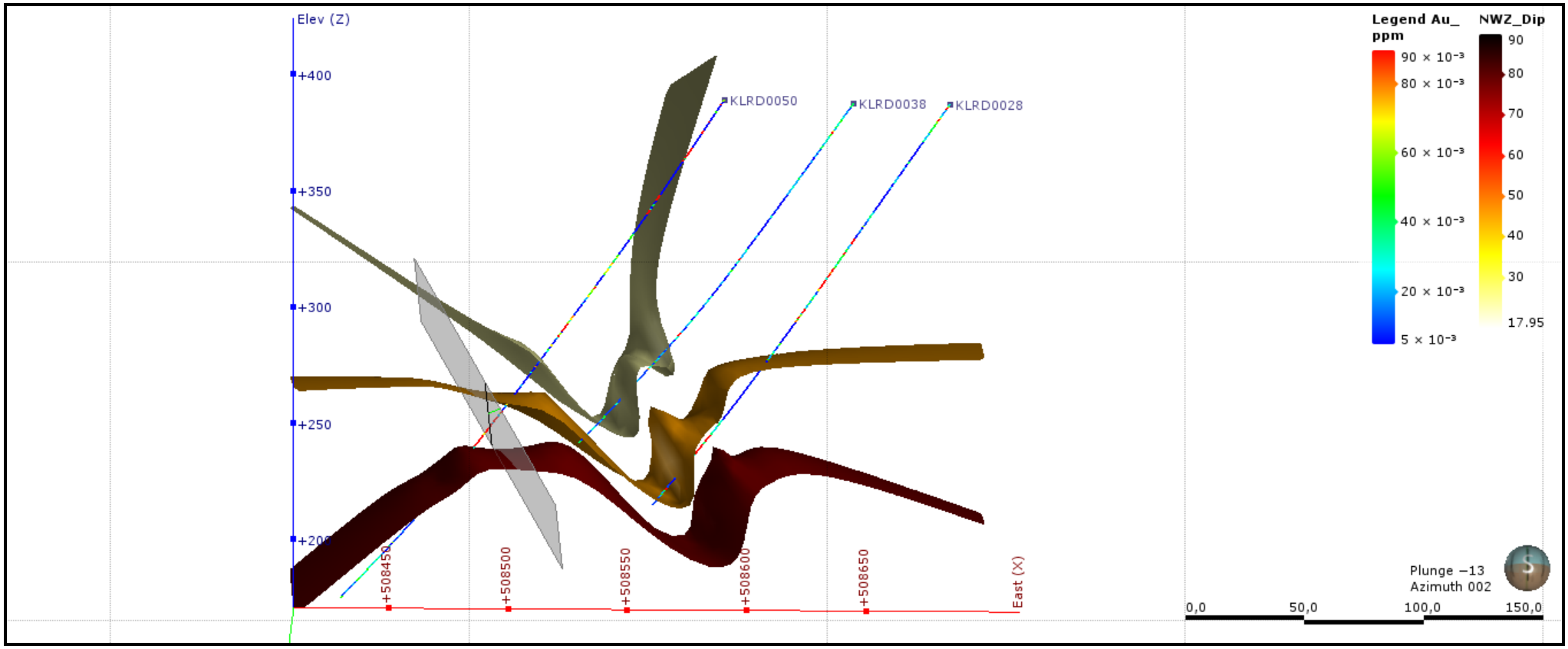

Figure 3.5.4: 3d interpolation of North-West Zone So plunge suggesting the presence of syncline or fold interference.

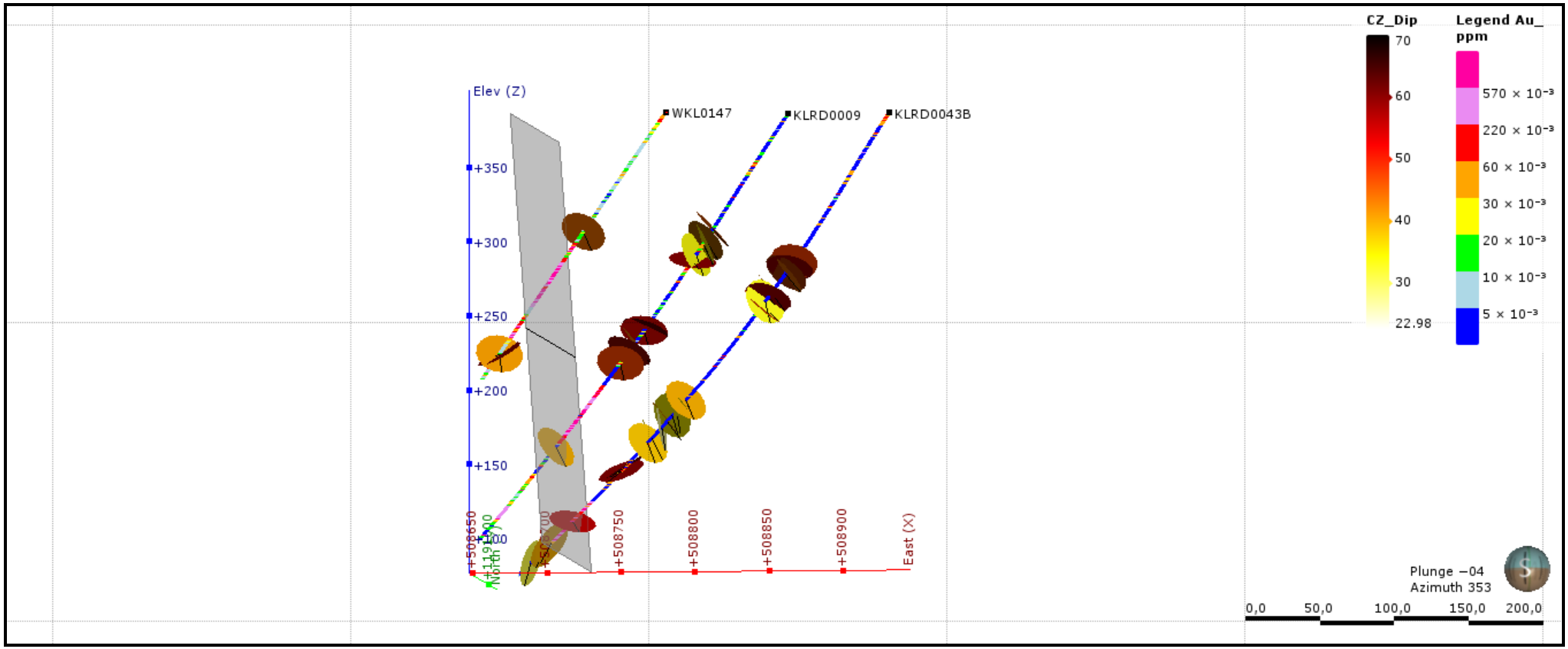

Figure 3.5.5: CZ S_o dip data with variable directions as shown on the corresponding pole points diagram.

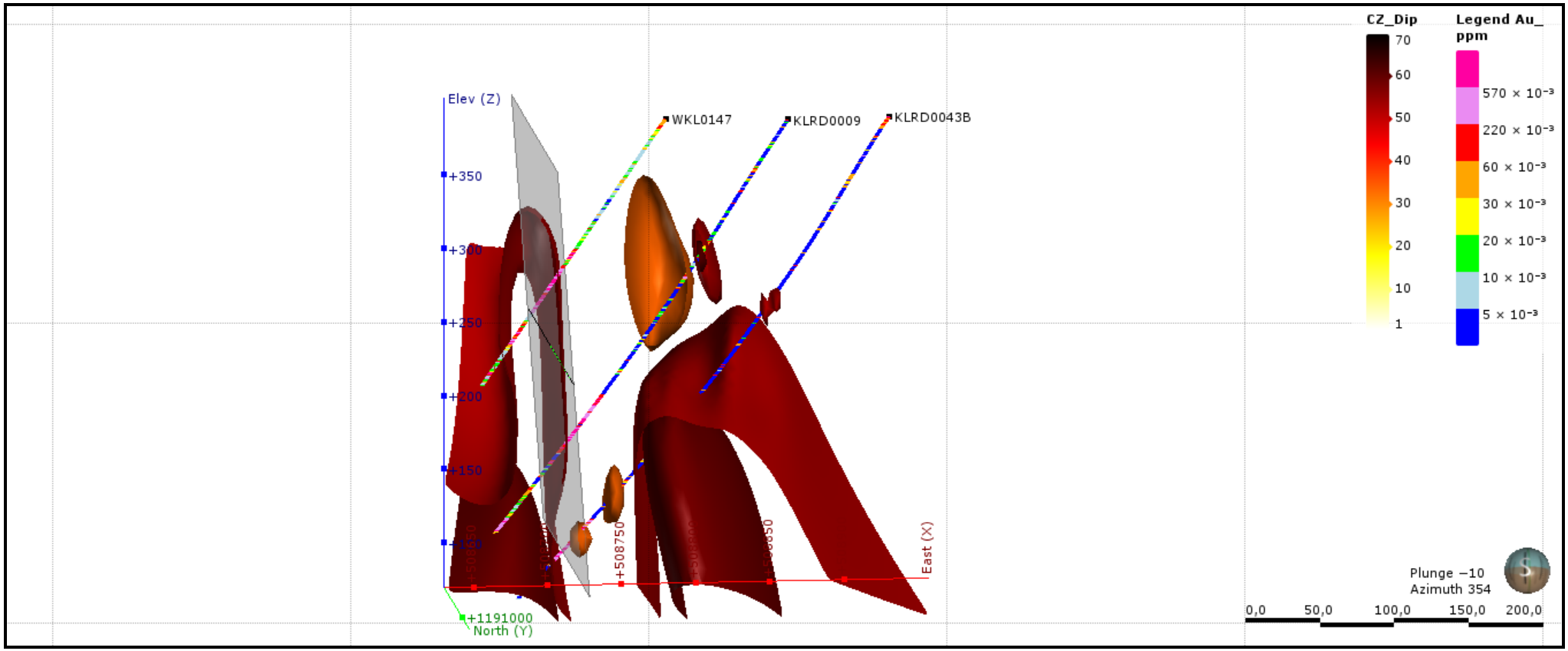

Figure 3.5.6: S_o 3d interpolation in Central Zone and resulted interference fold pattern.

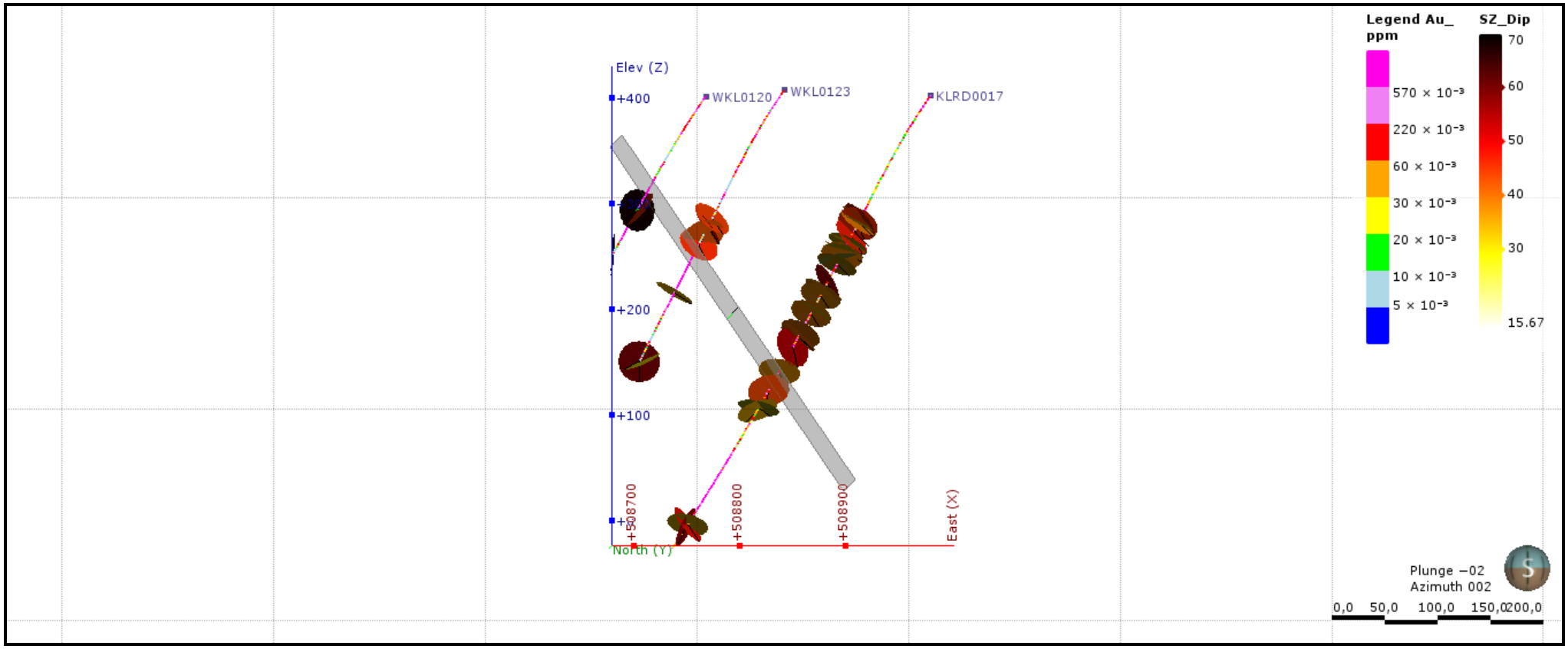

Figure 3.5.7: SZ So projection on drill section with regular S_o orientations and the 3d plane oriented parallel to the orebody.

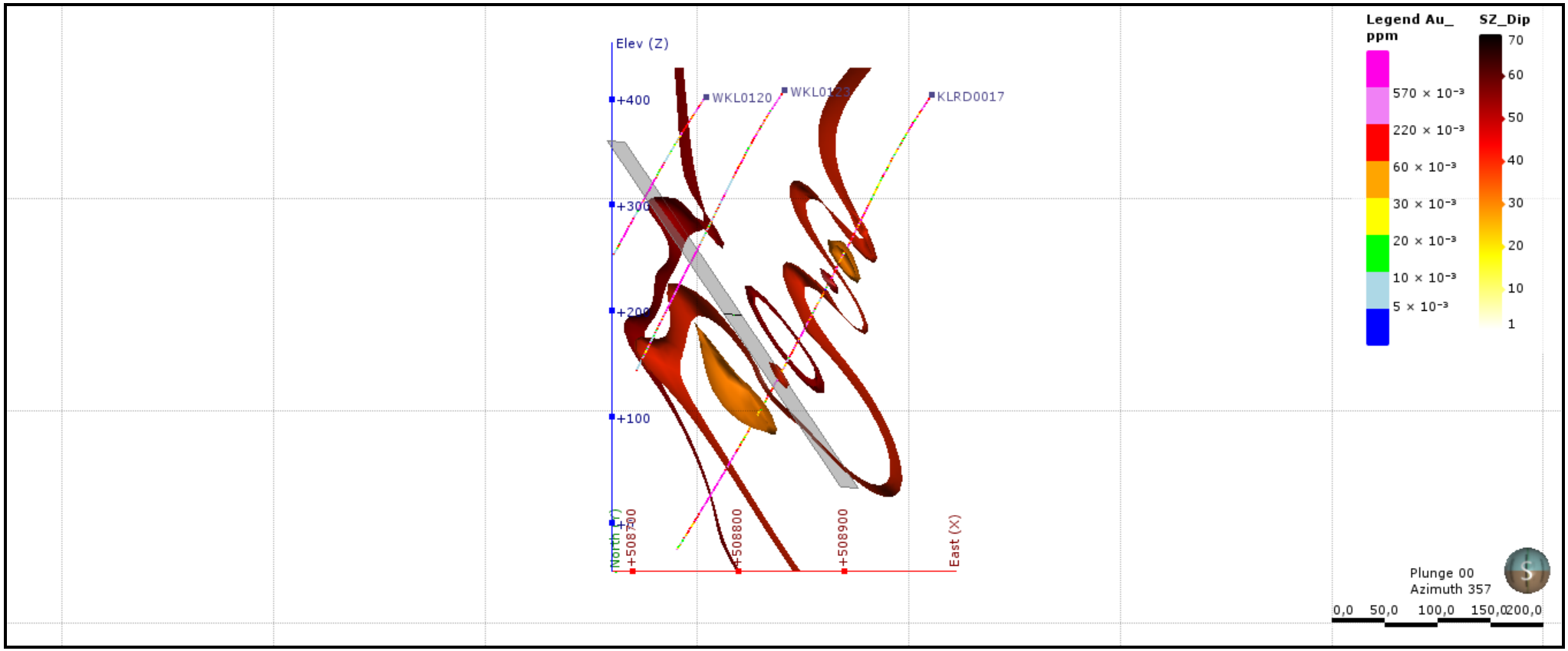

Figure 3.5.8: South Zone So 3d interpolation describing possible two generations of fold with mineralized body located at the axial plane of the presumed fold.

The axial surface (AS) orientation is determined from stereonet data by plotting of S_o readings representing the presumed fold pattern and the construction of the hinge line (HL) of the fold using the π-pole method. The determination of the nature of the fold referred to the commonly used classification scheme devised by Fleuty (1964) that classifies folds using the plunge of hinge lines and dip of axial surfaces.

Statistical analysis of S_o data was undertaken using the stereo32 software unregistered version 1.0.3. The procedure consists of the definition of main clusters point of S_o data that may represent the limbs of fold (cluster analysis technique). The great circle connecting the cluster centres is the π circle, the pole to which the π-pole plots at the same position like the hinge line of the fold at **036/26**. The interpolation of S_o planes in fig. 3.5.9 suggests a tight fold type. Therefore the pole to the AS was placed in the same acute angle between the two limb clusters producing a NE-dipping AS at **059/28**, on which of course also the hinge line plots (figure 3.5.9).

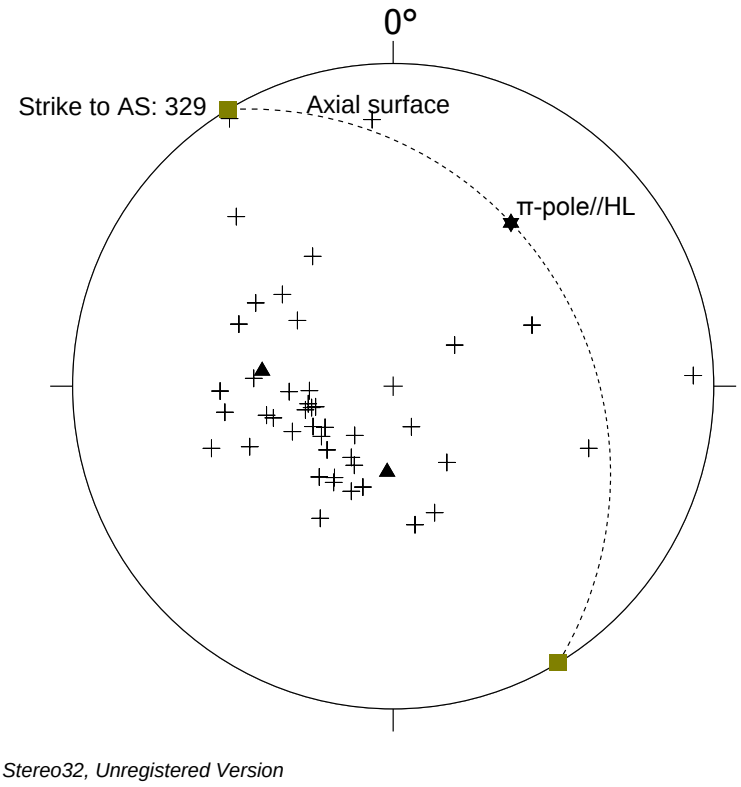

Figure 3.5.9: Determination of parameters of South Zone fold.

With the plunge of the hinge line of **26^0** and the dip of the axial surface of **28^0**; the South Zone fold is classified as a gently plunging and moderately inclined fold (figure 3.5.9).

The interlimb angle of the mentioned fold corresponds with the difference between the two main clusters. With Limb1 = 277/45 and Limb2 = 184/60; the interlimb angle is **93^o.** According to the interlimb angle, the South fold is classified as an open fold.

The normal direction to AS of the mentioned fold is **239/62** (figure 3.5.10). Since the mineralization occurs in the axial plane of the South Zone fold, the best drilling direction in South Zone should follow an azimuth of **N239**^{0} and plunge at **62^0**.

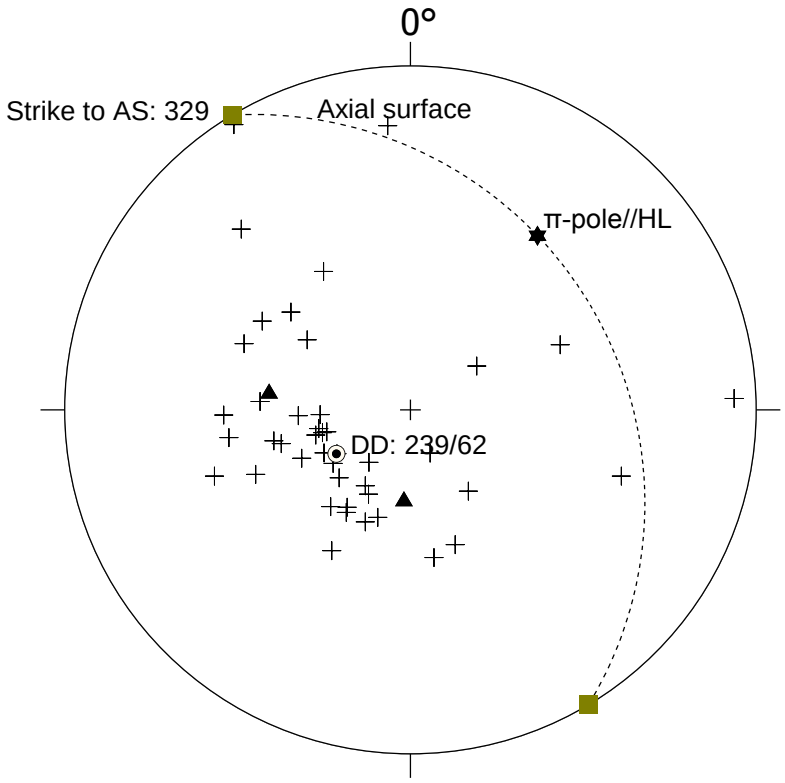

Stereo32, Unregistered Version

Figure 3.5.10: Parameters of fold and best drilling orientation in South zone.

CHAPTER 4 : DISCUSSION

Detailed stereonet analysis of structural data from designated zones of the Koulekoun Gold deposit characterized different types of structures in each zone and their relationship to each other were carried out in order to evaluate the possible structural control of gold mineralization. Despite the large variability in orientation of most structure types, this section will make an attempt to summarize the nature and geometry of the structural inventory.

4.1 *Principal structures orientations: relationships, similarities and differences*

The stereonet shows approximate principal S_o orientations of each structural domain (figure 4.1.1). The orientations reveal N, NE, E and SE dip directions and hence a large spectrum of orientations. This suggests complex and probably polyphase rotations of the once horizontal S_o planes. A typical structural pattern that produces such large variability in S_o orientation is polyphase non-coaxial folding and fold interference or sheath folding. Further evaluation of the S_o orientations follows below (section 4.2).

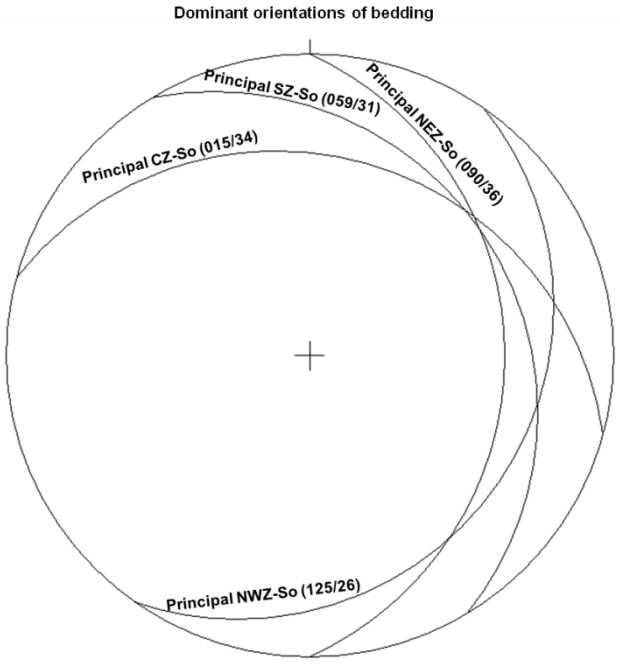

Figure 4.1.1: Dominant orientations of S_o showing their strike to N-S, NE-SW and NW-SE.

The stereonet presenting intrusive contact orientations (figure 4.1.2) shows sub-parallel relationship between North-East, North-West and Central Zones approximate contact principal orientations. Intrusive bodies are moderately dipping to the SE in general, except in the North-East Zone where they are sub-vertical. Crosscutting relationships also show that intrusive bodies are normally at high angle to S_o in North-East, North-West and Central Zones but are sub-parallel to the S_o in South Zone.

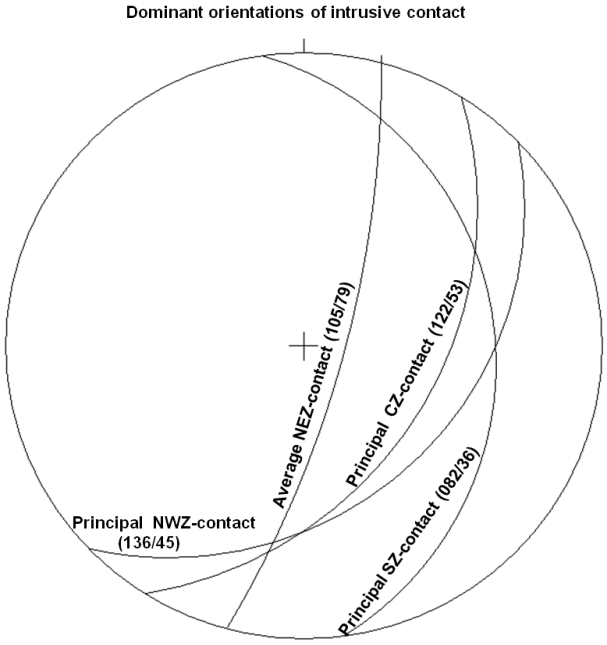

Figure 4.1.2: Principal orientations of steep to moderately E to SE dipping intrusive contacts.

Fault orientations are highly variable and dip respectively to S, SE, NW and NE (figure 4.1.3). The stereonet also shows that fault and intrusive contact are parallel in Central Zone.

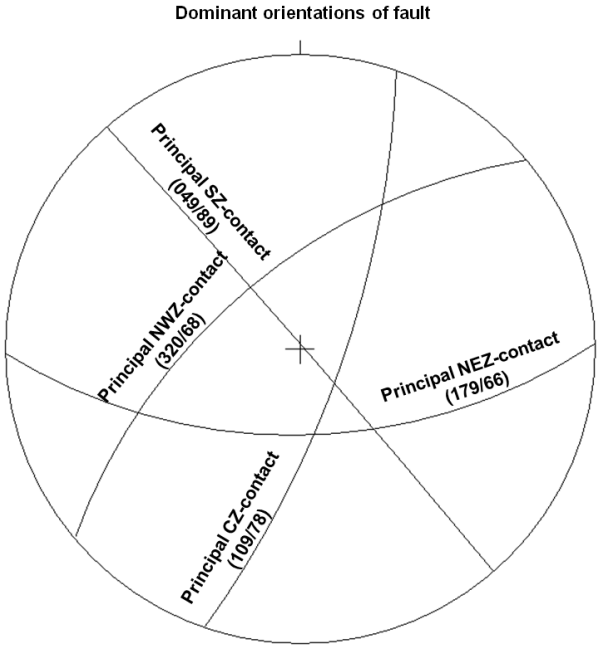

Figure 4.1.3: Dominant orientations of fault mainly striking to NE-SW, NW-SE and E-W.

Detailed vein orientation stereonets previously described (section 3.4) show highly variable directions and numerous vein orientation orders; which suggests stockworks pattern of polyphase vein formation in differently oriented stress fields. The geometrical relationships of vein approximate principal orientations (figure 4.1.4) show dominant SE-dip direction. It appears that the veins main directions are parallel to intrusive contacts. Although, vein in North-East and South Zones are steep is majority; while veins in Central and North-West Zones are moderate in general.

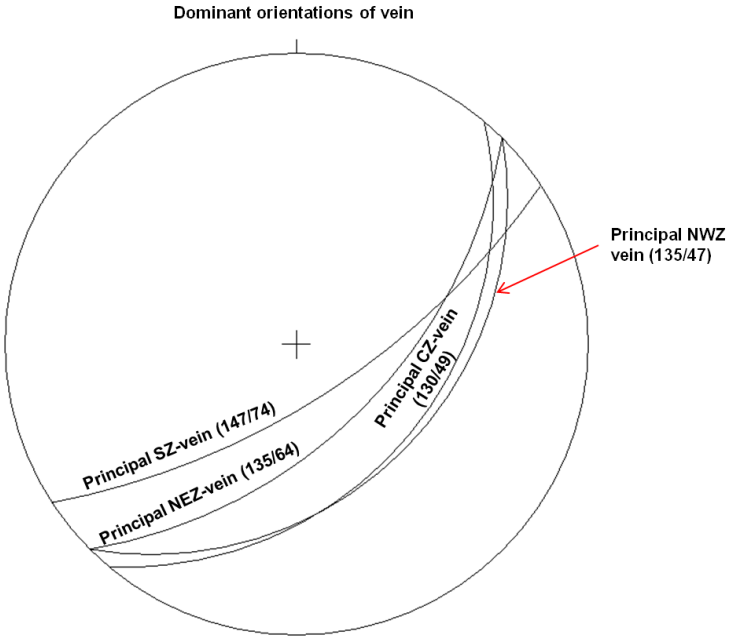

Figure 4.1.4: Dominant orientations of vein with their common NE-SW strike.

4.2 *Bedding 3d interpretation and evidence of folding*

The 3d analysis of S_o data in section 3.5 has led to the interpretation and identification of macro-structures in each zone.

It has been demonstrated that the 3d model of S_o data in the North-East Zone supports the presence of complex convoluted folds and fold interference (figure 4.2.1). The software algorithms may have affected the unusual geometry of fold which unlikely was not indentified on stereonet.

In the North-West Zone (figure 4.2.2), the 3d interpolation of S_o orientations shows the presence of synformal and open antiformal structures. Again, this interpretation is not obvious from stereonet analysis.

The dominant trend of modelled shapes of Central Zone S_o data (figure 4.2.3) shows possible antiforms or lenses. Like in the North-West Zone, S_o patterns in the Central Zone might also suggest an interference of two or more fold generations with some local dome structures.

The stereonet analysis of S_o data in the South Zone has recognized more or less cylindrical folds (figure 4.2.4). The 3d interpolation of S_o readings shows complex fold systems formed by two generations associated with some isolated basin-dome structures.

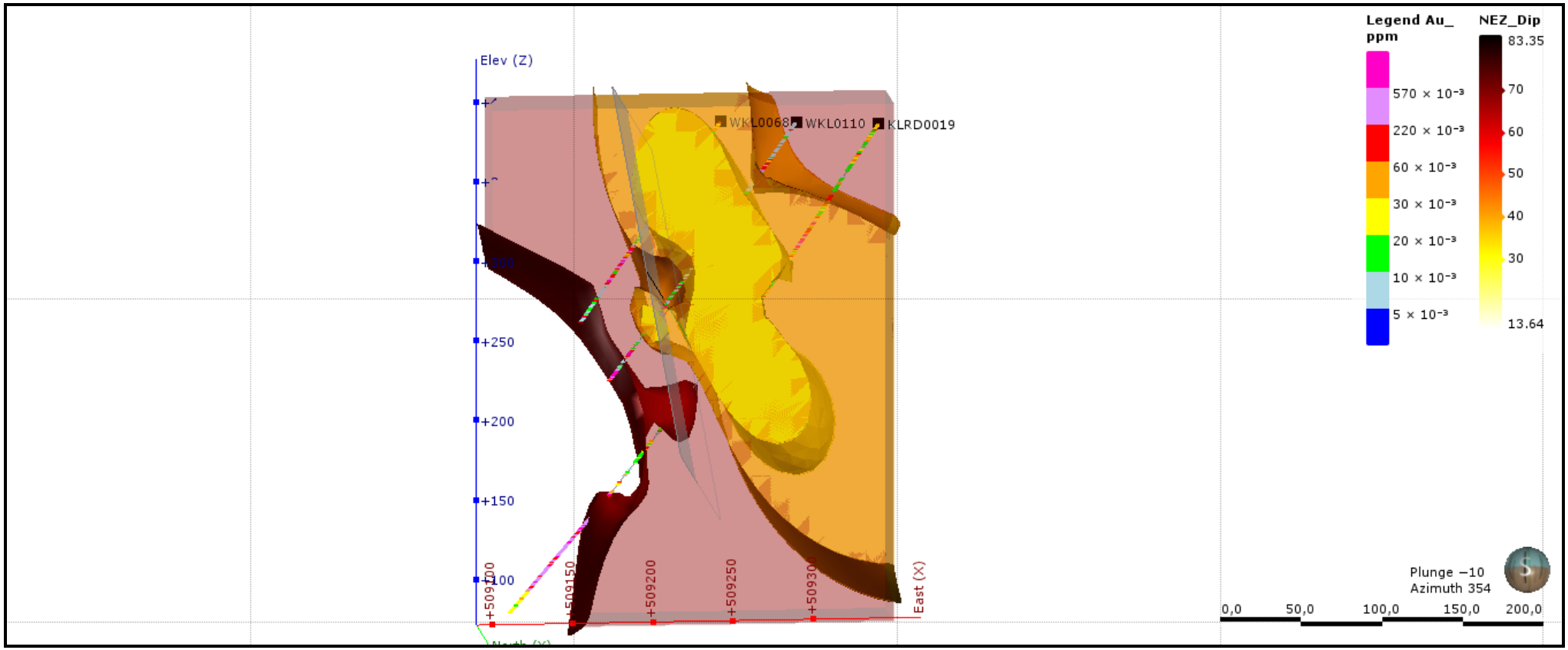

Figure 4.2.1: 3d model of NEZ So showing the possible convoluted folds and fold interference pattern.

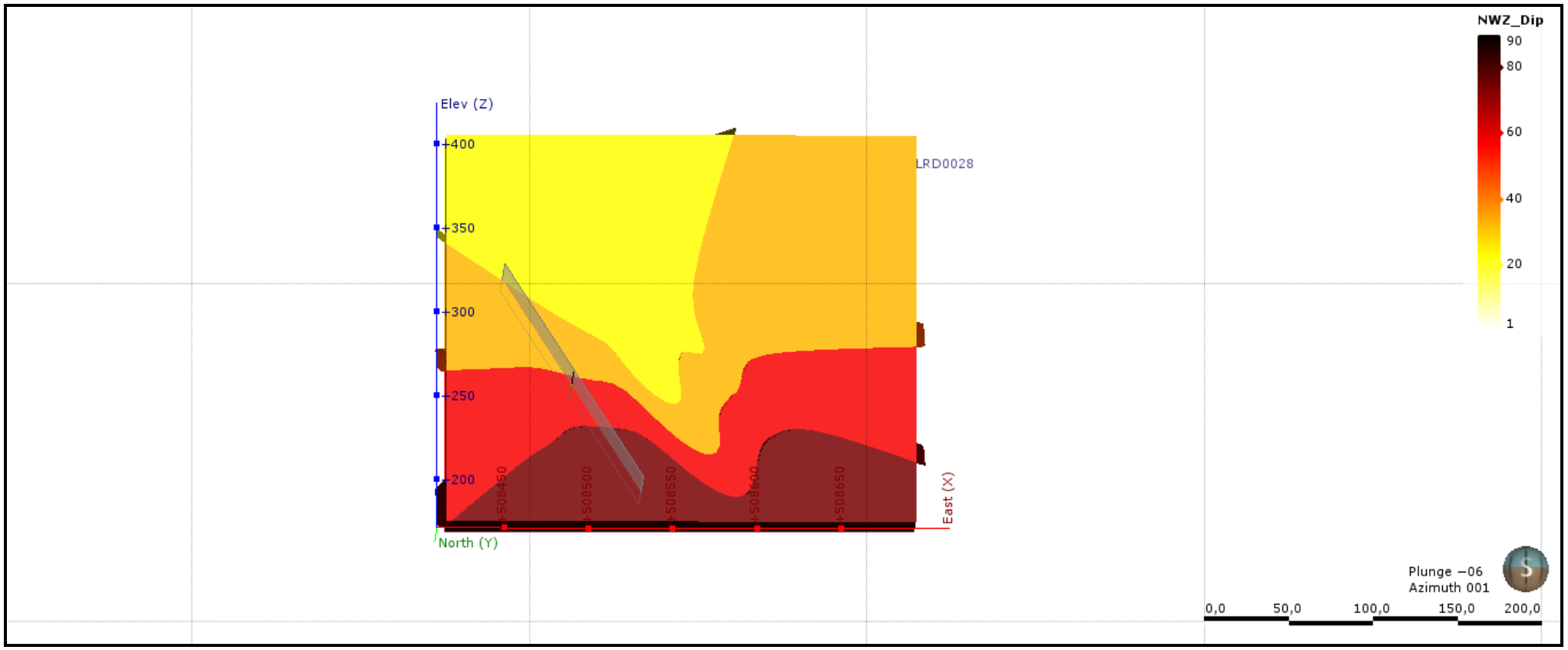

Figure 4.2.2: 3d model of NWZ So with synformal and open antiformal structures appearance.

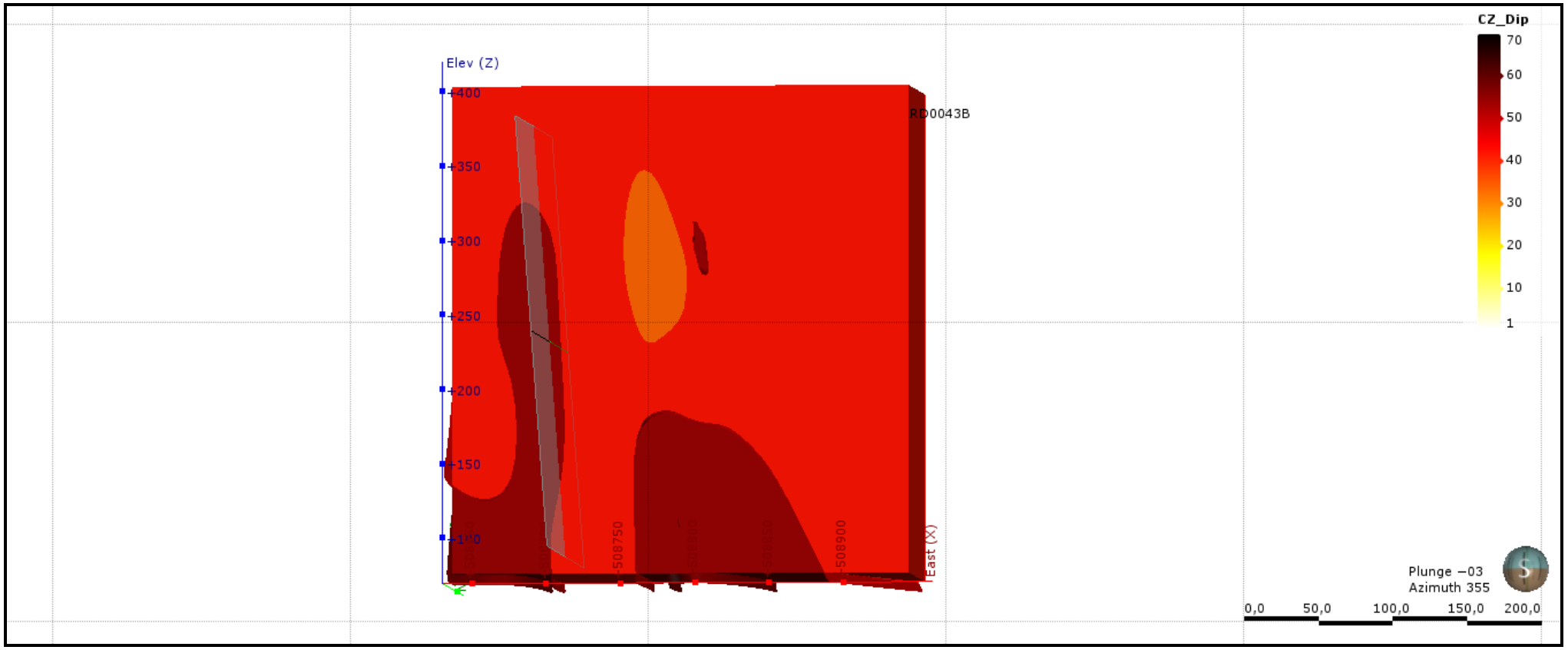

Figure 4.2.3: 3d model of CZ So with possible antiform and interference of several fold generations.

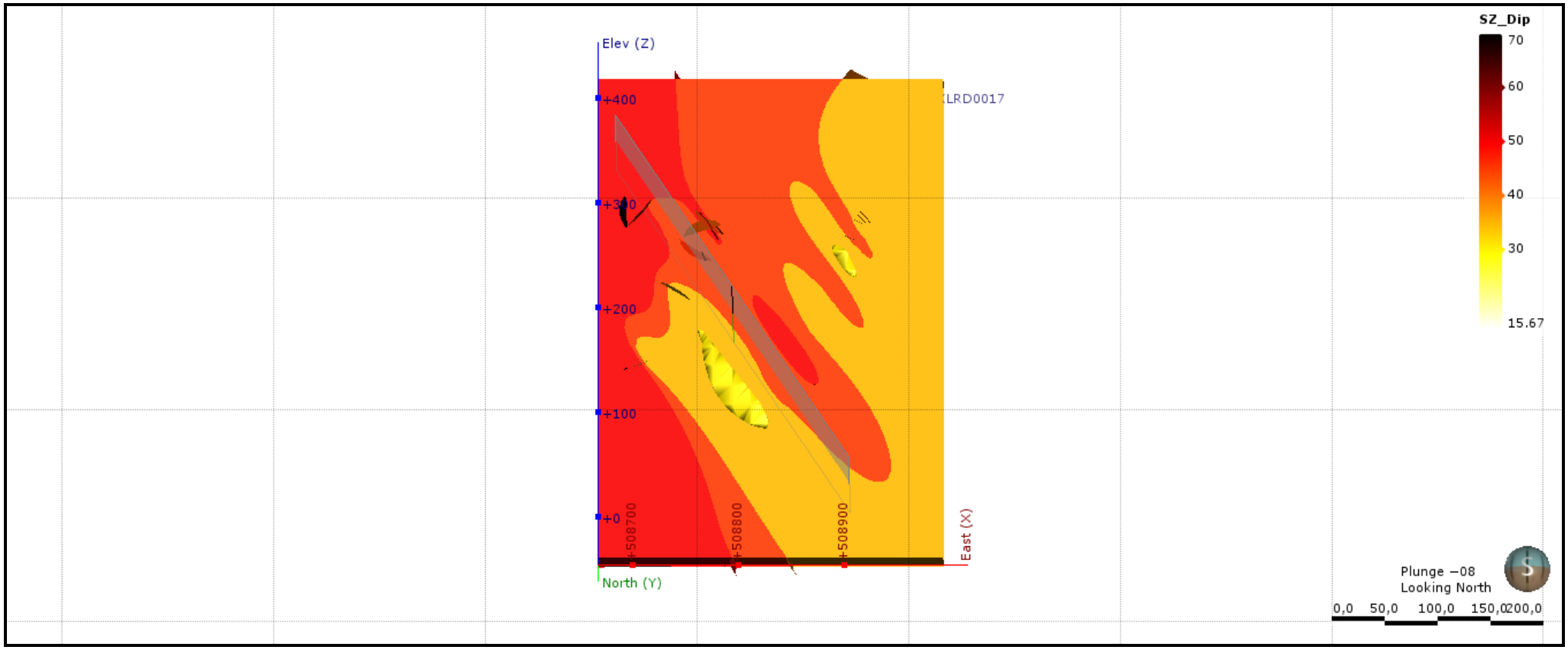

Figure 4.2.4: 3d model of SZ So showing a complex folds system associated with some isolated basin-dome structures.

The statistical analysis of S_o data has determined the plunge of hinge line of 26° and the dip of axial surface of 28°. This classifies the South Zone fold as a gently plunging and moderately inclined fold. With a corresponding interlimb angle of 93°, the presumed fold has been qualified as an open fold. The normal direction to the axial surface of this fold corresponds to the best drilling direction (figure 4.2.5) which could intersects the mineralized body located at the axial surface of the presumed fold at **239/62**.

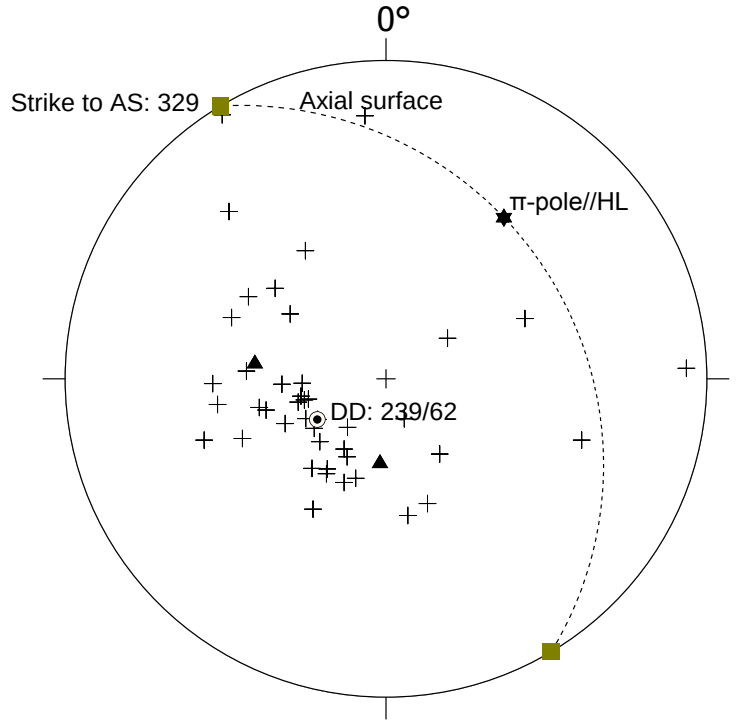

Figure 4.2.5: stereonet showing the orientation of the best drilling direction to intersect the mineralized zone situated at the SZ fold AS.

4.3 *Structure intersections and gold mineralization*

The determination of mineralized intervals and controlling structure intersection zones was conducted after plotting structure dip data across drill holes sections, using the Oasis montaj software version 6.3.0. Observations of drill sections suggest that:

Fault dip angle projections on drill sections of the North-East Zone shows two major directions (figure 4.3.1): (1) The NW-SE striking fault is visibly perpendicular to the drilling direction and parallel to the majority of S_o. (2) The dominant NE-SW fault which is slightly parallel to core axis and oblique to S_o. Each fault generation corresponds to veins orientation group to which they are parallel. Intrusive contacts on drill hole WKL0068@70m and S_2 on drill hole KLRD0019@80m are slightly oblique to core axis.

High gold grades zones (blue dashed delineations) in the North-East Zone are located where fault, veins and intrusive contact intersect (figure 4.3.2). These zones are preferably located within intrusive bodies (dacite cataclasite, dacite microporphyry and dacite porphyry), as seen on figure 4.3.1. Mineralized zones lying at the contacts or within sedimentary units also suggest the hydrothermal origin of gold mineralization.

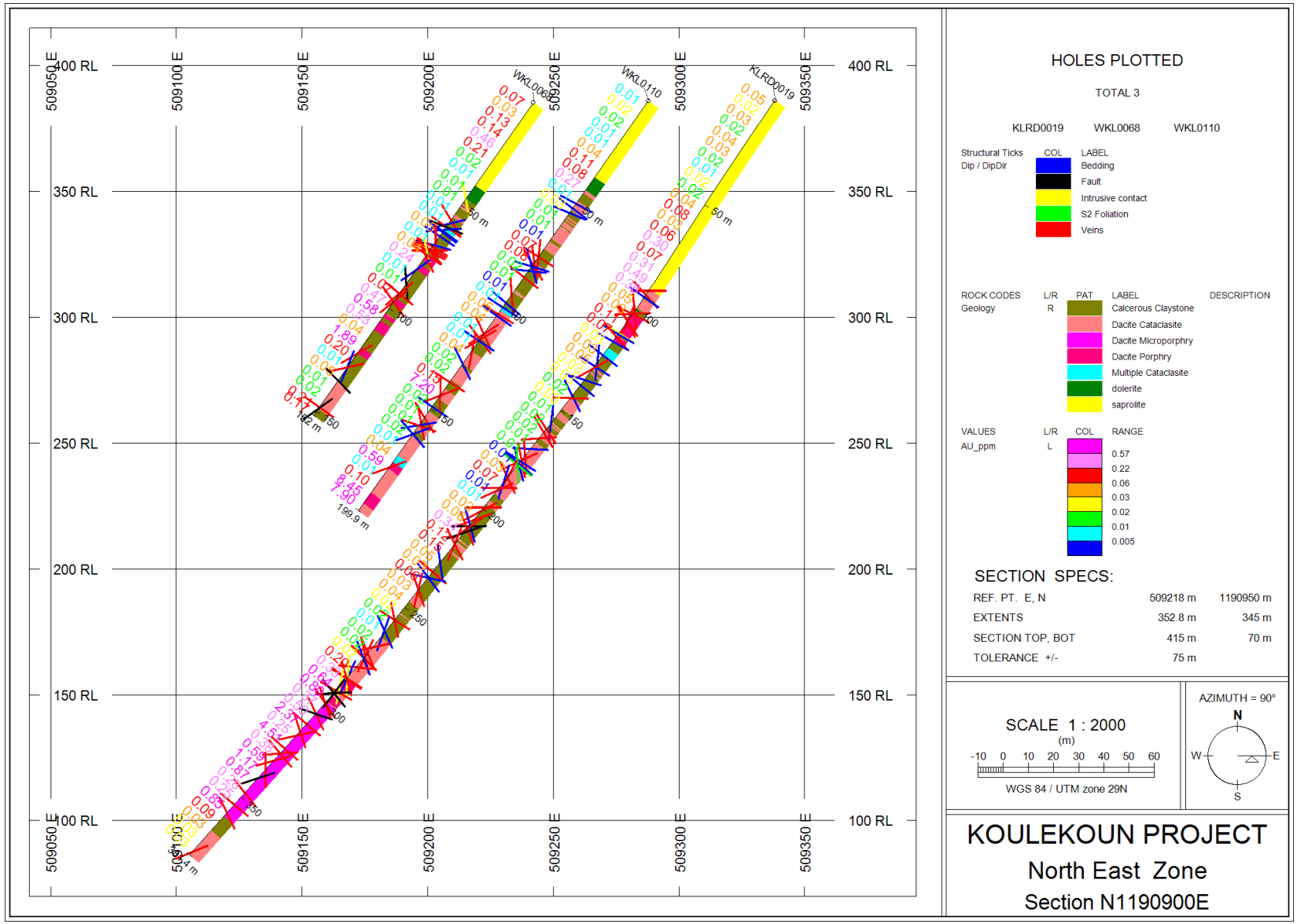

Figure 4.3.1: NE_Zone structures orientations on drill section with principal SE dip of So and crosscutting relation between fault and veins generations.

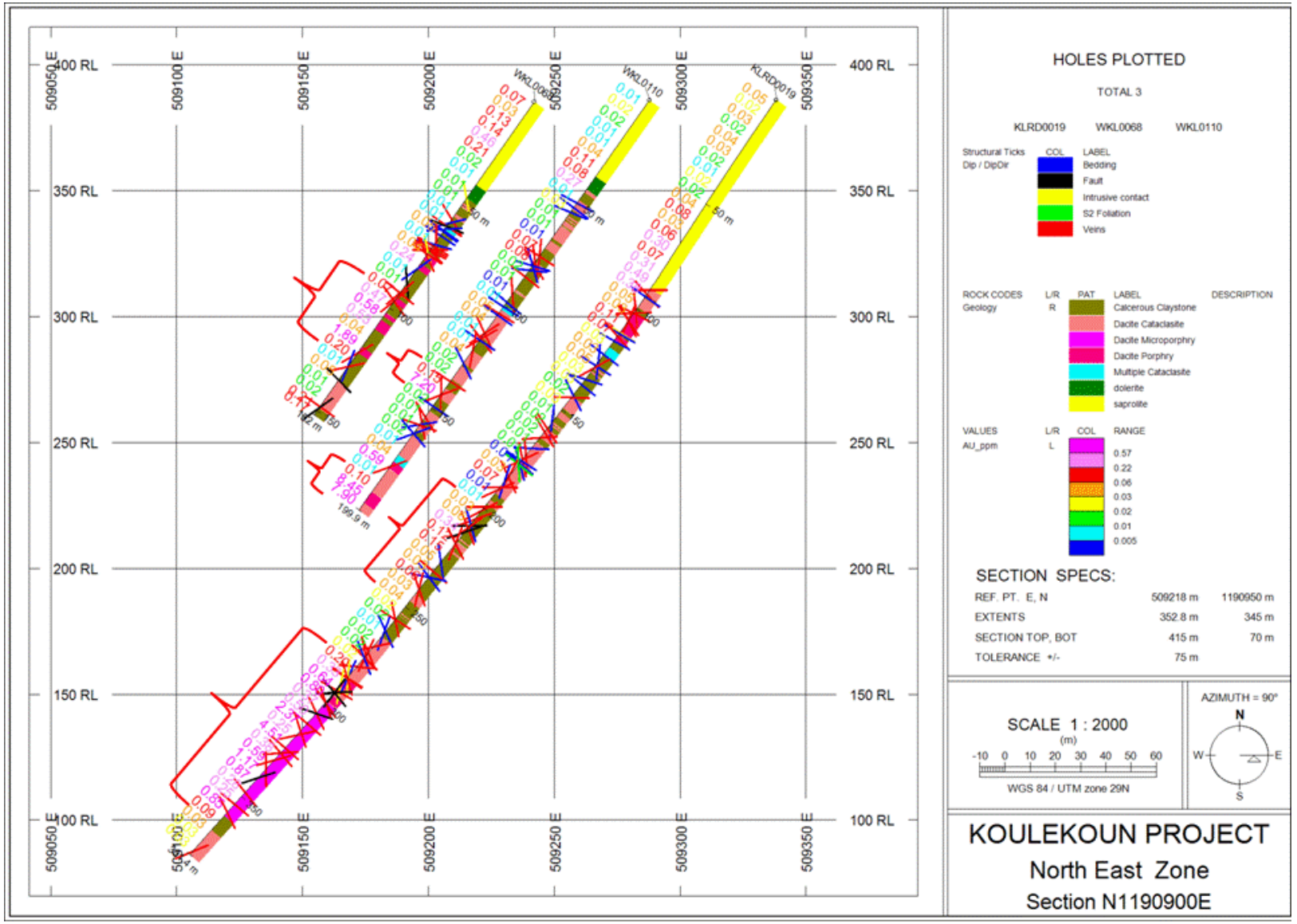

Figure 4.3.2: NE_Zone high grade intervals of gold, mainly related with crosscutting faults and veins generations.

The section of North-West Zone also show the two major fault orientations: (1) the parallel to S_o and perpendicular to core axis fault with NW-SE strike and (2) the sub-parallel to core axis fault at shallow angle. Here, again vein systems are associated with each fault generation. Intrusive contacts and S_2 are parallel to faults (figure 4.3.3).

Like in the North-East Zone, high gold grades intervals in the North-West Zone are located within intrusive bodies and where contacts, faults and veins intersect (figure 4.3.4). It appears again that S_2 are associated with mineralized zone on drill hole KLRD0028@175m.

Contrary to the North-East and North-West Zones, the section plot of Central zone structures shows one principal fault direction which is perpendicular to the core axis and sub-parallel to the S_o with a NW-SE strike (figure 4.3.5). Again, intrusive contacts, veins and S_2 are in many places sub-parallel or parallel to S_o planes.

High gold grade intervals in the Central Zone are preferably associated with intrusions. This is correlated to the intensity of contacts and veins within these zones (figure 4.3.6). Though, no S_2 or faults are present within these mineralized intervals, except at the bottom of the drill hole WKL0147@218m, where two intersected S_2 delineate low to medium gold grades.

Obviously, the drill section of the South Zone shows very deep mineralized intervals as drilling went through the mineralization (figure 4.3.7). Faults are present in two main directions, such as in the North-East and North-West zones. Here, majority of S_o, S_2, contact and veins are perpendicular to core axis.

High grade intervals in the South Zone are present where different generations of veins and contacts intersect (figure 3.4.8). This proves that high grade zones are controlled by magmatic hydrothermal fluids along contacts, additionally to structures. In some rare cases, S_1 is associated with low grade intervals like on drill hole KLRD0017@200m.

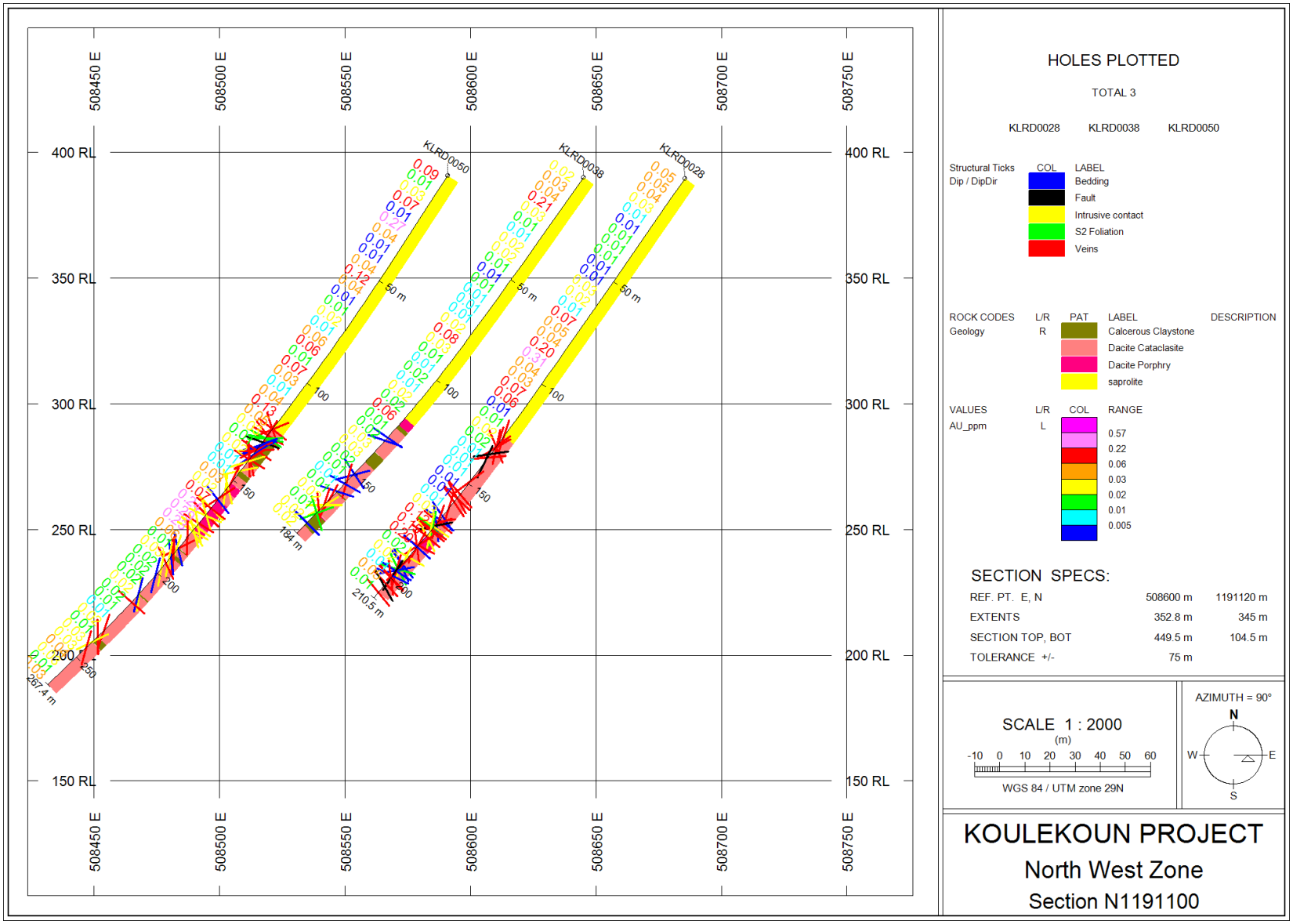

Figure 4.3.3: NW_Zone structures orientations on drill section with principal SE and N-S dip of So and contact; and fault and veins generations intersect.

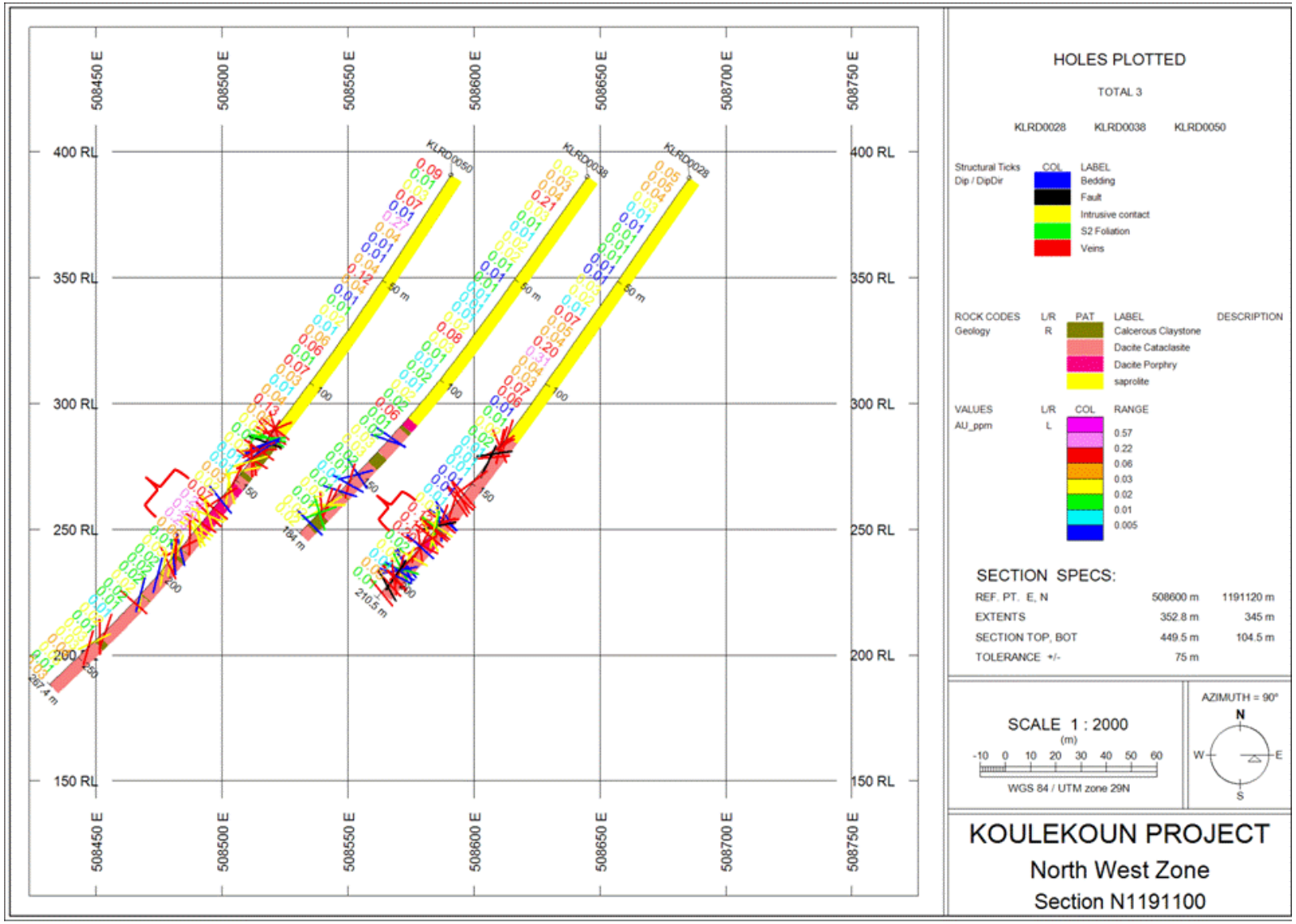

Figure 4.3.4: NE_Zone high grade intervals of gold, mainly related with crosscutting fault, contact and vein generations.

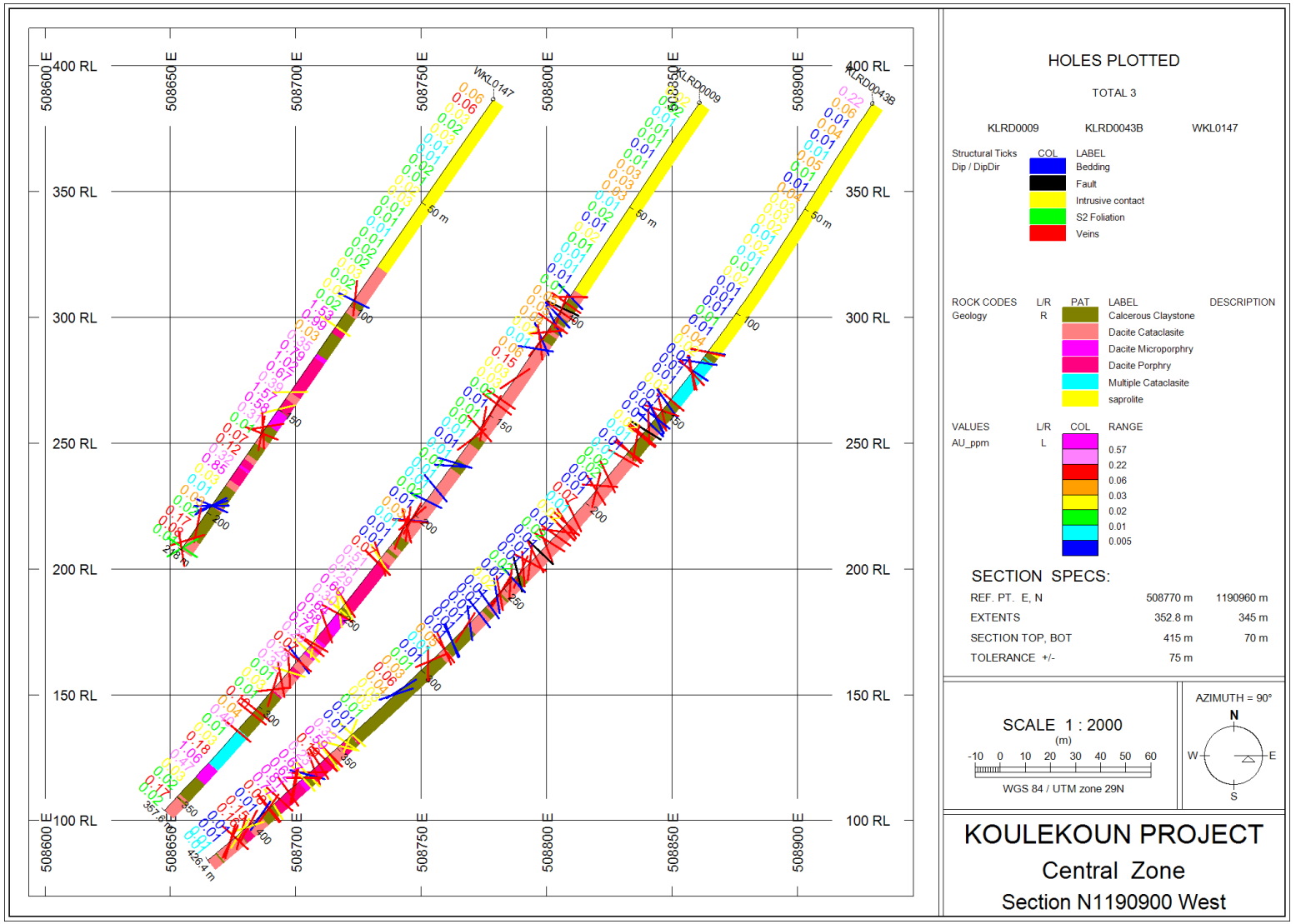

Figure 4.3.5: CZ structures orientations on drill section with principal SE dip of So and crosscutting fault, contact and vein generations**.**

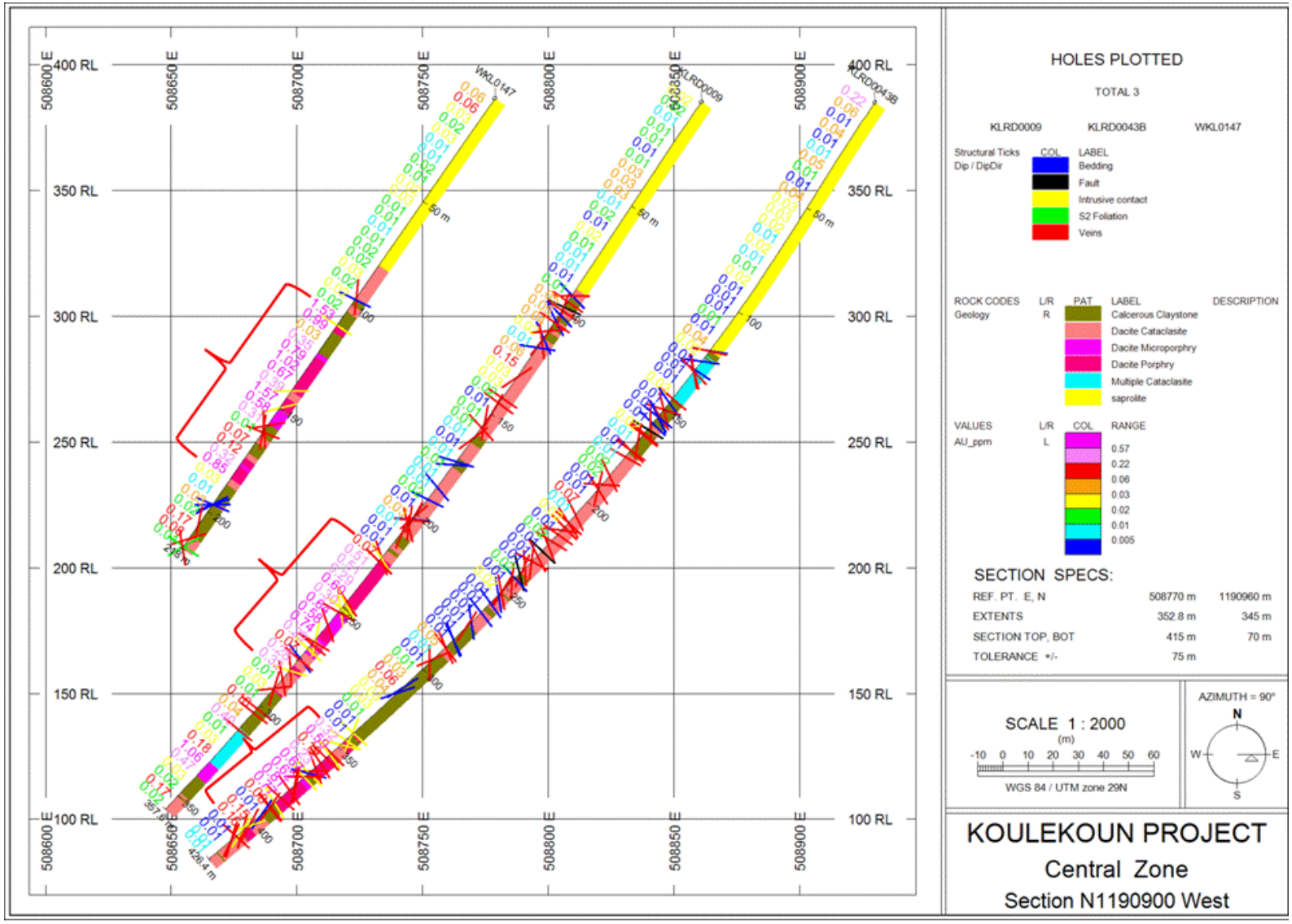

Figure 4.3.6: CZ high grade intervals of gold, mainly related with crosscutting contact and veins generations.

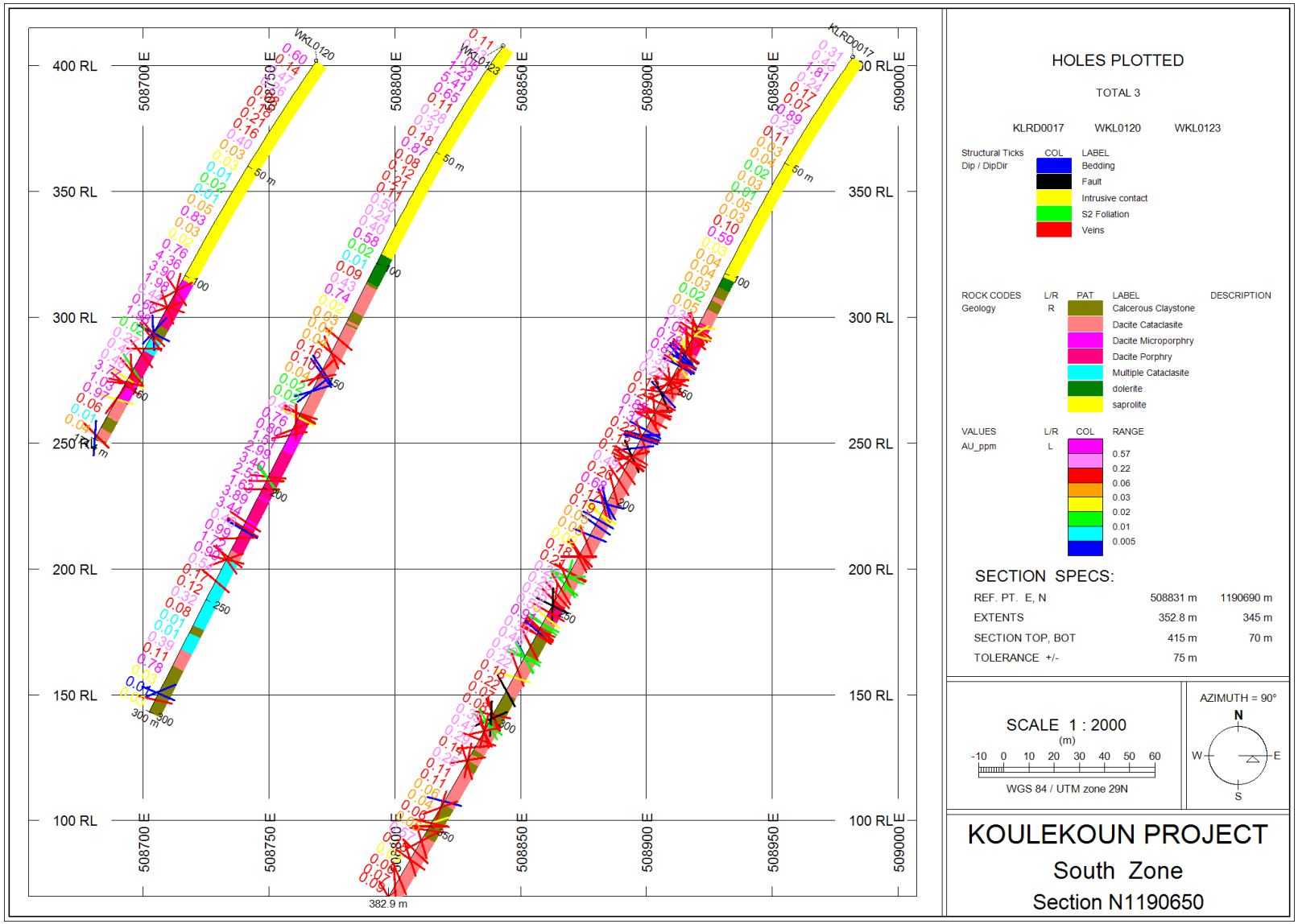

Figure 4.3.7: SZ structures orientations on drill section with principal SE dip of S_o, S_1, S_2, contact, fault, veins; and their corresponding crosscutting generations.

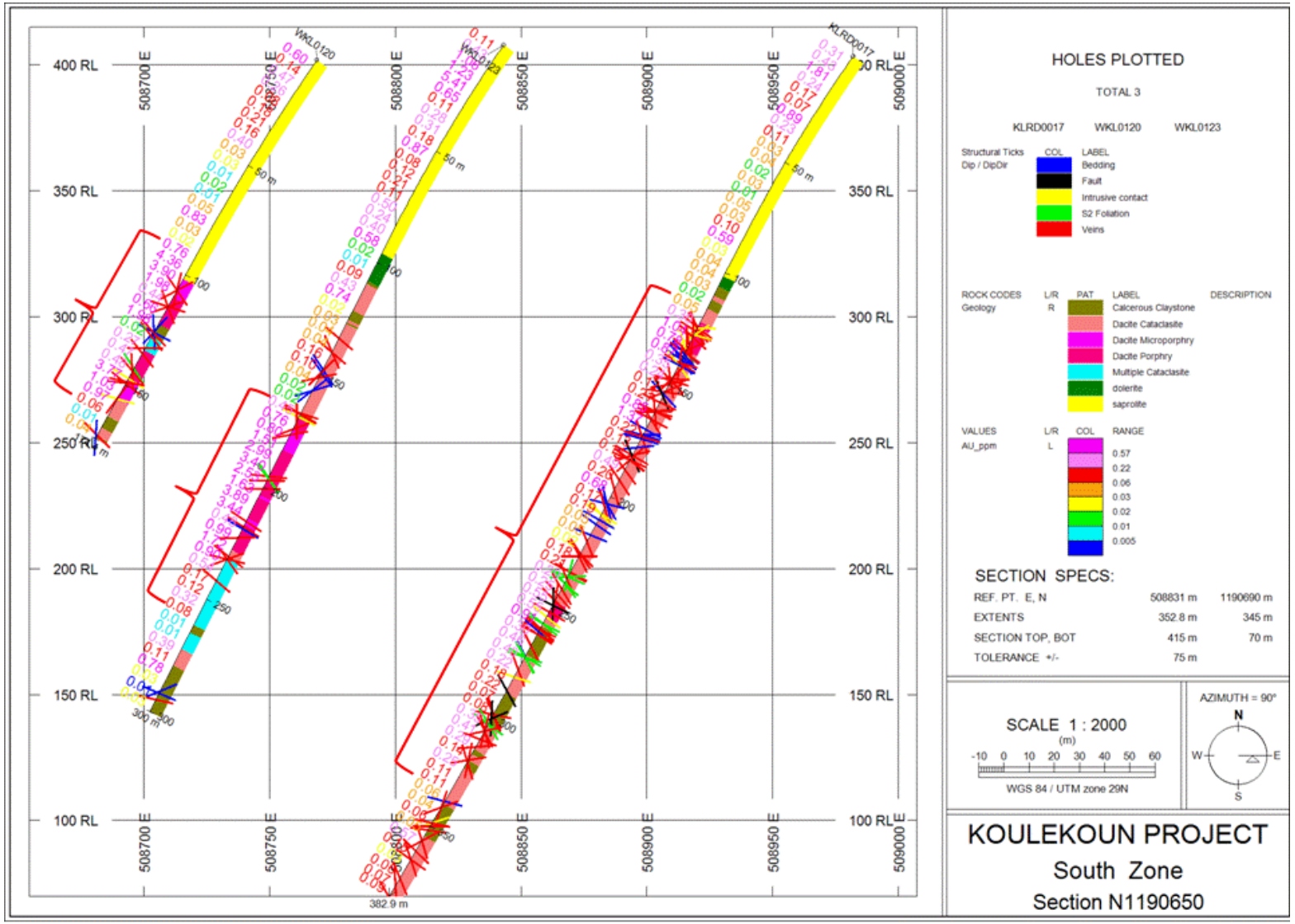

Figure 4.3.8: SZ high grade intervals of gold, mainly related with crosscutting fault, S2 and veins generations. S1 is associated with low grade intervals, suggesting the existence of pre-D2 mineralization.

In summary, the examination of the high gold grade intervals on drill sections shows the mineralized zone mostly located within intrusive bodies. Section interpretation suggests that gold occurs where faults, contacts and veins are present in close proximity to each other.

Two principal fault generations are present. The first fault type strikes NW-SE and in most cases is parallel to S_2. This may suggest its relation with D2 deformation event. The second fault generation (F2) is in general sub-parallel and strikes NE-SW and is often parallel to S_1.

Veins are likely oriented as faults; and vein high intensity domains are related to mineralization. The intersection zones of faults and veins always indicate gold mineralization.

Sections showing mineralized intervals confirm the NW-SE strike of S_2 in the North-West, Central and South Zones (figures 4.3.4; 4.3.6 and 4.3.8). Observations have also shown a sub-parallel relationship between S_1 and S_2 in South Zone (figure 4.3.8). This suggests a possible pre-D2 mineralization (low to medium grades), with a late reactivation during the D2 deformation.

The 3d model suggests that Koulekoun structures convoluted folding and perhaps fold interference and dome-basin structures explain the high variability of S_o plane orientations in all domains but particularly in the North-East, North-West and Central Zones (figures 4.2.1, 4.2.2 and 4.2.3), previously described in section 4.2 above.

Multiple folds generations may have affected these zones and favored interference folds pattern. The S_o 3d model of South Zone has permitted to determine the presence of a gently plunging and moderately inclined fold. The mineralized body in this zone is located within the axial surface (figure 3.5.8).

The relative timing of folding and vein or fault formation has not been worked out in this thesis. However, the large variety of vein orientations may at least in part be related to their folding, which implies that at least some vein generations were emplaced prior to folding.

4.4 *Structural model of the Koulekoun gold deposit*

It appears from the stereonet analysis that NW-SE structures (S_2, intrusive contact, fault, and vein) control the deposition of gold in the study area (figures 4.3.2; 4.3.4 and 4.3.8) shown in section 4.3 abow.

Ore shoot zones are located along the early NW-SE fault system, which was later intersected by the NE-SW F2 fault (figures 4.3.2, 4.3.4 and 4.3.8) of section 4.3. Each fault generation is accompanied by vein systems.

Local NE-SW gently plunging and moderately inclined folds recognized in the South Zone (figures 3.5.8 of section 3.5 and 4.2.4 of section 4.2) show a NE-dipping axial surface, along of which porphyry intrusions and the ore body occurs.

Numerous basin-dome structures occur in the study area (figures 3.5.2, 3.5.6 and 3.5.8 of section 3.5) and (figures 4.2.1, 4.2.3 and 4.2.4 of section 4.2), mainly presenting oval striking NW-SE shapes. The abundance of basin-domes structures indicates multiple phases of folding, that have led to fold interference patterns, adding to geometrical complexity of observed structures.

Regional structural interpretation suggests that NW-SE structures were subject of sinistral deformation; while NNE-SSW developed under dextral strike movement (Lahondere et al, 1999).

Consequently, the history of the emplacement of Koulekoun gold mineralization suggests multiple deformation phases started from the deposition of the sedimentary Lower Birimian (B1) on the D2 major transcurrent crustal contraction, passing through the Upper Birimian (B2) thickening.

The formation of F2 faults system was accompanied by intensive fracturing characterized by dominant S_2 foliations and veins; preferably associated with competent felsic intrusions (Lahondere et al., 1999b). This phenomenon led to gold mineralization which enriched felsic intrusions and filled intensive veins sets, possibly with the initial magma saturated with sulphide in melt.

The reactivation of F2 faults, possibly during the late-orogenic or post-D2 deformation events may have accounted for the dissemination of gold-bearing arsenopyrite and Au-quartz vein, sometimes with free gold often observed on the Koulekoun cores. F1 and F2 faults and their associated veins and foliations intersection points generally define the ore shoot zones (Central zone for instance).

In conclusion, the resulting structural model of the Koulekoun gold deposit proposed by the present study supports both the regional structural interpretation developed by Lahondere et al. (1999a) and the auriferous NE-SW trending fault zone, intersecting a major NW-striking and steeply E-dipping porphyry units previously mentioned by Tenova (2013). Additional characteristic of the Koulekoun deposit from the present study is the presence of numerous basin-dome structures that have affected the country meta-sedimentary units, particularly in the North-East, North-West and the Central zones of the deposit.

4.5 *Comparison between the Koulekoun gold deposit and the three industrial scale mines within the Siguiri Basin*

The style of gold deposits being mined in the three industrial scale gold mines (Siguiri, Lero and Kiniero) within the Siguiri Basin indicates the primary source of the gold to be mesothermal vein and lode mineralization hosted in Birimian meta-seimentary rocks (Lalande, 2005). These rocks have undergone a complex cycle of weathering, erosion and deposition resulting in truncated laterite profiles and alluvium that have been re-cemented (ferricrete) and themselves mineralized if derived from gold-bearing rocks (Lalande, 2005).

According to Lalande (2005), the styles of gold deposits within the three industrial gold mines within the Siguiri Basin are described as follow:

The Siguiri Mine exploites three tyes of gold deposits: (1) Laterite which occurs as aprons of colluviums or as paleo-channels of alluvial laterite gravel immediately above in-situ primary mineralization; (2) quartz vein related mineralization hosted in meta-sediments with the better grade associated with vein stockworks in brittle siltstones and sandstones; (3) lateritisation and weathering extends over 100 meters in places to form saprolite.

The Lero Mine exploites a series of laterite, saprolite and paleo-placer deposits. The concession is covered by the Birimian meta-sediments and is characterized by extensive laterisation and weathering extends up to 100 meters depth. The Lero deposit also presents

numerous ring and curved lineaments enhanced by drag folding; and these appear consistent with uplifting by an intrusion. Regional extensive NW structures with conjugate NS and WNW shorter lineaments.

The Kiniero Mine exploites a gold-bearing quartz vein and meta-sediments.

The early model of the Koulekoun gold deposit developed by Tenova (2013) and later confirmed by Fahey et al; (2013) presents the Koulekoun gold deposit as a porphyry hosted orogenic disseminated style mineralization system. This is markedly different to the typical orogenic lode or mesothermal lode style of the Birimian (Fahey et al; (2013)). The dominant geological feature is massive, NW-striking and steeply E-dipping quartz feldspath porphyry. The porphyry unit is the primary host to gold mineralization, and has intruded along the anticlinal axis of a folded sequence of volcanogenic sedimentary rocks (Fahey et al; (2013)). Although, the common character of the Koulekoun gold deposit with all industrial gold mines is the extends of weathering profile up to 80 meters, the presence of laterite cap and at some stages the existence of numerous ring and curved lineaments enhanced by drag folding (Lero).

CHAPTER 5 : CONCLUSIONS AND RECOMMENDATIONS

The Koulekoun gold deposit area is characterized by the high paucity of outcrops and raw data interpreted for the present study was mainly collected from core samples that had been already sampled (half-core). Therefore, the provisional findings of the present study are open for discussion due to high degree of statistical interpretation to which the data has been subjected to establish orientation patterns.

Although, it has been illustrated from structure data analysis and S_o data 3d interpolation that NW-SE structures (S_2, intrusive contact, fault and vein) have controlled the deposition of gold within the Koulekoun deposit area.

The geometrical relationships between structure main cluster orientations from stereonet analysis have demonstrated that S_o are in majority dipping at moderate angle and respectively strike to N-S, NE-SW and NW-SE. Intrusive bodies are moderately dipping to the SE in general, except in the North-East Zone where they are sub-vertical and SE dipping. Faults show variable orientations and strike to NE-SW, NW-SE and E-W and dip steeply in all zones. Like faults, vein orientations show highly variable directions due to the presence of numerous vein orientation orders in each domain.

High gold grades are found at the intersection of F1 and F2 faults and associated veins; preferably within competent felsic dykes. Other gold occurrences are found at the contact of intrusions and country rocks or where country rocks have been subjected of intensive fracturing and veining. Ore host rocks are formed by highly silicified, potassic and sometimes chloritized or carbonate associated porphyry dykes. High gold grade intervals are associated with fine-crystalline pyrite grains and arsenopyrite either disseminated in host rock (porphyry intrusions) or mobilized along contacts or veins.

It has also been demonstrated that two principal fault generations have plaid an important role in the localization of the Koulekoun ore body: the NE-SW fault (F1) and the NW-SE fault (F2). The two fault generations and their associated veins intersections defined ore shoot zones within the Koulkeoun deposit.

This study has made it possible for one to understand the reason for the occurrence of a limited mineralized orebody in the North-East and North-West zones. This may be related to dominant basin-dome structures in these zones. The study has also confirmed the axial surface mineralization style of Koulekoun ore body (South Zone). But, this concept may not be applied in all domains due to the difference in fold patterns that makes a successful drillholes planning difficult in certain domains.

The proposed structural model of the Koulekoun gold deposit in the present study supports both the regional structural interpretation developed by Lahondere et al (1999a) and the auriferous NE-SW trending fault zone, intersecting a major NW-striking and steeply E-dipping porphyry units previously mentioned by Tenova (2013). Additional characteristic of the Koulekoun deposit from the present study is the presence of numerous basin-dome structures that have affected the country meta-sedimentary units, particularly in the North-East, North-West and the Central zones of the deposit. This model is markedly different to the typical orogenic lode or mesothermal lode style of the Birimian (Fahey et al; (2013)).

Alternatively, the common character of the Koulekoun gold deposit with all industrial gold mines in the Siguiri Basin (Siguiri, Lero and Kiniero) is the extends of weathering profile, the presence of laterite cap and at some stages the existence of numerous ring and curved lineaments enhanced by drag folding (Lero).

It is therefore recommended that targets selection around the Koulekoun deposit and within the TriK-block for further exploration programs to be concentrated along NW-SE structures, in objective to determine possible intersection zones with NE-SW structures. Further exploration works may include:

a) an appropriate logging of bedding and interpretation for all diamond holes that have been drilled in the North-East, North-West and Central zones in order to refine interference fold structures and identify possible intersection zones where high gold grades may occur;

b) a detailed surface mapping to characterize the dilatant zones (shear or tension fractures and folds axial planes); mapping of artisanal mining sites, where outcrop of structures can be found will be helpful;

c) a systematic S_o mapping of Koulekoun cores in order to establish the stratigraphic younging direction and conduct a complete fold analysis;

d) the examination of structural relationships in field once mining has begun, to see how they compare with the results presented in this thesis.

REFERENCES

Allison D.T., 2004: Structural Geology Laboratory manual. Third Edition. Department of Earth Sciences; University of South Alabama.

Attoh K. & Ekwueme B.N., 1997: The West African Shield. In: Dirks P.H.G.M; Blenkinsop T.G; Jelsma H.A. : The Geological evolution of Africa. Geology. Vol. IV.

Aureus Mining Inc., 2015: Liberia Operation. Company presentation.

Avocet Mining plc. 2009: Core orientation methods and the measurements of geological structures in oriented diamond core. Company presentation.

Avocet Mining plc., 2011: Field photographs. Company presentation.

Avocet Mining plc. 2013: Guinea Exploration Update. Company presentation.

Core D., 2011: Interpretation of Magnetic and Electromagnetic data at the Tri-K Tenements, Guinea. Data Interpretation Report Tri-K, Guinea. Avocet Mining Plc. Fathom Geophysics. Competent persons report.

DePangher M., 2011: Petrographic Report #1LZ. Spectrum Petrographics, Inc.

Egal E., Thie´blemont D., Lahonde`re D., Guerrot C., Costea C. A, Iliescu D., Delor C., Goujou J.C, Lafon J.M, Tegyey M., Diaby S., Kolie P., 2002: Late Eburnean granitization and tectonics along the western and northwestern margin of the Archean Kenema–Man domain (Guinea, West African Craton); E. Egal et al. Precambrian Research 117 (2002) 57–84BRGM, BP 6009, 3, avenue C. Guillemin, 45060 Orleans Cedex 2, France. DNRGH, BP 295, Conakry, Guinee.

Fabre J., Ennih, N., Liegeois J.P., (eds): General Geology of the West Africa Craton. In: Youbi N., Ernst R., Soderland U., Bertrand H., Doblas M., Hachimi H.E., Kouyate D., Soulaimani A., Hafid A., Ikenne M., & Chaham K.R. : Large igneous provinces of the West African Craton: The record preserved in regional dyke swarms. Published on Large Igneous Provinces Commission - May 2011.

Fahey G., Bannister K., Gibbons T., 2013: West Africa Projects (Burkina Faso & Guinea). CSA Global. Avocet Mining Plc. Competent Persons Report (CPR).

Feybesse J., Billa M., Costea A., et al., 1999 : Carte Geologique au 1:200000. Feuille KANKAN NC-29-XV et Notice Explicative. In: Mamedov et al. :Geologie de la Republique de Guinee. VOLUME I ; 103-111.

Fleuty, 1964: In: Allison D.T: Structural Geology Laboratory manual. Department of Earth Sciences; University of South Alabama.

Lahondère D., Egal E., Lacomme A., Le Berre P., Costea C.A., Deynoux M., Guerrot C., Diabaté B., Diallo A., Diallo A.B., Diallo S., Gaye F. Iliescu D., Minthé D., Feybesse J.L., 1999a : Projet de cartographie géologique du Nord-Est de la République de Guinée et Notice explicative de la carte géologique à 1/200 000. Feuille n° 12*=

Siguiri. 1ère édition. Conakry. Edité sous la responsabilité du Ministère des Mines, de la Géologie et de l'Environnement.

Lahondère D., Lacomme A., Le Berre P., Iliescu D., Guerrot C., Diabaté B.,Gaye F., Minthé D., Feybesse J.L., 1999b : Projet de cartographie géologique du Nord-Est de la République de Guinée et Notice explicative de la carte géologique à 1/200 000. Feuille n° 20-21*= Falama – Manankoro. 1ère édition. Conakry. Edité sous la responsabilité du Ministère des Mines, de la Géologie et de l'Environnement.

Lalande P., 2005: Technical Report on Gold Geochemical Surveys of the bloc 29, Siguiri District, Guinea, West Africa. Societe Miniere de Siguiri (SMS). Competent Persons Report (CPR).

Mamedov V.I; Boufeev Y.V & Nikitine Y.A., 2010 : Geologie de la Republique de Guinee. Volume I. Geosprospects Ltd. Universite d'Etat de moscou Lomonossov M. (Faculté géologique).

Milési J.P; Ledru P.; Feybesse J.L; Dommanget A. & Marcoux E., 1992: Early proterozoic ore deposits and tectonics of the Birimian orogenic belt, West Africa. Précambrien Research 58, 305-344.

Scott W., 2009: Koulékoun Gold Project. Scoping study. Wega Mining Koulékoun. CPR Wega Mining ASA. Competent Persons Report.

Sibson R.H., 2001: Seismogenic framework for hydrothermal transport and ore deposition. Reviews in Economic Geology 14, 25-50.

Tenova Bateman, 2013: Kodieran and Koulekoun project Feasability Study. Section 2-Introduction and project background. Wega Mining Guinee SA. Competent Persons Report. Wega Mining Guinea SA & Tenova Bateman; M7430D-0760-002-Rev: A.

APPENDICES

Table A1-1: MSc project structural measurements data of the North-East zone

DH_Hole	DH_Depth	Structure Type	Alpha	Beta	Azimut	Dip	DH_East	DH_North	DH_RL	Plot_Dip	Plot_DipDir	Domain
KLRD0019	90.9	Vein	42	126	272.6543	-55.02	509287.681	1190926.19	310.6228889	36.9705156	177.2832632	NE zone
KLRD0019	92.8	Vein	60	292	272.6543	-55.02	509286.6106	1190926.18	309.0532148	52.4893409	53.85814904	NE zone
KLRD0019	93.9	S_0	86	280	272.6543	-55.02	509285.9888	1190926.18	308.1457902	35.3303729	83.10189699	NE zone
KLRD0019	100.7	Vein	25	302	277.0152	-54.257	509282.1159	1190926.28	302.5577325	85.9633669	42.53881325	NE zone
KLRD0019	102	Vein	42	124	277.0152	-54.257	509281.37	1190926.32	301.4939026	38.1522595	179.3508311	NE zone
KLRD0019	102	S_1	80	202	277.0152	-54.257	509281.37	1190926.32	301.4939026	26.0988043	85.04674088	NE zone
KLRD0019	105.6	Vein	50	60	277.0152	-54.257	509279.2975	1190926.48	298.5544924	64.0010278	133.3559753	NE zone
KLRD0019	105.6	Vein	10	24	277.0152	-54.257	509279.2975	1190926.48	298.5544924	67.6981193	300.7419565	NE zone
KLRD0019	105.7	Vein	11	350	277.0152	-54.257	509279.2398	1190926.48	298.4729782	66.1509983	264.3464114	NE zone
KLRD0019	105.7	Vein	44	54	277.0152	-54.257	509279.2398	1190926.48	298.4729782	71.2511864	133.0081196	NE zone
KLRD0019	111.4	Intrusive contact	77	100	279.2729	-53.284	509275.9411	1190926.85	293.839333	35.6254675	119.5725393	NE zone
KLRD0019	111.8	S_0	81	220	279.2729	-53.284	509275.7085	1190926.88	293.5153089	29.5477948	85.72535175	NE zone
KLRD0019	113.2	Vein	47	70	279.2729	-53.284	509274.893	1190926.99	292.3824751	63.0061071	143.7537316	NE zone
KLRD0019	115.5	S_0	78	116	279.2729	-53.284	509273.549	1190927.18	290.5256144	32.5996939	118.5710173	NE zone
KLRD0019	122.26	S_0	70	264	280.2585	-52.688	509269.5692	1190927.81	285.0977675	39.365522	67.11350227	NE zone
KLRD0019	126	S_0	30	348	280.2585	-52.688	509267.3525	1190928.19	282.1093617	83.641086	269.3344555	NE zone
KLRD0019	127.7	S_0	60	254	280.2585	-52.688	509266.3419	1190928.36	280.7538824	39.3324411	50.68568938	NE zone
KLRD0019	128.8	Vein	24	150	280.2585	-52.688	509265.687	1190928.48	279.8777706	36.5911573	230.2081545	NE zone
KLRD0019	134.55	S_0	53	232	281.2569	-52.096	509262.2515	1190929.11	275.3105311	30.8019102	32.84714556	NE zone
KLRD0019	137.26	S_0	83	276	281.2569	-52.096	509260.6254	1190929.42	273.1651815	38.9632888	89.80244917	NE zone
KLRD0019	142.62	S_0	62	330	279.8432	-51.631	509257.395	1190930.06	268.935204	63.5485538	85.75998218	NE zone
KLRD0019	143.77	Vein	55	160	279.8432	-51.631	509256.6987	1190930.19	268.0296354	12.2579604	168.1919552	NE zone
KLRD0019	156.6	S_0	31	350	276.114	-51.356	509248.8481	1190931.49	257.9668196	82.9379646	268.8631505	NE zone
KLRD0019	159.45	Vein	55	58	276.114	-51.356	509247.0838	1190931.7	255.7385805	63.2238745	129.3034633	NE zone
KLRD0019	161.12	Vein	31	76	272.3514	-51.138	509246.0468	1190931.81	254.4341834	74.1828906	155.5183822	NE zone
KLRD0019	164.2	Vein	45	160	272.3514	-51.138	509244.1287	1190931.98	252.0304562	14.6833554	201.9193952	NE zone
KLRD0019	169.6	S_0	52	202	272.3514	-51.138	509240.7531	1190932.19	247.8208383	13.6498092	14.52243685	NE zone
KLRD0019	173.1	Vein	30	52	271.0454	-50.97	509238.5577	1190932.28	245.0962772	86.8929123	135.1052424	NE zone
KLRD0019	175.4	Vein	25	200	271.0454	-50.97	509237.1131	1190932.32	243.3071459	30.2286534	309.6940423	NE zone
KLRD0019	175.4	Vein	38	310	271.0454	-50.97	509237.1131	1190932.32	243.3071459	80.7681138	53.98791324	NE zone
KLRD0019	176	S_0	77	116	271.0454	-50.97	509236.736	1190932.33	242.8405723	34.9359736	112.3659415	NE zone
KLRD0019	177.1	S_0	85	286	271.0454	-50.97	509236.0444	1190932.35	241.9853545	40.6011891	83.99367056	NE zone
KLRD0019	177.1	Vein	52	22	271.0454	-50.97	509236.0444	1190932.35	241.9853545	75.3190413	105.1831598	NE zone
KLRD0019	177.65	S_2	80	270	271.0454	-50.97	509235.6985	1190932.36	241.5578265	40.0467795	75.73268322	NE zone
KLRD0019	177.65	Vein	40	22	271.0454	-50.97	509235.6985	1190932.36	241.5578265	86.9714236	108.0905395	NE zone
KLRD0019	183.6	Vein	8	40	271.9326	-51.346	509231.9565	1190932.44	236.9324928	68.4208488	314.6010562	NE zone
KLRD0019	184.1	Vein	45	60	271.9326	-51.346	509231.6427	1190932.44	236.543288	70.8180985	131.8228532	NE zone
KLRD0019	186.57	S_0	17	330	271.9326	-51.346	509230.0946	1190932.48	234.6191009	73.1048974	241.6786322	NE zone
KLRD0019	189.5	Vein	50	150	271.9326	-51.346	509228.2624	1190932.54	232.3332947	18.9274105	174.1498451	NE zone
KLRD0019	190.85	Vein	27	166	272.8124	-51.725	509227.4198	1190932.57	231.2789294	26.5463228	243.0810271	NE zone
KLRD0019	199.42	Vein	50	154	272.8124	-51.725	509222.0943	1190932.79	224.5681514	16.4168946	178.2554325	NE zone
KLRD0019	201.3	Vein	23	154	273.52	-51.798	509220.9312	1190932.85	223.0922544	35.0042452	228.270952	NE zone
KLRD0019	205.75	Vein	32	166	273.52	-51.798	509218.1802	1190933	219.597557	22.2642148	240.5006106	NE zone
KLRD0019	208.12	S_0	52	339	273.52	-51.798	509216.7162	1190933.08	217.7356947	74.7282462	80.06509435	NE zone
KLRD0019	209	Fault	17	100	273.52	-51.798	509216.1729	1190933.11	217.044256	70.5842024	180.5243752	NE zone
KLRD0019	210.1	Vein	17	170	273.9943	-51.593	509215.4938	1190933.15	216.1798729	35.6545638	257.0435218	NE zone
KLRD0019	210.1	Vein	40	58	273.9943	-51.593	509215.4938	1190933.15	216.1798729	75.3086146	135.7863624	NE zone
KLRD0019	212.4	Fault	30	150	273.9943	-51.593	509214.0734	1190933.24	214.3730994	31.0268706	216.4467484	NE zone
KLRD0019	218	Fault	16	350	273.9943	-51.593	509210.6094	1190933.47	209.9788857	68.2116088	263.5037719	NE zone
KLRD0019	218	Vein	60	32	273.9943	-51.593	509210.6094	1190933.47	209.9788857	65.4115397	110.8004776	NE zone
KLRD0019	227.4	S_0	46	350	274.4708	-51.389	509204.7778	1190933.89	202.6184929	82.2227393	87.46025757	NE zone
KLRD0019	232.19	Vein	70	272	274.6667	-51.303	509201.7984	1190934.12	198.8750393	43.37224	64.60292079	NE zone
KLRD0019	235	S_0	65	300	274.6667	-51.303	509200.0492	1190934.26	196.6802479	54.8005786	67.84439598	NE zone
KLRD0019	235	Vein	55	222	274.6667	-51.303	509200.0492	1190934.26	196.6802479	25.0277998	29.33210466	NE zone
KLRD0019	241.35	Vein	55	332	274.6001	-51.342	509196.0936	1190934.58	191.7231014	71.1426475	78.07312972	NE zone
KLRD0019	241.35	Vein	25	354	274.6001	-51.342	509196.0936	1190934.58	191.7231014	76.5187302	269.0145484	NE zone

DH_Hole	DH_Depth	Structure Type	Alpha	Beta	Azimut	Dip	DH_East	DH_North	DH_RL	Plot_Dip	Plot_DipDir	Domain
KLRD0019	256.5	S_0	25	89	274.5335	-51.381	509186.6595	1190935.34	179.8933806	71.3305571	167.6433672	NE zone
KLRD0019	256.5	Vein	40	43	274.5335	-51.381	509186.6595	1190935.34	179.8933806	81.2638218	126.5142465	NE zone
KLRD0019	262.6	S_0	40	62	275.1064	-50.902	509182.8618	1190935.65	175.1294191	73.9057132	139.3513444	NE zone
KLRD0019	263.75	S_0	18	23	275.1064	-50.902	509182.1441	1190935.71	174.2328214	72.0518776	297.7762136	NE zone
KLRD0019	270.4	Vein	16	238	276.3314	-49.908	509177.9784	1190936.07	169.061789	57.6393091	349.9486291	NE zone
KLRD0019	273.5	Vein	40	62	276.3314	-49.908	509176.0238	1190936.25	166.6626187	74.444111	140.101321	NE zone
KLRD0019	274.9	Vein	15	356	276.3314	-49.908	509175.1373	1190936.34	165.5825836	65.5245291	271.4456402	NE zone
KLRD0019	275.1	Vein	45	34	276.3314	-49.908	509175.0105	1190936.35	165.428469	80.1167979	119.3548267	NE zone
KLRD0019	275.9	Vein	67	278	276.3314	-49.908	509174.5027	1190936.4	164.812452	47.6779017	64.32183692	NE zone
KLRD0019	276.1	S_0	46	302	276.3314	-49.908	509174.3756	1190936.41	164.658558	71.4530146	57.46042469	NE zone
KLRD0019	280.84	Vein	45	124	277.5794	-48.92	509171.3502	1190936.74	161.0242541	37.307381	171.7124584	NE zone
KLRD0019	285.9	S_0	16	0	277.5794	-48.92	509168.0918	1190937.12	157.1723106	65.3897846	276.9901427	NE zone
KLRD0019	286.17	Intrusive contact	30	40	277.5794	-48.92	509167.9172	1190937.15	156.967576	86.8826742	311.0623466	NE zone
KLRD0019	286.6	S_2	85	152	277.5794	-48.92	509167.6388	1190937.18	156.6416857	36.4057996	101.1328119	NE zone
KLRD0019	286.6	Vein	22	87	277.5794	-48.92	509167.6388	1190937.18	156.6416857	75.3996554	170.2790471	NE zone
KLRD0019	286.6	Vein	42	52	277.5794	-48.92	509167.6388	1190937.18	156.6416857	77.9861287	133.9578464	NE zone
KLRD0019	291	Intrusive contact	30	350	278.3675	-48.234	509164.7789	1190937.55	153.318792	79.4328009	268.7740347	NE zone
KLRD0019	293.1	Vein	60	102	278.3675	-48.234	509163.4077	1190937.74	151.7392293	43.9582847	142.544848	NE zone
KLRD0019	294.4	Fault	5	0	278.3675	-48.234	509162.5571	1190937.86	150.7631482	53.6145574	277.9312375	NE zone
KLRD0019	294.4	Vein	29	226	278.3675	-48.234	509162.5571	1190937.86	150.7631482	40.0561093	355.7924791	NE zone
KLRD0019	294.4	Fault	80	0	278.3675	-48.234	509162.5571	1190937.86	150.7631482	51.3854426	97.93123753	NE zone
KLRD0019	299.7	Vein	32	76	278.3675	-48.234	509159.0763	1190938.36	146.7975762	74.9800819	156.7253821	NE zone
KLRD0019	299.7	S_2	60	352	278.3675	-48.234	509159.0763	1190938.36	146.7975762	71.5072044	94.09155487	NE zone
KLRD0019	305.3	Vein	35	68	278.9043	-47.902	509155.3812	1190938.91	142.6261073	77.2234757	149.8615048	NE zone
KLRD0019	305.4	Fault	42	240	278.9043	-47.902	509155.3151	1190938.92	142.5517273	41.7587846	23.61863704	NE zone
KLRD0019	310.9	Vein	70	88	279.4444	-47.571	509151.6757	1190939.48	138.466793	46.4411734	127.0701333	NE zone
KLRD0019	314.7	Vein	35	63	279.4444	-47.571	509149.1554	1190939.88	135.6513394	79.9448022	146.9808201	NE zone
KLRD0019	317	Vein	35	152	279.4444	-47.571	509147.6277	1190940.13	133.949968	24.3288845	210.3730849	NE zone
KLRD0019	323.9	Vein	80	85	280.2972	-47.402	509143.0366	1190940.9	128.8567562	44.3040492	114.2320748	NE zone
KLRD0019	326.7	Vein	60	70	280.2972	-47.402	509141.1725	1190941.23	126.7929912	58.4831619	133.3383461	NE zone
KLRD0019	326.7	Vein	42	140	280.2972	-47.402	509141.1725	1190941.23	126.7929912	28.6068009	185.9872185	NE zone
KLRD0019	330.7	Vein	22	210	281.4917	-47.408	509138.509	1190941.7	123.8473954	34.9912493	334.3947389	NE zone
KLRD0019	335.5	Vein	35	42	281.4917	-47.408	509135.3164	1190942.31	120.3139094	89.4123238	134.2659103	NE zone
KLRD0019	339.9	Fault	20	106	281.4917	-47.408	509132.3955	1190942.89	117.0746527	64.7171506	189.0114773	NE zone
KLRD0019	347.9	Vein	60	64	282.7203	-47.419	509127.0996	1190944.01	111.1846551	60.7015006	133.4623112	NE zone
KLRD0019	354.3	Vein	70	86	283.2833	-47.4	509122.8758	1190944.96	106.4723486	47.4963711	130.6516587	NE zone
KLRD0019	358.8	Vein	40	64	283.2833	-47.4	509119.9092	1190945.65	103.1595093	75.7628684	148.3462106	NE zone
KLRD0019	380	Vein	20	196	283.2833	-47.4	509105.9432	1190948.95	87.55420422	30.3250203	314.1457305	NE zone
WKL0068	46.7	Intrusive contact	45	346	271.1829	-54.892	509215.0521	1190901.95	347.238358	79.4063554	81.18245938	NE zone
WKL0068	57.1	Vein	57	46	271.3983	-54.873	509209.0717	1190902.07	338.7307956	62.0644963	117.5291764	NE zone
WKL0068	59	S_0	35	214	271.3983	-54.873	509207.9789	1190902.1	337.1767523	30.6926422	335.363757	NE zone
WKL0068	60.32	Vein	86	90	271.6138	-54.854	509207.2196	1190902.12	336.0971417	35.3374127	98.47188004	NE zone
WKL0068	60.45	Fault	40	100	271.6138	-54.854	509207.1448	1190902.12	335.9908183	52.9720463	162.448025	NE zone
WKL0068	62	S_0	46	210	271.6138	-54.854	509206.2532	1190902.14	334.7231406	20.8524554	348.9001466	NE zone
WKL0068	62.47	S_0	65	90	271.6138	-54.854	509205.9828	1190902.15	334.338757	42.1718023	130.5581009	NE zone
WKL0068	62.85	S_0	72	80	271.6138	-54.854	509205.7642	1190902.16	334.0279818	41.6823388	118.7790067	NE zone
WKL0068	64.9	S_0	87	104	271.6138	-54.854	509204.5849	1190902.19	332.3514782	34.5209717	96.6859256	NE zone
WKL0068	67.56	Vein	35	344	271.6138	-54.854	509203.0544	1190902.23	330.1762302	89.0930944	78.49395353	NE zone
WKL0068	69.1	S_0	64	224	271.6138	-54.854	509202.1683	1190902.25	328.9169367	23.5817954	41.97608103	NE zone
WKL0068	69.85	Vein	72	102	271.6138	-54.854	509201.7368	1190902.26	328.3036605	35.4415142	122.961738	NE zone
WKL0068	71.29	Vein	65	104	271.8295	-54.836	509200.9081	1190902.29	327.1262009	36.8716376	134.6558542	NE zone
WKL0068	71.8	Vein	52	206	271.8295	-54.836	509200.6146	1190902.3	326.7091933	15.6577374	1.767873673	NE zone
WKL0068	72.1	S_0	74	241	271.8295	-54.836	509200.442	1190902.3	326.463897	30.3462273	63.04414475	NE zone
WKL0068	72.1	Vein	70	300	271.8295	-54.836	509200.442	1190902.3	326.463897	47.9323766	68.0293243	NE zone
WKL0068	73.2	Intrusive contact	45	26	271.8295	-54.836	509199.809	1190902.32	325.5644915	77.7347378	110.0395219	NE zone
WKL0068	73.82	Vein	85	266	271.8295	-54.836	509199.4522	1190902.33	325.0575638	35.1010099	82.84836891	NE zone
WKL0068	74.4	Vein	55	30	271.8295	-54.836	509199.1184	1190902.34	324.5833475	67.420865	109.6400009	NE zone
WKL0068	81.5	S_0	20	176	272.0453	-54.817	509195.0317	1190902.47	318.7787946	34.9630557	265.3173463	NE zone
WKL0068	87.7	Fault	32	320	272.0453	-54.817	509191.4622	1190902.59	313.7107964	86.6176689	58.788113	NE zone
WKL0068	92.7	Vein	12	134	272.2579	-54.799	509188.5831	1190902.69	309.6242171	55.8370259	213.9716391	NE zone
WKL0068	92.7	Vein	64	278	272.2579	-54.799	509188.5831	1190902.69	309.6242171	45.6290268	54.82832743	NE zone

DH_Hole	DH_Depth	Structure Type	Alpha	Beta	Azimut	Dip	DH_East	DH_North	DH_RL	Plot_Dip	Plot_DipDir	Domain
WKL0068	96.7	Vein	11	221	272.2579	-54.799	509186.2795	1190902.78	306.355281	54.3421506	324.651964	NE zone
WKL0068	96.7	Vein	48	65	272.2579	-54.799	509186.2795	1190902.78	306.355281	63.6228717	134.8247146	NE zone
WKL0068	122.25	Vein	20	210	272.9095	-54.745	509171.5588	1190903.41	285.4818641	41.4942185	318.0688017	NE zone
WKL0068	128.6	S_0	12	350	272.9095	-54.745	509167.8987	1190903.59	280.2959645	67.2795159	262.2914734	NE zone
WKL0068	128.7	Vein	34	218	272.9095	-54.745	509167.841	1190903.59	280.2143025	33.5172545	340.470863	NE zone
WKL0068	135	Fault	15	85	273.1235	-54.726	509164.2091	1190903.78	275.0699816	80.6329617	170.1298077	NE zone
WKL0068	148	Vein	67	86	273.1235	-54.726	509156.7121	1190904.19	264.4573851	42.6385766	128.2861266	NE zone
WKL0068	148.9	Fault	14	218	273.1235	-54.726	509156.1928	1190904.22	263.7228248	50.270973	324.119687	NE zone
WKL0110	50	S_0	59	262	266.7334	-54.664	509258.9101	1190912.74	345.2086012	42.1833531	37.69681445	NE zone
WKL0110	52.34	S_0	65	276	266.7334	-54.664	509257.5598	1190912.67	343.2986672	44.4255198	50.21719042	NE zone
WKL0110	54.35	S_0	60	250	266.7334	-54.664	509256.3997	1190912.61	341.6582975	36.3292547	34.64397739	NE zone
WKL0110	75.85	Vein	83	112	265.7221	-54.569	509243.9811	1190911.85	324.1243623	33.3569808	97.63639229	NE zone
WKL0110	75.85	Vein	20	48	265.7221	-54.569	509243.9811	1190911.85	324.1243623	85.0801754	310.2776518	NE zone
WKL0110	78.8	Vein	43	350	265.7221	-54.569	509242.276	1190911.73	321.7202683	82.0528244	78.410277	NE zone
WKL0110	79.58	Vein	65	338	265.7221	-54.569	509241.8251	1190911.69	321.0846773	59.2431181	75.16144743	NE zone
WKL0110	80.45	S_0	65	143	265.2153	-54.524	509241.3221	1190911.66	320.3757846	20.9064527	131.2362388	NE zone
WKL0110	80.45	Vein	40	50	265.2153	-54.524	509241.3221	1190911.66	320.3757846	76.2094733	122.9519133	NE zone
WKL0110	82.59	S_0	60	204	265.2153	-54.524	509240.0849	1190911.56	318.6322261	13.9764493	28.08872007	NE zone
WKL0110	85.75	Vein	50	90	265.2153	-54.524	509238.2578	1190911.42	316.0580112	51.3917117	140.7869826	NE zone
WKL0110	94.35	Vein	38	340	264.7077	-54.479	509233.284	1190911	309.0545655	85.9024468	69.43206664	NE zone
WKL0110	98.32	S_0	80	302	264.7077	-54.479	509230.9875	1190910.8	305.822717	41.5705763	71.95092283	NE zone
WKL0110	100.37	S_0	80	260	264.1994	-54.435	509229.8015	1190910.69	304.1541561	35.0040219	67.42898067	NE zone
WKL0110	103.8	Vein	75	110	264.1994	-54.435	509227.8171	1190910.5	301.3628007	33.1333534	110.8589593	NE zone
WKL0110	104.63	S_0	88	278	264.1994	-54.435	509227.3369	1190910.45	300.6874195	35.8702529	81.05688579	NE zone
WKL0110	113.5	Vein	21	204	263.6902	-54.392	509222.2044	1190909.94	293.4716891	38.0348592	302.1482589	NE zone
WKL0110	113.5	Vein	46	308	263.6902	-54.392	509222.2044	1190909.94	293.4716891	70.3486394	48.56386315	NE zone
WKL0110	116	Vein	23	170	263.6902	-54.392	509220.7577	1190909.78	291.4385666	32.2828772	246.3522177	NE zone
WKL0110	116	Vein	56	65	263.6902	-54.392	509220.7577	1190909.78	291.4385666	57.5539189	120.6756163	NE zone
WKL0110	116.9	S_0	84	110	263.6902	-54.392	509220.2368	1190909.73	290.7067081	33.9581718	93.89424168	NE zone
WKL0110	121.7	Vein	22	326	263.1803	-54.35	509217.4591	1190909.42	286.8040548	81.7850853	232.1755808	NE zone
WKL0110	128	S_0	40	66	263.1803	-54.35	509213.8132	1190909	281.6833212	70.0649189	131.5395804	NE zone
WKL0110	137	Vein	70	102	262.6695	-54.309	509208.605	1190908.37	274.3708877	36.4140121	117.0620461	NE zone
WKL0110	143.5	Vein	32	344	262.1579	-54.27	509204.8439	1190907.88	269.0917711	87.3909988	248.8939432	NE zone
WKL0110	143.5	Vein	32	216	262.1579	-54.27	509204.8439	1190907.88	269.0917711	33.8253656	325.9940567	NE zone
WKL0110	149.04	S_0	86	104	262.1579	-54.27	509201.6387	1190907.45	264.5936934	34.9546906	88.87836609	NE zone
WKL0110	154.43	Vein	60	48	261.6455	-54.231	509198.5207	1190907.02	260.2185956	59.4974124	107.6409969	NE zone
WKL0110	156.74	Vein	45	352	261.6455	-54.231	509197.1845	1190906.83	258.3439044	80.5266479	76.03467529	NE zone
WKL0110	158.15	S_0	42	162	261.6455	-54.231	509196.369	1190906.71	257.1997143	17.0570567	210.2334324	NE zone
WKL0110	158.21	Vein	60	248	261.6455	-54.231	509196.3343	1190906.7	257.1510271	35.6873123	29.13458968	NE zone
WKL0110	162.43	S_0	65	64	261.1322	-54.193	509193.8939	1190906.34	253.7270532	51.1797747	110.6059816	NE zone
WKL0110	162.43	S_2	31	166	261.1322	-54.193	509193.8939	1190906.34	253.7270532	25.2917102	232.3898972	NE zone
WKL0110	178.8	Vein	32	172	260.4952	-53.955	509184.4315	1190904.86	240.4514272	22.8756351	243.0367661	NE zone

Table A1-2: MSc project structural measurements data of the North-West zone

DH_Hole	DH_Depth	Structure Type	Alpha	Beta	Azimut	Dip	DH_East	DH_North	DH_RL	Plot_Dip	Plot_DipDir	Domain
KLRD0028	126.2	Vein	15	330	286.5509	-52.189	508613.0732	1191108.22	287.0457583	72.2093842	255.6662708	NW zone
KLRD0028	129.8	Vein	20	350	286.5509	-52.189	508610.9601	1191108.84	284.1978545	72.6697711	276.8061003	NW zone
KLRD0028	131.25	Vein	25	30	287.5681	-51.707	508610.1078	1191109.1	283.0526943	81.4889568	313.9193405	NW zone
KLRD0028	131.25	Vein	35	58	287.5681	-51.707	508610.1078	1191109.1	283.0526943	79.253045	151.6463496	NW zone
KLRD0028	131.25	Vein	17	168	287.5681	-51.707	508610.1078	1191109.1	283.0526943	36.4002059	267.0726522	NW zone
KLRD0028	131.9	Vein	25	150	287.5681	-51.707	508609.7255	1191109.21	282.5397004	35.377651	235.1399693	NW zone
KLRD0028	134.8	Fault	45	164	287.5681	-51.707	508608.0181	1191109.73	280.2536113	12.6174162	223.9996018	NW zone
KLRD0028	136.6	Vein	15	80	287.5681	-51.707	508606.9571	1191110.06	278.8368405	84.2497501	180.1106602	NW zone
KLRD0028	138.8	Fault	15	24	287.5681	-51.707	508605.659	1191110.46	277.1075013	69.9699877	312.1284552	NW zone
KLRD0028	149	Vein	15	165	288.2736	-50.901	508599.6004	1191112.41	269.1370872	37.9525842	264.226373	NW zone
KLRD0028	155.4	Vein	65	54	289.0618	-49.903	508595.7535	1191113.7	264.1859565	57.4112687	132.694466	NW zone
KLRD0028	157.4	S_0	35	260	289.0618	-49.903	508594.543	1191114.11	262.6479893	57.9000178	36.65903427	NW zone
KLRD0028	157.4	Vein	55	46	289.0618	-49.903	508594.543	1191114.11	262.6479893	68.083378	135.2960787	NW zone
KLRD0028	159.4	Vein	50	57	289.0618	-49.903	508593.3287	1191114.52	261.1144748	68.8232107	144.3433638	NW zone
KLRD0028	163	Vein	25	22	289.8648	-48.908	508591.133	1191115.29	258.3654646	77.1458024	309.6708334	NW zone
KLRD0028	166.9	S_0	75	344	289.8648	-48.908	508588.7406	1191116.13	255.4038282	55.2634604	104.5866962	NW zone
KLRD0028	168.8	S_0	85	98	289.8648	-48.908	508587.5699	1191116.55	253.967211	40.4418743	117.3513367	NW zone
KLRD0028	169.83	Vein	18	58	289.8648	-48.908	508586.9339	1191116.78	253.1901265	84.3668863	343.9912201	NW zone
KLRD0028	169.83	Vein	60	74	289.8648	-48.908	508586.9339	1191116.78	253.1901265	55.7826054	145.388375	NW zone
KLRD0028	169.83	Vein	22	214	289.8648	-48.908	508586.9339	1191116.78	253.1901265	38.0538064	347.110584	NW zone
KLRD0028	171	S_0	40	312	290.3508	-48.131	508586.2103	1191117.04	252.3087756	81.6461678	74.8379007	NW zone
KLRD0028	171.4	Vein	30	158	290.3508	-48.131	508585.9626	1191117.13	252.0077415	25.1285529	240.1495128	NW zone
KLRD0028	171.8	Fault	40	158	290.3508	-48.131	508585.7149	1191117.22	251.7068504	17.9016939	220.9662433	NW zone
KLRD0028	172.45	Intrusive contact	80	102	290.3508	-48.131	508585.312	1191117.37	251.2182075	40.1633364	125.2336638	NW zone
KLRD0028	173.4	Vein	80	77	290.3508	-48.131	508584.7226	1191117.58	250.5047173	44.559126	124.0310479	NW zone
KLRD0028	173.4	S_2	30	24	290.3508	-48.131	508584.7226	1191117.58	250.5047173	81.4526322	310.9440038	NW zone
KLRD0028	173.7	Vein	80	98	290.3508	-48.131	508584.5364	1191117.65	250.2795725	41.0299981	125.2627764	NW zone
KLRD0028	174.5	Vein	55	76	290.3508	-48.131	508584.0393	1191117.83	249.6795811	58.509775	150.81911	NW zone
KLRD0028	174.7	Intrusive contact	20	315	290.3508	-48.131	508583.915	1191117.88	249.529673	79.4412796	247.5522858	NW zone
KLRD0028	177.2	Intrusive contact	60	36	290.3508	-48.131	508582.3582	1191118.45	247.6588545	67.7334447	128.7059454	NW zone
KLRD0028	177.3	Vein	45	75	290.3508	-48.131	508582.2958	1191118.47	247.5841388	65.9725206	158.5907351	NW zone
KLRD0028	182.4	Vein	70	107	290.6539	-47.592	508579.1057	1191119.65	243.7848253	40.0519407	140.9615369	NW zone
KLRD0028	182.4	Vein	15	174	290.6539	-47.592	508579.1057	1191119.65	243.7848253	33.3932561	279.8408493	NW zone
KLRD0028	183.28	Vein	40	312	290.6539	-47.592	508578.5536	1191119.86	243.1310863	82.239961	75.34386051	NW zone
KLRD0028	183.28	Fault	17	28	290.6539	-47.592	508578.5536	1191119.86	243.1310863	69.6724476	319.0169579	NW zone
KLRD0028	183.3	S_0	60	72	290.6539	-47.592	508578.5411	1191119.86	243.1162342	57.2840358	144.827005	NW zone
KLRD0028	188.8	Intrusive contact	50	85	290.6539	-47.592	508575.0817	1191121.16	239.0414921	58.1209029	159.5829413	NW zone
KLRD0028	191.8	Intrusive contact	20	32	290.8	-47.322	508573.1885	1191121.87	236.8264578	73.4727058	321.9309665	NW zone
KLRD0028	192.45	S_0	58	58	290.8	-47.322	508572.7779	1191122.03	236.3469607	64.2355193	140.6721887	NW zone
KLRD0028	193.12	S_0	47	50	290.8	-47.322	508572.3546	1191122.19	235.8528506	75.9867678	143.3173424	NW zone
KLRD0028	194.55	Vein	14	114	290.8	-47.322	508571.4508	1191122.53	234.7987352	63.5684402	208.8941806	NW zone
KLRD0028	195.2	Vein	50	216	290.8	-47.322	508571.0398	1191122.69	234.3198071	23.6570501	40.41883054	NW zone
KLRD0028	195.2	S_2	60	35	290.8	-47.322	508571.0398	1191122.69	234.3198071	68.8494781	128.6468856	NW zone
KLRD0028	195.8	S_0	37	118	290.8	-47.322	508570.6603	1191122.83	233.8778391	45.8240177	190.2206168	NW zone
KLRD0028	196.35	S_0	80	130	290.8	-47.322	508570.3123	1191122.96	233.4728026	36.7893012	123.5716883	NW zone
KLRD0028	196.5	Vein	27	352	290.8	-47.322	508570.2174	1191123	233.3623548	74.7855199	283.3546731	NW zone
KLRD0028	198.5	Fault	15	40	290.8	-47.322	508568.9513	1191123.48	231.8904035	71.9486925	331.5083332	NW zone
KLRD0028	198.72	S_0	70	116	290.8	-47.322	508568.812	1191123.53	231.7285667	37.4834403	141.0800054	NW zone
KLRD0028	199.4	Vein	80	290	290.8	-47.322	508568.3812	1191123.69	231.2284417	46.861987	97.87799479	NW zone
KLRD0028	199.9	Vein	30	260	290.8	-47.322	508568.0644	1191123.81	230.8607969	61.996009	35.79002041	NW zone
KLRD0028	199.9	Fault	40	312	290.8	-47.322	508568.0644	1191123.81	230.8607969	82.813118	75.7846703	NW zone
KLRD0028	203	Vein	80	295	290.8	-47.322	508566.1	1191124.56	228.5817457	47.6024473	98.49491504	NW zone
KLRD0028	204.1	Fault	70	340	290.8	-47.322	508565.4029	1191124.83	227.7730506	61.7715963	103.170037	NW zone
KLRD0028	207.6	Vein	65	278	290.8	-47.322	508563.185	1191125.67	225.1999301	51.2124028	78.32623122	NW zone
KLRD0038	130.4	S_0	70	232	282.8833	-45.892	508566.8815	1191110.98	286.7018019	33.7398761	73.85487277	NW zone
KLRD0038	132	S_0	65	174	282.8833	-45.892	508565.817	1191111.22	285.5323547	18.4000808	110.9283203	NW zone
KLRD0038	150.3	S_0	65	286	292.2583	-44.326	508553.4987	1191114.46	272.40274	56.0807838	79.94311984	NW zone

DH_Hole	DH_Depth	Structure Type	Alpha	Beta	Azimut	Dip	DH_East	DH_North	DH_RL	Plot_Dip	Plot_DipDir	Domain
KLRD0038	151.1	S_0	35	150	292.2583	-44.326	508552.9643	1191114.65	271.8379415	24.8534034	212.4644828	NW zone
KLRD0038	154.6	Vein	22	60	292.2583	-44.326	508550.6306	1191115.5	269.3727221	86.2107224	344.0639577	NW zone
KLRD0038	156	S_0	70	110	292.2583	-44.326	508549.6993	1191115.86	268.3892389	42.006773	139.6762312	NW zone
KLRD0038	160.4	S_0	65	166	285.9992	-44.497	508546.7811	1191117.02	265.307841	22.0770475	127.730043	NW zone
KLRD0038	165.4	Vein	18	40	285.9992	-44.497	508543.4333	1191118.27	261.8104923	72.3136913	328.8584918	NW zone
KLRD0038	168.1	Intrusive contact	33	210	285.9992	-44.497	508541.6016	1191118.86	259.9186821	25.8760437	1.105433268	NW zone
KLRD0038	168.2	Vein	27	354	285.9992	-44.497	508541.5335	1191118.88	259.8485636	71.7305853	281.5642319	NW zone
KLRD0038	168.8	Intrusive contact	14	170	285.9992	-44.497	508541.1243	1191119.01	259.4277704	31.7102024	267.9964375	NW zone
KLRD0038	171.2	Vein	50	350	282.8833	-44.283	508539.4803	1191119.48	257.7448942	85.1258951	99.2243691	NW zone
KLRD0038	172.62	S_2	25	174	282.8833	-44.283	508538.5031	1191119.75	256.7503679	20.0419546	269.1101986	NW zone
KLRD0038	172.62	Intrusive contact	60	330	282.8833	-44.283	508538.5031	1191119.75	256.7503679	72.710225	89.97873238	NW zone
KLRD0038	178.2	S_0	90	280	282.8833	-44.283	508534.6395	1191120.74	252.847084	45.6658278	103.4088703	NW zone
KLRD0038	182.9	S_1	42	340	282.8833	-44.283	508531.3616	1191121.49	249.5646875	88.1266071	268.1588227	NW zone
KLRD0050	123.4	Vein	52	254	292.121	-50.36	508520.9128	1191104.98	290.0416013	44.1237191	52.26976724	NW zone
KLRD0050	123.4	S_2	52	317	292.121	-50.36	508520.9128	1191104.98	290.0416013	70.9801875	84.11914986	NW zone
KLRD0050	123.4	Vein	7	219	292.121	-50.36	508520.9128	1191104.98	290.0416013	54.4033526	340.6768882	NW zone
KLRD0050	126.6	Vein	72	90	292.121	-50.36	508519.0185	1191105.71	287.565547	42.7229236	138.4255127	NW zone
KLRD0050	126.6	S_2	60	283	292.121	-50.36	508519.0185	1191105.71	287.565547	53.3067673	73.91550802	NW zone
KLRD0050	126.6	Vein	8	0	292.121	-50.36	508519.0185	1191105.71	287.565547	58.5743718	291.3301715	NW zone
KLRD0050	128	Vein	52	140	292.121	-50.36	508518.1905	1191106.03	286.4845663	24.7630242	182.4839935	NW zone
KLRD0050	128	Vein	65	160	292.121	-50.36	508518.1905	1191106.03	286.4845663	17.8326491	139.7763521	NW zone
KLRD0050	128	S_0	65	160	292.121	-50.36	508518.1905	1191106.03	286.4845663	17.8326491	139.7763521	NW zone
KLRD0050	128	S_2	75	102	292.121	-50.36	508518.1905	1191106.03	286.4845663	38.7759403	135.4554461	NW zone
KLRD0050	130	Fault	70	122	294.6953	-49.722	508517.0084	1191106.51	284.9427147	32.9423645	144.4003304	NW zone
KLRD0050	131.35	S_0	34	160	294.6953	-49.722	508516.2108	1191106.83	283.9037664	21.8824765	242.9096728	NW zone
KLRD0050	132	S_0	40	148	294.6953	-49.722	508515.827	1191106.99	283.4039922	24.5403974	214.9354844	NW zone
KLRD0050	133	S_0	30	172	294.6953	-49.722	508515.2368	1191107.24	282.6356912	21.0221386	273.3787958	NW zone
KLRD0050	133.8	S_0	30	174	294.6953	-49.722	508514.7649	1191107.44	282.0215573	20.6417555	278.1316088	NW zone
KLRD0050	134.25	Vein	25	170	294.6953	-49.722	508514.4995	1191107.55	281.6763045	26.2422256	272.4457298	NW zone
KLRD0050	134.25	Vein	75	78	294.6953	-49.722	508514.4995	1191107.55	281.6763045	45.0739207	134.2467144	NW zone
KLRD0050	134.25	Vein	42	104	294.6953	-49.722	508514.4995	1191107.55	281.6763045	51.0591856	181.2783796	NW zone
KLRD0050	137.1	S_0	19	82	294.6953	-49.722	508512.8207	1191108.29	279.4929925	80.5336601	185.5333455	NW zone
KLRD0050	138.45	Vein	40	40	294.6953	-49.722	508512.0267	1191108.64	278.4607653	83.5581121	144.1437319	NW zone
KLRD0050	139	S_2	80	102	294.6953	-49.722	508511.7035	1191108.79	278.0405902	39.1495772	130.0456218	NW zone
KLRD0050	139	S_0	18	170	294.6953	-49.722	508511.7035	1191108.79	278.0405902	32.8004299	276.6888765	NW zone
KLRD0050	139	Vein	42	360	294.6953	-49.722	508511.7035	1191108.79	278.0405902	88.1995403	114.4388558	NW zone
KLRD0050	139	Vein	15	174	294.6953	-49.722	508511.7035	1191108.79	278.0405902	35.1418742	284.3363158	NW zone
KLRD0050	140.14	Intrusive contact	20	200	295.4506	-48.834	508511.0339	1191109.1	277.1703719	33.6882452	330.1278711	NW zone
KLRD0050	145.05	Intrusive contact	40	170	295.4506	-48.834	508508.1408	1191110.44	273.4372544	11.7280519	254.1341424	NW zone
KLRD0050	151.4	Vein	20	42	295.7861	-48.501	508504.3749	1191112.22	268.6448395	78.3108938	335.4331856	NW zone
KLRD0050	153.3	S_1	45	330	295.7861	-48.501	508503.2446	1191112.76	267.2162285	82.604225	94.59850719	NW zone
KLRD0050	153.4	Intrusive contact	45	310	295.7861	-48.501	508503.1851	1191112.79	267.1410767	76.544364	81.63902724	NW zone
KLRD0050	155.4	Intrusive contact	30	40	295.7861	-48.501	508501.9943	1191113.36	265.6388464	86.3818702	329.5498712	NW zone
KLRD0050	159	Vein	17	166	295.7861	-48.501	508499.8487	1191114.39	262.9386989	33.4850884	271.0197679	NW zone
KLRD0050	160.16	S_0	70	290	296.1237	-48.168	508499.1568	1191114.72	262.0697121	51.2461463	91.47337645	NW zone
KLRD0050	164.65	Intrusive contact	60	60	296.1237	-48.168	508496.4755	1191116.02	258.7110241	61.2837925	145.5637831	NW zone
KLRD0050	164.8	Vein	85	88	296.1237	-48.168	508496.3859	1191116.07	258.5989525	42.104505	123.4416486	NW zone
KLRD0050	168	Vein	80	292	296.1237	-48.168	508494.4721	1191117	256.2101578	46.1970556	103.0871424	NW zone
KLRD0050	168.1	Intrusive contact	50	30	296.1237	-48.168	508494.4123	1191117.03	256.1355716	78.3547149	135.1336911	NW zone
KLRD0050	168.7	Intrusive contact	30	74	296.1237	-48.168	508494.0532	1191117.21	255.6881356	77.6835958	174.557814	NW zone
KLRD0050	172.84	Vein	60	80	296.4373	-47.583	508491.5722	1191118.42	252.6058149	54.1753939	153.6170047	NW zone
KLRD0050	173.65	Intrusive contact	50	340	296.4373	-47.583	508491.0858	1191118.66	252.0040714	80.5118521	103.3435414	NW zone
KLRD0050	174.6	Intrusive contact	70	80	296.4373	-47.583	508490.5149	1191118.95	251.2988943	48.8220776	142.8065162	NW zone
KLRD0050	176.38	Intrusive contact	55	340	296.4373	-47.583	508489.444	1191119.47	249.9792776	75.8282056	104.6470437	NW zone
KLRD0050	176.76	Intrusive contact	80	118	296.4373	-47.583	508489.2151	1191119.59	249.6978428	38.3403263	130.6300643	NW zone
KLRD0050	177.2	Intrusive contact	75	0	296.4373	-47.583	508488.9501	1191119.72	249.3720946	57.1972119	116.3204333	NW zone
KLRD0050	180.5	Vein	35	39	296.7476	-46.751	508486.9589	1191120.71	246.9332583	89.6979804	327.4452844	NW zone
KLRD0050	186.2	Vein	20	174	296.7476	-46.751	508483.501	1191122.43	242.7439597	27.4931079	284.3504849	NW zone
KLRD0050	186.56	S_0	40	48	296.7476	-46.751	508483.2818	1191122.54	242.4804493	83.0329415	151.6311799	NW zone
KLRD0050	188.15	Intrusive contact	25	46	296.7476	-46.751	508482.3122	1191123.03	241.3181478	82.9882035	337.7680711	NW zone

DH_Hole	DH_Depth	Structure Type	Alpha	Beta	Azimut	Dip	DH_East	DH_North	DH_RL	Plot_Dip	Plot_DipDir	Domain
KLRD0050	189.5	Vein	40	348	296.7476	-46.751	508481.4875	1191123.45	240.333258	87.5196885	287.5343781	NW zone
KLRD0050	190.63	Vein	40	338	297.0623	-45.918	508480.796	1191123.8	239.510264	88.8662555	280.0980386	NW zone
KLRD0050	191.1	S_o	50	340	297.0623	-45.918	508480.5081	1191123.94	239.1683319	81.7915285	103.944065	NW zone
KLRD0050	192.37	Intrusive contact	30	334	297.0623	-45.918	508479.7294	1191124.33	238.2454898	80.0126348	274.1764888	NW zone
KLRD0050	194.5	Vein	60	306	297.0623	-45.918	508478.4205	1191125	236.7013501	64.9821643	90.41068772	NW zone
KLRD0050	197.5	Intrusive contact	33	350	297.0623	-45.918	508476.571	1191125.94	234.5342209	79.6122141	288.4816034	NW zone
KLRD0050	201.2	So	33	359	297.9939	-44.503	508474.2804	1191127.11	231.8744234	78.7675522	296.3099243	NW zone
KLRD0050	211.5	Intrusive contact	31	320	299.6052	-42.513	508467.8318	1191130.49	224.5896997	83.62472	264.5341311	NW zone
KLRD0050	212	So	31	44	299.6052	-42.513	508467.5159	1191130.66	224.241401	85.1481865	335.0302671	NW zone
KLRD0050	216.25	Vein	80	80	299.6052	-42.513	508464.8191	1191132.13	221.3060929	49.2062173	132.0416703	NW zone
KLRD0050	233.45	Vein	30	344	302.0504	-39.315	508453.7246	1191138.64	209.8923541	71.6154883	287.0000141	NW zone
KLRD0050	237.25	Vein	40	48	302.0504	-39.315	508451.2432	1191140.17	207.4557923	89.0569175	156.4981685	NW zone
KLRD0050	240.4	Intrusive contact	18	50	302.3855	-38.945	508449.1799	1191141.46	205.4538048	73.9063266	351.3733879	NW zone
KLRD0050	244	Vein	30	330	302.3855	-38.945	508446.8184	1191142.94	203.1768673	74.5771787	275.5081252	NW zone

Table A1-3: MSc project structural measurements data of the Central zone

DH_Hole	DH_Depth	Structure Type	Alpha	Beta	Azimut	Dip	DH_East	DH_North	DH_RL	Plot_Dip	Plot_DipDir	Domain
KLRD0009	92.9	S_o	74	320	275.4542	-56.153	508809.3632	1190908.25	308.3485964	46.9589461	80.80126563	C zone
KLRD0009	93	Vein	45	122	275.4542	-56.153	508809.3078	1190908.25	308.2654312	37.233105	177.1710832	C zone
KLRD0009	95.9	Vein	46	84	275.4542	-56.153	508807.7026	1190908.39	305.85433	56.1159707	151.4783475	C zone
KLRD0009	95.9	S_2	55	84	275.4542	-56.153	508807.7026	1190908.39	305.85433	49.6457752	143.6191551	C zone
KLRD0009	98.5	Fault	70	240	275.4542	-56.153	508806.2623	1190908.52	303.6937813	28.8773503	57.65191158	C zone
KLRD0009	99.85	Vein	85	271	275.4542	-56.153	508805.514	1190908.6	302.5723778	34.2621342	86.57791804	C zone
KLRD0009	99.85	Vein	12	30	275.4542	-56.153	508805.514	1190908.6	302.5723778	72.5896935	306.3166297	C zone
KLRD0009	101.8	S_o	55	284	276.2275	-55.991	508804.4326	1190908.7	300.9530999	52.9155871	51.24466076	C zone
KLRD0009	104.54	S_o	55	323	276.2275	-55.991	508802.912	1190908.85	298.678819	64.9066973	73.40856072	C zone
KLRD0009	105.6	Vein	82	273	276.2275	-55.991	508802.3234	1190908.91	297.7993035	35.149007	81.84428689	C zone
KLRD0009	109.87	Vein	42	128	276.2275	-55.991	508799.9507	1190909.16	294.2581289	35.8474823	186.6519263	C zone
KLRD0009	113.23	S_o	53	30	276.9023	-55.6	508798.0799	1190909.37	291.4748452	68.3522	115.2993877	C zone
KLRD0009	114.7	Vein	28	52	276.9023	-55.6	508797.2597	1190909.46	290.258514	85.2928378	140.9309927	C zone
KLRD0009	114.7	Vein	5	110	276.9023	-55.6	508797.2597	1190909.46	290.258514	74.7031993	200.6057298	C zone
KLRD0009	117.76	S_o	60	134	276.9023	-55.6	508795.549	1190909.66	287.7292094	24.3129944	157.5310453	C zone
KLRD0009	132.25	Vein	14	210	278.1287	-54.405	508787.365	1190910.7	275.8168095	47.1015231	319.0464968	C zone
KLRD0009	142.34	Vein	65	260	278.7852	-53.901	508781.5721	1190911.51	267.5953706	38.8649475	56.74616857	C zone
KLRD0009	144.8	Vein	85	280	278.7852	-53.901	508780.1493	1190911.72	265.59953	37.0324186	90.30762912	C zone
KLRD0009	148.1	Vein	7	354	278.7852	-53.901	508778.2349	1190912.01	262.9270715	61.1737831	271.9049187	C zone
KLRD0009	154.38	Vein	24	342	279.5591	-53.503	508774.5752	1190912.58	257.855831	79.2461447	262.481713	C zone
KLRD0009	156.74	Vein	55	68	279.5591	-53.503	508773.1954	1190912.8	255.9543302	57.8933421	138.3204382	C zone
KLRD0009	162	Vein	12	200	280.34	-53.108	508770.1117	1190913.32	251.7244792	44.4002089	308.2412535	C zone
KLRD0009	173.53	S_o	60	220	280.9853	-52.6	508763.3119	1190914.54	242.4932196	22.8137957	44.61987447	C zone
KLRD0009	175.3	S_o	38	226	280.9853	-52.6	508762.2621	1190914.74	241.0817951	34.7912094	4.041510188	C zone
KLRD0009	186.42	S_o	70	302	281.5595	-52.002	508755.6239	1190916.03	232.2550196	50.7901799	79.33061468	C zone
KLRD0009	192.57	S_o	55	242	282.141	-51.404	508751.9167	1190916.79	227.4066299	35.8163509	41.7039768	C zone
KLRD0009	201.7	Vein	12	108	282.8343	-51.001	508746.3665	1190917.96	220.253635	69.4337027	198.8458291	C zone
KLRD0009	201.7	Fault	10	6	282.8343	-51.001	508746.3665	1190917.96	220.253635	61.4975857	289.0867264	C zone
KLRD0009	202.75	S_o	31	232	282.8343	-51.001	508745.7253	1190918.1	219.4340162	42.9504714	4.808624976	C zone
KLRD0009	203.1	Vein	45	214	282.8343	-51.001	508745.5114	1190918.15	219.1609176	23.3092941	10.18356321	C zone
KLRD0009	204.6	Vein	30	348	282.8343	-51.001	508744.5945	1190918.35	217.9911056	81.9629407	271.8826531	C zone
KLRD0009	205.34	Vein	45	316	282.8343	-51.001	508744.1418	1190918.45	217.4143631	76.6122603	72.26357662	C zone
KLRD0009	209	Vein	15	344	282.8343	-51.001	508741.8999	1190918.95	214.5653714	67.4841909	266.0766372	C zone
KLRD0009	222.5	Vein	55	334	284.5788	-50.61	508733.6136	1190920.92	204.0903966	72.0594982	88.66425662	C zone
KLRD0009	222.66	Intrusive contact	46	284	284.5788	-50.61	508733.5153	1190920.94	203.9664865	63.2156018	54.96080618	C zone
KLRD0009	224.3	Vein	65	274	284.5788	-50.61	508732.5083	1190921.19	202.6967211	46.9140169	68.73107991	C zone
KLRD0009	245	Vein	60	50	286.0608	-49.603	508719.7574	1190924.59	186.7490944	62.8684051	131.1495082	C zone
KLRD0009	245.75	Intrusive contact	62	30	286.0608	-49.603	508719.2922	1190924.73	186.1755767	65.6827775	120.7703585	C zone
KLRD0009	248.75	Intrusive contact	54	76	286.0608	-49.603	508717.4284	1190925.26	183.8852853	58.3787393	148.076866	C zone
KLRD0009	248.95	Intrusive contact	47	14	286.0608	-49.603	508717.304	1190925.29	183.7328145	82.6094113	115.6050119	C zone
KLRD0009	250.4	Vein	60	237	286.7777	-49.007	508716.4012	1190925.55	182.6282113	33.257766	56.15278862	C zone
KLRD0009	257.3	Vein	30	64	286.7777	-49.007	508712.0899	1190926.81	177.3913369	82.5251082	158.3118055	C zone
KLRD0009	264.85	Intrusive contact	25	334	287.3507	-48.55	508707.3455	1190928.25	171.6963425	77.4239657	262.9493905	C zone
KLRD0009	266.15	Vein	55	88	287.3507	-48.55	508706.5263	1190928.5	170.7188626	52.9707866	153.0523666	C zone
KLRD0009	267.3	Vein	85	256	287.3507	-48.55	508705.8012	1190928.73	169.8549077	40.3272267	99.65134584	C zone
KLRD0009	269.8	Intrusive contact	80	62	287.3507	-48.55	508704.2229	1190929.22	167.9791401	46.8346008	119.5039349	C zone
KLRD0009	274.92	S_o	70	42	287.8537	-48.251	508700.9855	1190930.23	164.1456803	57.7177293	123.2933647	C zone
KLRD0009	275.2	Vein	90	274	287.8537	-48.251	508700.8083	1190930.29	163.9362996	41.5900826	107.5875086	C zone
KLRD0009	280.75	Vein	45	346	288.3595	-47.954	508697.2929	1190931.42	159.7916773	85.9189039	97.93427111	C zone
KLRD0009	281.39	Intrusive contact	45	96	288.3595	-47.954	508696.8872	1190931.55	159.314428	54.8294412	167.3797101	C zone
KLRD0009	285.75	Vein	51	340	288.3595	-47.954	508694.1209	1190932.45	156.0669412	79.5061844	95.60720321	C zone
KLRD0009	291	Vein	25	352	288.9351	-47.517	508690.7853	1190933.55	152.1653796	73.2336902	280.8877008	C zone
KLRD0009	291	Vein	42	130	288.9351	-47.517	508690.7853	1190933.55	152.1653796	35.2444909	189.0356667	C zone
KLRD0009	301.8	Vein	80	92	289.6089	-46.952	508683.8981	1190935.89	144.180869	43.1563749	123.7239454	C zone
KLRD0009	304	Vein	75	86	289.6089	-46.952	508682.49	1190936.37	142.562665	45.7734916	130.3274317	C zone
KLRD0009	313.34	Vein	60	78	290.2894	-46.39	508676.4895	1190938.5	135.7287367	55.9089596	145.9524281	C zone
KLRD0043B	119.5	S_o	30	230	290.6902	-50.933	508864.2402	1190909.94	286.4868499	42.3691901	10.4637822	C zone

DH_Hole	DH_Depth	Structure Type	Alpha	Beta	Azimut	Dip	DH_East	DH_North	DH_RL	Plot_Dip	Plot_DipDir	Domain
KLRD0043B	119.7	Vein	40	226	290.6902	-50.933	508864.1224	1190909.99	286.3314616	33.444549	19.58998354	C zone
KLRD0043B	125	S_0	40	218	292.0837	-50.002	508860.9899	1190911.19	282.2292772	28.3580823	14.58200709	C zone
KLRD0043B	129.3	S_0	45	248	292.0837	-50.002	508858.4361	1190912.21	278.9223538	44.5903346	42.98201359	C zone
KLRD0043B	130.2	S_0	58	268	293.5021	-49.078	508857.9002	1190912.42	278.2326341	48.5505192	67.07486009	C zone
KLRD0043B	130.2	Vein	23	64	293.5021	-49.078	508857.9002	1190912.42	278.2326341	87.6851294	167.9266328	C zone
KLRD0043B	130.2	Vein	41	44	293.5021	-49.078	508857.9002	1190912.42	278.2326341	81.1247781	144.0780158	C zone
KLRD0043B	144.45	Vein	88	308	294.3675	-48.417	508849.3606	1190916.07	267.4222369	42.487549	111.5766365	C zone
KLRD0043B	146.55	S_0	65	290	294.3675	-48.417	508848.0946	1190916.63	265.8442202	54.2306603	84.79732727	C zone
KLRD0043B	150.25	S_0	40	226	294.9043	-48.085	508845.86	1190917.63	263.0720558	33.4876791	27.23171379	C zone
KLRD0043B	150.25	Vein	54	344	294.9043	-48.085	508845.86	1190917.63	263.0720558	76.6559525	104.7368655	C zone
KLRD0043B	153.2	Vein	53	52	294.9043	-48.085	508844.0758	1190918.45	260.8674286	69.5089875	144.9444525	C zone
KLRD0043B	154.1	S_0	58	36	294.9043	-48.085	508843.5312	1190918.7	260.1954974	69.6190109	133.9360045	C zone
KLRD0043B	154.1	Vein	42	54	294.9043	-48.085	508843.5312	1190918.7	260.1954974	77.9213396	152.4682147	C zone
KLRD0043B	154.1	Vein	75	74	294.9043	-48.085	508843.5312	1190918.7	260.1954974	47.6272312	134.2085893	C zone
KLRD0043B	157.6	S_0	80	276	294.9043	-48.085	508841.4124	1190919.67	257.5853981	43.7904862	100.2930848	C zone
KLRD0043B	158.7	Vein	43	345	294.9043	-48.085	508840.7462	1190919.98	256.7660562	87.8627547	103.8252433	C zone
KLRD0043B	160.8	Fault	60	80	295.4445	-47.754	508839.4739	1190920.57	255.2031598	54.1213945	152.3829845	C zone
KLRD0043B	163	Vein	75	64	295.4445	-47.754	508838.1404	1190921.19	253.5676748	50.0165114	132.6326158	C zone
KLRD0043B	163.8	Vein	70	72	295.4445	-47.754	508837.6553	1190921.42	252.9734163	51.1992126	139.8445113	C zone
KLRD0043B	167.3	Vein	32	350	295.4445	-47.754	508835.5323	1190922.42	250.3764418	80.2907401	286.7938817	C zone
KLRD0043B	172	Vein	53	66	295.7308	-47.236	508832.6784	1190923.77	246.8969827	64.8549487	152.9179255	C zone
KLRD0043B	172	Vein	80	90	295.7308	-47.236	508832.6784	1190923.77	246.8969827	43.32855	130.1794533	C zone
KLRD0043B	175.6	Vein	75	112	295.7308	-47.236	508830.4866	1190924.82	244.2403577	39.0129873	138.0300473	C zone
KLRD0043B	185.7	Vein	44	54	295.7926	-46.542	508824.3008	1190927.8	236.8328267	77.4100701	152.368129	C zone
KLRD0043B	190.7	Vein	55	140	295.8553	-45.847	508821.2112	1190929.29	233.1959623	26.2872096	172.1535806	C zone
KLRD0043B	193.1	S_1	70	308	295.8553	-45.847	508819.7214	1190930.01	231.4576684	57.7392714	97.22991008	C zone
KLRD0043B	193.1	Vein	30	351	295.8553	-45.847	508819.7214	1190930.01	231.4576684	76.7258207	287.8139542	C zone
KLRD0043B	207.45	Vein	65	317	296.1192	-44.867	508810.7175	1190934.38	221.1749257	64.8626607	97.47498044	C zone
KLRD0043B	211.8	Vein	70	294	296.5957	-43.601	508807.9505	1190935.74	218.1047638	55.8849593	94.04466397	C zone
KLRD0043B	211.8	Vein	90	244	296.5957	-43.601	508807.9505	1190935.74	218.1047638	45.392545	116.2171302	C zone
KLRD0043B	214.45	Vein	80	262	296.5957	-43.601	508806.2548	1190936.58	216.2482999	45.2322915	102.3444129	C zone
KLRD0043B	216.3	Vein	45	196	296.5957	-43.601	508805.0663	1190937.17	214.9588527	11.4300183	36.84984606	C zone
KLRD0043B	218.4	Vein	60	236	296.5957	-43.601	508803.7126	1190937.84	213.5017366	36.7188573	72.61389261	C zone
KLRD0043B	222.45	Vein	54	230	297.0811	-42.336	508801.0883	1190939.15	210.7114685	33.9337193	62.95503501	C zone
KLRD0043B	224.5	Vein	60	310	297.0811	-42.336	508799.7532	1190939.83	209.3091471	69.0901083	92.58671511	C zone
KLRD0043B	228.1	Fault	70	248	297.0811	-42.336	508797.3978	1190941.02	206.8629566	43.1536817	89.39160456	C zone
KLRD0043B	230.9	Vein	55	282	297.854	-41.568	508795.5568	1190941.96	204.9746596	62.3978149	77.83041511	C zone
KLRD0043B	234.3	Fault	30	316	297.854	-41.568	508793.316	1190943.12	202.693597	82.6284375	260.0699039	C zone
KLRD0043B	234.3	Vein	50	226	297.854	-41.568	508793.316	1190943.12	202.693597	32.3879541	57.73438484	C zone
KLRD0043B	234.3	Vein	40	28	297.854	-41.568	508793.316	1190943.12	202.693597	85.846074	318.5503824	C zone
KLRD0043B	238.35	Vein	45	318	297.854	-41.568	508790.6419	1190944.52	199.9914605	85.5242478	89.39292495	C zone
KLRD0043B	239.9	Vein	20	334	297.854	-41.568	508789.617	1190945.06	198.9616393	66.1073862	271.1267555	C zone
KLRD0043B	241.6	Fault	60	344	298.9975	-41.307	508788.4931	1190945.65	197.8341021	77.6500555	110.0409502	C zone
KLRD0043B	244.3	S_0	75	58	298.9975	-41.307	508786.7105	1190946.61	196.0453338	57.5531998	133.4790996	C zone
KLRD0043B	246	Vein	30	308	298.9975	-41.307	508785.5899	1190947.21	194.9203385	86.0172903	255.4915765	C zone
KLRD0043B	251.6	Vein	25	26	300.1459	-41.052	508781.9076	1190949.24	191.22141	70.5206554	324.0826526	C zone
KLRD0043B	252.3	Fault	20	20	300.1459	-41.052	508781.4484	1190949.5	190.759801	64.0192378	320.1066129	C zone
KLRD0043B	252.4	Vein	20	24	300.1459	-41.052	508781.3828	1190949.54	190.6938702	65.1905094	324.0604246	C zone
KLRD0043B	252.7	Vein	55	326	300.1459	-41.052	508781.186	1190949.65	190.4960979	79.5118942	100.3735796	C zone
KLRD0043B	254.35	S_0	46	308	300.1459	-41.052	508780.1048	1190950.26	189.4088856	81.2424002	85.77932292	C zone
KLRD0043B	259.3	S_0	20	256	300.1459	-41.052	508776.869	1190952.11	186.1526657	66.6721347	36.97445232	C zone
KLRD0043B	265.1	S_0	60	264	300.5467	-40.667	508773.0851	1190954.31	182.3500731	52.6840489	81.63434957	C zone
KLRD0043B	270.9	S_0	50	314	300.239	-40.201	508769.2974	1190956.54	178.5645796	80.7306408	92.55722164	C zone
KLRD0043B	273.6	Vein	25	20	300.239	-40.201	508767.5296	1190957.58	176.8088534	68.107713	319.9638529	C zone
KLRD0043B	281.8	S_0	60	286	299.9293	-39.735	508762.1311	1190960.74	171.5043318	63.046508	87.58609949	C zone
KLRD0043B	281.8	Vein	60	38	299.9293	-39.735	508762.1311	1190960.74	171.5043318	75.0786099	138.7920653	C zone
KLRD0043B	286.5	S_0	75	50	299.9293	-39.735	508759.0169	1190962.54	168.4827801	60.6095853	133.137486	C zone
KLRD0043B	286.5	Vein	55	49	299.9293	-39.735	508759.0169	1190962.54	168.4827801	76.3774504	146.434196	C zone
KLRD0043B	293.8	Vein	9	39	299.9867	-39.284	508754.1529	1190965.35	163.8169254	60.5698895	345.4763005	C zone
KLRD0043B	296.1	Vein	33	58	299.9867	-39.284	508752.6155	1190966.23	162.3535955	89.8421539	165.3025281	C zone
KLRD0043B	311.9	S_0	10	162	300.8052	-38.419	508742.0165	1190972.39	152.386531	32.980931	266.4666688	C zone

DH_Hole	DH_Depth	Structure Type	Alpha	Beta	Azimut	Dip	DH_East	DH_North	DH_RL	Plot_Dip	Plot_DipDir	Domain
KLRD0043B	315	S_0	30	144	300.8052	-38.419	508739.9328	1190973.62	150.4481987	30.7427647	215.8583101	C zone
KLRD0043B	341.1	Intrusive contact	80	100	302.1608	-37.203	508722.3545	1190984.25	134.3483671	51.3492565	134.3626281	C zone
KLRD0043B	342.15	Intrusive contact	13	310	302.1608	-37.203	508721.6466	1190984.69	133.7086385	68.9543506	248.6068693	C zone
KLRD0043B	345.6	Intrusive contact	60	220	302.1608	-37.203	508719.3206	1190986.14	131.610951	33.8381179	86.62999387	C zone
KLRD0043B	348.7	Intrusive contact	30	214	302.1608	-37.203	508717.2305	1190987.45	129.731672	29.0590958	27.64251438	C zone
KLRD0043B	354.24	Vein	40	246	302.6199	-36.846	508713.4952	1190989.8	126.3859609	50.5210222	57.34681212	C zone
KLRD0043B	355.1	Intrusive contact	85	316	302.6199	-36.846	508712.9154	1190990.17	125.8679669	56.6496285	118.2388765	C zone
KLRD0043B	357.34	Vein	38	70	302.6199	-36.846	508711.4054	1190991.13	124.5204999	81.1454919	171.1147481	C zone
KLRD0043B	360.7	Vein	52	62	303.0885	-36.541	508709.1406	1190992.57	122.5039659	76.0100425	156.645244	C zone
KLRD0043B	363.5	Vein	50	54	303.0885	-36.541	508707.2538	1190993.79	120.8273882	81.0443888	154.5267445	C zone
KLRD0043B	366.1	Vein	40	170	303.0885	-36.541	508705.5024	1190994.92	119.2735181	8.53245641	186.6609407	C zone
KLRD0043B	367.24	Intrusive contact	85	98	303.0885	-36.541	508704.7347	1190995.41	118.5931025	52.8346159	129.1690806	C zone
KLRD0043B	367.6	So	60	148	303.0885	-36.541	508704.4923	1190995.57	118.378348	31.0190183	153.8929811	C zone
KLRD0043B	369.7	Vein	45	156	303.0885	-36.541	508703.0784	1190996.49	117.1267002	19.9652471	180.524625	C zone
KLRD0043B	370.1	Intrusive contact	87	90	303.0885	-36.541	508702.8091	1190996.67	116.8885014	53.5500404	126.8704825	C zone
KLRD0043B	374.8	Vein	45	354	303.556	-36.239	508699.6465	1190998.74	114.0948259	81.5665269	299.0439744	C zone
KLRD0043B	376	Vein	42	340	303.556	-36.239	508698.8393	1190999.27	113.3830649	80.488818	288.3947382	C zone
KLRD0043B	378.9	Vein	60	63	303.556	-36.239	508696.8894	1191000.55	111.6655253	70.7770745	151.6645127	C zone
KLRD0043B	384	Vein	70	82	303.9367	-35.78	508693.4606	1191002.83	108.6555393	58.9771504	146.9407371	C zone
KLRD0043B	387.6	Intrusive contact	45	262	303.9367	-35.78	508691.0389	1191004.45	106.5408858	60.3424536	70.10833578	C zone
KLRD0043B	390	Vein	88	296	304.2445	-35.174	508689.4239	1191005.54	105.1357822	55.1013148	121.7285854	C zone
KLRD0043B	390.6	So	22	352	304.2445	-35.174	508689.02	1191005.81	104.7851303	58.2896456	295.1959514	C zone
KLRD0043B	390.6	Vein	88	304	304.2445	-35.174	508689.02	1191005.81	104.7851303	55.3398964	121.9046098	C zone
KLRD0043B	395.4	So	22	350	304.2445	-35.174	508685.7854	1191007.99	101.9910526	58.2117023	293.193836	C zone
KLRD0043B	402.3	Vein	27	342	304.5546	-34.568	508681.1251	1191011.16	98.00935989	64.3620106	286.5147748	C zone
KLRD0043B	403.2	Intrusive contact	35	109	304.5546	-34.568	508680.5164	1191011.58	97.493044	56.7808771	192.0895301	C zone
KLRD0043B	406.7	Vein	22	308	304.5546	-34.568	508678.1471	1191013.2	95.49182094	75.1693311	255.3878263	C zone
KLRD0043B	407.5	Intrusive contact	25	350	304.5546	-34.568	508677.6051	1191013.57	95.03589064	60.4560728	294.0618123	C zone
KLRD0043B	410.5	Vein	35	70	304.7	-34.264	508675.5713	1191014.97	93.33105225	84.6041977	175.2252081	C zone
KLRD0043B	413	Vein	37	32	304.7	-34.264	508673.8753	1191016.14	91.91449332	77.4540257	330.2791643	C zone
KLRD0043B	413.2	So	36	336	304.7	-34.264	508673.7396	1191016.23	91.80128685	73.9728757	284.5641687	C zone
KLRD0043B	413.2	Vein	26	336	304.7	-34.264	508673.7396	1191016.23	91.80128685	64.6390933	280.7215317	C zone
WKL0147	96.3	Vein	28	346	271.2833	-55.2	508723.5742	1190900.25	307.7870073	84.0529387	258.8745507	C zone
WKL0147	97.44	So	45	260	271.2833	-55.2	508722.9237	1190900.26	306.8509279	49.4084182	24.77995176	C zone
WKL0147	99.4	S1	40	154	271.2833	-55.2	508721.8053	1190900.29	305.2415281	22.9558624	211.8461163	C zone
WKL0147	109.9	Intrusive contact	90	114	271.2833	-55.2	508715.8139	1190900.42	296.6197439	34.8102535	91.2760089	C zone
WKL0147	141.8	Intrusive contact	55	176	271.2833	-55.2	508697.6115	1190900.83	270.425942	2.29640944	184.3726168	C zone
WKL0147	150.2	Intrusive contact	40	162	271.2833	-55.2	508692.8184	1190900.93	263.5285146	19.3243861	225.6041318	C zone
WKL0147	158.4	Vein	44	160	271.2833	-55.2	508688.1394	1190901.04	256.7953116	17.0156002	214.0572253	C zone
WKL0147	160.5	Vein	37	346	271.2833	-55.2	508686.9411	1190901.07	255.0709548	87.0335356	80.12084471	C zone
WKL0147	161.7	Vein	12	62	271.2833	-55.2	508686.2564	1190901.08	254.085608	84.7534884	331.4208451	C zone
WKL0147	161.7	S2	70	130	271.2833	-55.2	508686.2564	1190901.08	254.085608	26.2291745	127.6331187	C zone
WKL0147	196.8	So	38	98	271.2833	-55.2	508666.228	1190901.53	225.2642148	55.3826302	162.7552821	C zone
WKL0147	196.8	So	47	140	271.2833	-55.2	508666.228	1190901.53	225.2642148	26.0100977	182.7718763	C zone
WKL0147	197	Vein	30	140	271.2833	-55.2	508666.1138	1190901.53	225.0999903	37.8854219	206.2493001	C zone
WKL0147	197	So	27	160	271.2833	-55.2	508666.1138	1190901.53	225.0999903	31.7106705	235.8419601	C zone
WKL0147	206.4	Vein	20	330	271.2833	-55.2	508660.7501	1190901.65	217.3814406	79.4117176	242.7221282	C zone
WKL0147	213.42	Vein	33	146	271.2833	-55.2	508656.7444	1190901.74	211.6171619	32.4256944	210.2753839	C zone
WKL0147	217	Vein	15	232	271.2833	-55.2	508654.7017	1190901.79	208.677544	56.4967806	337.1741193	C zone
WKL0147	217	S2	81	268	271.2833	-55.2	508654.7017	1190901.79	208.677544	35.5059495	75.6602449	C zone
WKL0147	217.8	Vein	43	344	271.2833	-55.2	508654.2452	1190901.8	208.0206462	80.8728999	79.49489024	C zone

Table A1-4: MSc project structural measurements data of the South zone

DH_Hole	DH_Depth	Structure Type	Alpha	Beta	Azimut	Dip	DH_East	DH_North	DH_RL	Plot_Dip	Plot_DipDir	Domain
KLRD0017	124.2	Vein	60	66	275.0023	-63.051	508920.1385	1190659.38	296.0379371	47.133491	133.105598	S zone
KLRD0017	124.2	Vein	60	356	275.0023	-63.051	508920.1385	1190659.38	296.0379371	56.8638873	92.16782528	S zone
KLRD0017	124.56	Intrusive contact	65	160	275.0023	-63.051	508919.9762	1190659.39	295.7168702	8.91568902	163.4077765	S zone
KLRD0017	124.8	Vein	25	62	275.0023	-63.051	508919.868	1190659.4	295.5028311	79.3756185	149.0613349	S zone
KLRD0017	124.8	Vein	30	60	275.0023	-63.051	508919.868	1190659.4	295.5028311	75.5241544	145.3229468	S zone
KLRD0017	126	Vein	34	82	275.0023	-63.051	508919.3269	1190659.44	294.4327031	63.4987331	161.5167911	S zone
KLRD0017	127.6	Vein	65	242	275.0023	-63.051	508918.6051	1190659.51	293.0060401	26.1251959	37.04079528	S zone
KLRD0017	127.6	Intrusive contact	30	172	275.0023	-63.051	508918.6051	1190659.51	293.0060401	33.4559544	262.3450882	S zone
KLRD0017	128.7	Vein	40	280	275.0023	-63.051	508918.1088	1190659.55	292.0253247	59.1531647	33.48656907	S zone
KLRD0017	128.7	Vein	22	340	275.0023	-63.051	508918.1088	1190659.55	292.0253247	86.5125736	256.4492939	S zone
KLRD0017	131.9	Vein	28	40	275.5393	-62.953	508916.664	1190659.68	289.1728759	83.5668178	129.8034661	S zone
KLRD0017	134	Vein	15	60	275.5393	-62.953	508915.7152	1190659.76	287.3013906	89.3594628	152.1603899	S zone
KLRD0017	134.5	Intrusive contact	25	60	275.5393	-62.953	508915.4892	1190659.78	286.8558492	80.1747573	148.1845685	S zone
KLRD0017	134.7	Vein	30	74	275.5393	-62.953	508915.3988	1190659.79	286.677638	70.3060709	157.5337358	S zone
KLRD0017	134.7	Vein	40	170	275.5393	-62.953	508915.3988	1190659.79	286.677638	23.7460738	256.0915122	S zone
KLRD0017	135.5	S_0	80	330	275.5393	-62.953	508915.0372	1190659.82	285.9648242	35.9999628	86.88638715	S zone
KLRD0017	135.6	Vein	25	82	275.5393	-62.953	508914.9919	1190659.83	285.875726	71.3855748	166.6484159	S zone
KLRD0017	136.2	S_1	60	312	275.5393	-62.953	508914.7207	1190659.85	285.3411527	51.7181255	67.12841773	S zone
KLRD0017	136.2	S_0	60	312	275.5393	-62.953	508914.7207	1190659.85	285.3411527	51.7181255	67.12841773	S zone
KLRD0017	137.45	S_0	70	320	275.5393	-62.953	508914.1554	1190659.91	284.2275476	44.1004254	76.96520978	S zone
KLRD0017	138.65	S_0	70	64	275.5393	-62.953	508913.6125	1190659.96	283.1586	39.7330328	124.12598	S zone
KLRD0017	138.65	Vein	35	64	275.5393	-62.953	508913.6125	1190659.96	283.1586	69.6437664	147.1285633	S zone
KLRD0017	140.15	Vein	20	360	275.9837	-62.834	508912.9337	1190660.02	281.8225724	82.9822585	275.3808653	S zone
KLRD0017	140.15	S_0	45	268	275.9837	-62.834	508912.9337	1190660.02	281.8225724	50.1225567	28.33029453	S zone
KLRD0017	140.15	Vein	52	250	275.9837	-62.834	508912.9337	1190660.02	281.8225724	37.0921886	21.79061628	S zone
KLRD0017	141	Intrusive contact	12	272	275.9837	-62.834	508912.549	1190660.06	281.0655788	80.2402057	13.06043962	S zone
KLRD0017	141.1	S_0	80	274	275.9837	-62.834	508912.5037	1190660.06	280.9765252	29.412264	75.11158995	S zone
KLRD0017	147.2	Vein	13	210	275.9837	-62.834	508909.7391	1190660.34	275.5460531	54.2151264	312.676339	S zone
KLRD0017	147.2	Vein	65	160	275.9837	-62.834	508909.7391	1190660.34	275.5460531	8.99208411	163.4041343	S zone
KLRD0017	148	S_0	70	354	275.9837	-62.834	508909.3761	1190660.38	274.834122	47.0408912	92.96629193	S zone
KLRD0017	148	Vein	25	48	275.9837	-62.834	508909.3761	1190660.38	274.834122	84.2687782	138.3683326	S zone
KLRD0017	148	Vein	77	136	275.9837	-62.834	508909.3761	1190660.38	274.834122	19.7677978	123.284785	S zone
KLRD0017	149.6	Vein	45	140	275.9837	-62.834	508908.6498	1190660.45	273.4104419	28.7696865	205.3273248	S zone
KLRD0017	152.9	Vein	35	206	276.3521	-62.701	508907.1506	1190660.61	270.4749231	32.1334858	318.5911014	S zone
KLRD0017	153.1	Vein	40	100	276.3521	-62.701	508907.0597	1190660.62	270.2970499	50.7685883	173.0167084	S zone
KLRD0017	154.1	S_0	60	42	276.3521	-62.701	508906.605	1190660.67	269.4077478	53.1171552	120.8534284	S zone
KLRD0017	155	Fault	40	310	276.3521	-62.701	508906.1956	1190660.72	268.6074664	69.732971	57.40474763	S zone
KLRD0017	157.7	Vein	80	92	276.3521	-62.701	508904.9666	1190660.85	266.2071373	28.5341543	117.4305815	S zone
KLRD0017	161.52	S_0	70	260	276.722	-62.568	508903.2256	1190661.04	262.8124388	30.4580695	54.82560666	S zone
KLRD0017	161.52	Vein	60	172	276.722	-62.568	508903.2256	1190661.04	262.8124388	4.66449637	217.6296784	S zone
KLRD0017	161.83	Vein	25	42	276.722	-62.568	508903.0842	1190661.06	262.537021	86.2111664	133.8953473	S zone
KLRD0017	161.9	S_0	80	264	276.722	-62.568	508903.0522	1190661.06	262.4748313	27.9770743	74.86676571	S zone
KLRD0017	161.9	Vein	60	170	276.722	-62.568	508903.0522	1190661.06	262.4748313	5.47731039	211.015073	S zone
KLRD0017	162	Vein	70	222	276.722	-62.568	508903.0066	1190661.07	262.3859898	17.9254811	48.43064594	S zone
KLRD0017	165.2	Vein	30	66	276.722	-62.568	508901.546	1190661.23	259.5436204	73.5982876	152.0267543	S zone
KLRD0017	165.2	S_2	85	69	276.722	-62.568	508901.546	1190661.23	259.5436204	29.4751675	105.9855551	S zone
KLRD0017	169.8	S_0	85	288	276.722	-62.568	508899.4434	1190661.48	255.4596166	29.372701	87.05721742	S zone
KLRD0017	169.8	S_2	85	288	276.722	-62.568	508899.4434	1190661.48	255.4596166	29.372701	87.05721742	S zone
KLRD0017	172.3	Vein	55	130	277.0171	-62.4	508898.2989	1190661.61	253.2410723	26.2511332	180.197745	S zone
KLRD0017	172.3	S_0	60	242	277.0171	-62.4	508898.2989	1190661.61	253.2410723	28.7578216	30.20629445	S zone
KLRD0017	173.2	Vein	30	52	277.0171	-62.4	508897.8866	1190661.66	252.4426033	78.5991338	140.9074513	S zone
KLRD0017	173.2	Vein	75	128	277.0171	-62.4	508897.8866	1190661.66	252.4426033	21.4839496	130.6269278	S zone
KLRD0017	174	S_0	50	250	277.0171	-62.4	508897.5199	1190661.71	251.7329452	38.639994	21.4733446	S zone
KLRD0017	178	S_0	52	202	277.0171	-62.4	508895.6843	1190661.93	248.1859556	15.663772	335.7140014	S zone
KLRD0017	181.5	Vein	75	274	277.2519	-62.2	508894.075	1190662.13	245.0841509	32.0654796	67.94105658	S zone
KLRD0017	181.5	S_2	50	178	277.2519	-62.2	508894.075	1190662.13	245.0841509	12.4236715	271.0556946	S zone
KLRD0017	181.5	S_2	40	134	277.2519	-62.2	508894.075	1190662.13	245.0841509	35.2884835	204.5111776	S zone

DH_Hole	DH_Depth	Structure Type	Alpha	Beta	Azimut	Dip	DH_East	DH_North	DH_RL	Plot_Dip	Plot_DipDir	Domain
KLRD0017	181.7	Fault	45	32	277.2519	-62.2	508893.983	1190662.14	244.9069619	69.6075387	120.6043196	S zone
KLRD0017	183.5	Vein	70	48	277.2519	-62.2	508893.154	1190662.24	243.3125522	43.4099949	118.7476756	S zone
KLRD0017	183.5	S_0	65	256	277.2519	-62.2	508893.154	1190662.24	243.3125522	31.7449708	45.83668544	S zone
KLRD0017	183.5	S_2	70	58	277.2519	-62.2	508893.154	1190662.24	243.3125522	41.5366255	122.9800077	S zone
KLRD0017	183.5	Fault	15	118	277.2519	-62.2	508893.154	1190662.24	243.3125522	63.9228318	205.323596	S zone
KLRD0017	187.9	Vein	35	65	277.2519	-62.2	508891.1236	1190662.5	239.4173152	69.7602175	149.5525029	S zone
KLRD0017	192.6	Vein	42	54	277.4883	-62.001	508888.9489	1190662.77	235.2599666	67.1563459	137.9705631	S zone
KLRD0017	196.8	Vein	30	48	277.4883	-62.001	508887.0002	1190663.02	231.5479314	80.2184126	138.2270281	S zone
KLRD0017	203.3	S_0	52	320	277.9008	-61.817	508883.9748	1190663.42	225.8087208	61.7801752	71.04903004	S zone
KLRD0017	203.3	Vein	75	140	277.9008	-61.817	508883.9748	1190663.42	225.8087208	19.0192412	128.4337689	S zone
KLRD0017	203.3	S_2	35	320	277.9008	-61.817	508883.9748	1190663.42	225.8087208	77.8618977	65.14928645	S zone
KLRD0017	205	Vein	28	52	277.9008	-61.817	508883.1819	1190663.53	224.3087635	80.9104552	142.5352969	S zone
KLRD0017	207.83	Intrusive contact	75	280	277.9008	-61.817	508881.8604	1190663.71	221.8127413	33.8170384	70.4793956	S zone
KLRD0017	208.06	Intrusive contact	68	334	277.9008	-61.817	508881.7529	1190663.72	221.6099374	48.7621507	85.12256051	S zone
KLRD0017	210.3	S_0	80	272	278.5041	-61.652	508880.7055	1190663.87	219.6352212	30.1373286	77.84262782	S zone
KLRD0017	212.44	S_0	70	284	278.5041	-61.652	508879.7038	1190664.01	217.7493315	37.9259244	65.38562364	S zone
KLRD0017	217.17	S_0	55	254	278.5041	-61.652	508877.487	1190664.33	213.5831997	37.2423969	32.77567326	S zone
KLRD0017	220.15	Vein	30	56	279.1105	-61.488	508876.0883	1190664.54	210.960013	77.8575849	145.6829271	S zone
KLRD0017	221.2	Vein	50	254	279.1105	-61.488	508875.5951	1190664.61	210.0360289	40.6778846	26.99176037	S zone
KLRD0017	221.2	S_1	50	248	279.1105	-61.488	508875.5951	1190664.61	210.0360289	37.9477753	22.69149543	S zone
KLRD0017	225.7	Vein	42	66	279.1105	-61.488	508873.4791	1190664.93	206.0777933	63.6031319	148.0677635	S zone
KLRD0017	225.7	Vein	30	66	279.1105	-61.488	508873.4791	1190664.93	206.0777933	74.2134362	154.0885824	S zone
KLRD0017	226.8	S_2	53	214	279.1105	-61.488	508872.9614	1190665.01	205.1106426	19.9743596	358.9038948	S zone
KLRD0017	226.8	Vein	26	64	279.1105	-61.488	508872.9614	1190665.01	205.1106426	78.5813096	154.2882934	S zone
KLRD0017	234.2	Vein	30	80	279.6836	-61.367	508869.4735	1190665.58	198.6083339	68.4696972	166.0067862	S zone
KLRD0017	234.2	S_0	72	262	279.6836	-61.367	508869.4735	1190665.58	198.6083339	31.175426	63.30007203	S zone
KLRD0017	236.1	S_0	53	254	279.6836	-61.367	508868.5769	1190665.72	196.9397592	38.685536	31.78883076	S zone
KLRD0017	236.1	S_2	52	210	279.6836	-61.367	508868.5769	1190665.72	196.9397592	18.7213297	353.0900226	S zone
KLRD0017	236.1	Fault	12	340	279.6836	-61.367	508868.5769	1190665.72	196.9397592	75.0796011	259.2817951	S zone
KLRD0017	237.15	Vein	36	50	279.6836	-61.367	508868.0813	1190665.81	196.0178072	74.5075258	139.5621488	S zone
KLRD0017	239	Vein	40	70	279.6836	-61.367	508867.2078	1190665.95	194.3936839	63.9648493	152.7773499	S zone
KLRD0017	239	S_2	28	70	279.6836	-61.367	508867.2078	1190665.95	194.3936839	74.4775655	158.9792022	S zone
KLRD0017	241.6	Vein	40	54	280.2515	-61.302	508865.9797	1190666.16	192.1116605	69.630827	141.3103288	S zone
KLRD0017	244.4	Vein	40	64	280.2515	-61.302	508864.6569	1190666.39	189.6545396	66.2363541	148.7179416	S zone
KLRD0017	247	Vein	15	46	280.2515	-61.302	508863.4285	1190666.61	187.3733091	84.5649775	324.1920843	S zone
KLRD0017	247	Vein	65	46	280.2515	-61.302	508863.4285	1190666.61	187.3733091	49.1217209	123.6356571	S zone
KLRD0017	249	Vein	60	83	280.2515	-61.302	508862.4835	1190666.78	185.6187658	43.0872241	146.9186688	S zone
KLRD0017	249	Fault	10	70	280.2515	-61.302	508862.4835	1190666.78	185.6187658	89.456852	348.0632962	S zone
KLRD0017	252.17	Vein	65	76	280.8206	-61.237	508860.9856	1190667.05	182.8382674	41.7716526	138.3184897	S zone
KLRD0017	254.2	Intrusive contact	72	300	280.8206	-61.237	508860.0262	1190667.23	181.0579826	40.5403117	76.01228143	S zone
KLRD0017	257.35	Vein	50	68	280.8206	-61.237	508858.5376	1190667.51	178.2959082	56.2357031	146.5156136	S zone
KLRD0017	257.35	S_2	60	260	280.8206	-61.237	508858.5376	1190667.51	178.2959082	36.7723885	45.3764233	S zone
KLRD0017	257.35	S_0	55	260	280.8206	-61.237	508858.5376	1190667.51	178.2959082	39.9976292	39.21681685	S zone
KLRD0017	259.45	Vein	45	68	280.8206	-61.237	508857.5451	1190667.69	176.4548189	60.4938796	149.5952912	S zone
KLRD0017	260	Vein	50	68	281.4342	-61.117	508857.2852	1190667.74	175.9726675	56.2357031	146.5156136	S zone
KLRD0017	260	Intrusive contact	80	102	281.4342	-61.117	508857.2852	1190667.74	175.9726675	28.2657176	121.7350829	S zone
KLRD0017	261	S_0	70	300	281.4342	-61.117	508856.8125	1190667.83	175.0960986	42.1335065	74.51548496	S zone
KLRD0017	262	Vein	44	75	281.4342	-61.117	508856.3397	1190667.93	174.2196306	58.7424123	155.4750472	S zone
KLRD0017	262	S_1	50	258	281.4342	-61.117	508856.3397	1190667.93	174.2196306	42.6425297	32.95684097	S zone
KLRD0017	267.47	Vein	30	60	281.4342	-61.117	508853.7523	1190668.43	169.4271302	76.740911	151.5056554	S zone
KLRD0017	272.33	S_0	41	46	282.1044	-60.952	508851.4514	1190668.9	165.1717142	71.2709188	136.4445793	S zone
KLRD0017	272.5	Vein	43	48	282.1044	-60.952	508851.3708	1190668.92	165.0229178	68.8590214	137.1097511	S zone
KLRD0017	272.5	S_2	77	130	282.1044	-60.952	508851.3708	1190668.92	165.0229178	22.6381979	128.0634551	S zone
KLRD0017	272.5	S_2	88	84	282.1044	-60.952	508851.3708	1190668.92	165.0229178	29.1633105	105.5519675	S zone
KLRD0017	272.5	S_2	31	60	282.1044	-60.952	508851.3708	1190668.92	165.0229178	75.8857932	151.413371	S zone
KLRD0017	278.12	Vein	25	60	282.1044	-60.952	508848.7062	1190669.47	160.1061446	81.3645445	154.3804512	S zone
KLRD0017	281.6	Intrusive contact	52	244	282.778	-60.789	508847.0541	1190669.83	157.0638017	34.9274305	27.06710055	S zone
KLRD0017	287.65	Fault	25	280	282.778	-60.789	508844.1785	1190670.46	151.7786808	72.9988072	33.59716482	S zone
KLRD0017	291.33	Vein	40	73	283.4857	-60.501	508842.4271	1190670.86	148.5665046	63.1713522	158.0705692	S zone
KLRD0017	291.33	S_1	60	240	283.4857	-60.501	508842.4271	1190670.86	148.5665046	28.6301392	38.24262885	S zone
KLRD0017	294.9	S_1	35	240	283.4857	-60.501	508840.7248	1190671.25	145.4532486	45.5130371	7.127563901	S zone

DH_Hole	DH_Depth	Structure Type	Alpha	Beta	Azimut	Dip	DH_East	DH_North	DH_RL	Plot_Dip	Plot_DipDir	Domain
KLRD0017	298.7	S_2	25	58	283.4857	-60.501	508838.9087	1190671.68	142.1428581	82.4549162	154.3193184	S zone
KLRD0017	298.7	Vein	29	58	283.4857	-60.501	508838.9087	1190671.68	142.1428581	78.8310298	152.6028183	S zone
KLRD0017	298.7	So	46	238	283.4857	-60.501	508838.9087	1190671.68	142.1428581	36.1624169	16.7765517	S zone
KLRD0017	300.5	S1	14	230	284.2617	-60.103	508838.047	1190671.88	140.5760332	58.8220935	343.8027998	S zone
KLRD0017	300.5	Fault	18	310	284.2617	-60.103	508838.047	1190671.88	140.5760332	88.1601822	236.6900542	S zone
KLRD0017	303	S2	40	52	284.2617	-60.103	508836.848	1190672.17	138.4016282	71.0082741	143.4347096	S zone
KLRD0017	303	Vein	50	70	284.2617	-60.103	508836.848	1190672.17	138.4016282	56.1460409	150.4253631	S zone
KLRD0017	306.1	Vein	50	318	284.2617	-60.103	508835.3576	1190672.54	135.7083405	64.6822981	75.62315382	S zone
KLRD0017	306.1	Vein	14	40	284.2617	-60.103	508835.3576	1190672.54	135.7083405	80.8402315	323.2146198	S zone
KLRD0017	306.1	Vein	32	218	284.2617	-60.103	508835.3576	1190672.54	135.7083405	37.641767	342.7846507	S zone
KLRD0017	306.1	Vein	45	358	284.2617	-60.103	508835.3576	1190672.54	135.7083405	74.7666222	102.569694	S zone
KLRD0017	310	Vein	55	88	285.0467	-59.707	508833.4768	1190673.01	132.3246983	45.5727336	157.6936198	S zone
KLRD0017	313.5	Vein	45	212	285.0467	-59.707	508831.7835	1190673.45	129.2925869	24.1653272	350.8331588	S zone
KLRD0017	319.55	So	26	228	285.0467	-59.707	508828.8449	1190674.22	124.0613345	46.9912022	351.1120191	S zone
KLRD0017	319.55	Vein	16	46	285.0467	-59.707	508828.8449	1190674.22	124.0613345	84.2964616	329.150685	S zone
KLRD0017	320.4	Vein	36	42	285.7686	-59.317	508828.4308	1190674.33	123.3273831	78.2508327	138.6980688	S zone
KLRD0017	338.56	So	60	224	286.5098	-58.953	508819.5185	1190676.85	107.7056252	21.9530788	38.19615967	S zone
KLRD0017	341.4	Vein	14	30	287.2585	-58.59	508818.1142	1190677.26	105.2724492	76.9429305	316.3554054	S zone
KLRD0017	341.4	So	30	202	287.2585	-58.59	508818.1142	1190677.26	105.2724492	32.6058953	323.5028679	S zone
KLRD0017	348.46	Intrusive contact	20	222	287.2585	-58.59	508814.6119	1190678.33	99.23523357	49.0762017	343.3626734	S zone
KLRD0017	348.6	Vein	45	234	287.2585	-58.59	508814.5423	1190678.35	99.11568038	34.9032675	18.26689837	S zone
KLRD0017	350	Vein	32	228	288.1021	-58.251	508813.8459	1190678.56	97.92050174	41.576004	359.0634193	S zone
KLRD0017	352	Vein	60	206	288.1021	-58.251	508812.85	1190678.87	96.21419881	13.2698516	34.58928789	S zone
KLRD0017	357	Vein	40	34	288.1021	-58.251	508810.3559	1190679.67	91.95384014	77.6632252	133.9140562	S zone
KLRD0017	357	Vein	33	150	288.1021	-58.251	508810.3559	1190679.67	91.95384014	32.3433116	236.2949341	S zone
KLRD0017	361.7	Vein	55	56	289.1105	-57.955	508808.0061	1190680.43	87.95610723	58.1669956	142.2399017	S zone
KLRD0017	365.6	Vein	20	64	289.1105	-57.955	508806.0538	1190681.08	84.64356483	85.8174784	166.3966817	S zone
KLRD0017	365.6	Vein	40	70	289.1105	-57.955	508806.0538	1190681.08	84.64356483	65.9507677	160.5507715	S zone
KLRD0017	374.5	Vein	35	50	290.1272	-57.663	508801.592	1190682.63	77.09968874	78.1497523	149.3767967	S zone
KLRD0017	377.7	Vein	28	40	290.1272	-57.663	508799.9859	1190683.21	74.39254479	87.9288974	144.4295392	S zone
KLRD0017	383	Vein	33	278	290.7337	-57.4	508797.3236	1190684.18	69.91485435	66.5720901	45.33076266	S zone
KLRD0017	390.7	Vein	40	90	290.9978	-57.203	508793.4477	1190685.64	63.42194969	57.225375	176.4226021	S zone
KLRD0017	392.6	Vein	20	40	290.9978	-57.203	508792.4898	1190686	61.82186871	84.2543803	328.1452894	S zone
KLRD0017	392.6	Vein	55	56	290.9978	-57.203	508792.4898	1190686	61.82186871	58.8743021	144.5114151	S zone
KLRD0017	396.8	Vein	20	60	290.9978	-57.203	508790.3699	1190686.81	58.28722135	88.102687	165.4973025	S zone
KLRD0017	399.1	Vein	40	76	290.9978	-57.203	508789.2077	1190687.25	56.35296781	63.8939488	166.8512978	S zone
KLRD0017	404.2	Vein	13	162	291.2673	-57.004	508786.6271	1190688.24	52.06755765	46.1613436	266.5132749	S zone
KLRD0017	408.1	Vein	60	78	291.2673	-57.004	508784.6504	1190689.01	48.79389345	47.9082694	152.4149475	S zone
KLRD0017	409.65	Intrusive contact	46	78	291.2673	-57.004	508783.8641	1190689.32	47.49364506	58.3179848	164.1705735	S zone
KLRD0017	409.9	Vein	40	120	292.1053	-56.619	508783.7372	1190689.37	47.28397495	41.606059	198.7681127	S zone
KLRD0017	421.8	Vein	44	238	293.5259	-56.06	508777.6818	1190691.78	37.32972198	37.8401992	28.32042034	S zone
KLRD0017	421.8	Vein	70	94	293.5259	-56.06	508777.6818	1190691.78	37.32972198	37.1305445	146.6795404	S zone
KLRD0017	425.3	Vein	25	130	293.5259	-56.06	508775.8948	1190692.53	34.41379701	47.5707399	222.6789305	S zone
KLRD0017	425.3	S2	25	38	293.5259	-56.06	508775.8948	1190692.53	34.41379701	87.4691077	326.7863806	S zone
KLRD0017	429.1	Vein	60	98	293.5259	-56.06	508773.9518	1190693.36	31.25537985	40.7362389	162.7590885	S zone
KLRD0017	444.3	Vein	40	78	294.9665	-55.509	508766.1556	1190696.9	18.69843974	64.0373599	171.8388698	S zone
KLRD0017	447.4	Intrusive contact	75	280	294.9665	-55.509	508764.5611	1190697.66	16.15011817	39.9407482	92.34405628	S zone
KLRD0017	454.9	Intrusive contact	30	62	295.7169	-55.133	508760.698	1190699.52	9.996787032	79.7650927	166.7247515	S zone
KLRD0017	460.2	Vein	70	312	295.951	-55	508757.9655	1190700.85	5.653532808	50.3370407	96.70255883	S zone
KLRD0017	469.55	So	70	350	295.951	-55	508753.1403	1190703.21	-1.99949953	54.9135714	112.002659	S zone
KLRD0017	469.7	So	45	226	295.951	-55	508753.0628	1190703.25	-2.12218056	30.5756248	26.73444247	S zone
KLRD0017	473	So	10	352	296.1858	-54.867	508751.3568	1190704.09	-4.81832236	65.0755961	287.6772925	S zone
KLRD0017	474.9	Vein	55	78	296.1858	-54.867	508750.3725	1190704.58	-6.36771298	53.2481707	161.0149789	S zone
WKL0120	107	Vein	60	330	273.1891	-61.037	508713.0736	1190650.58	310.734199	56.7661649	75.75347489	S zone
WKL0120	107	Vein	25	129	273.1891	-61.037	508713.0736	1190650.58	310.734199	49.7634212	205.8280386	S zone
WKL0120	107	Vein	15	0	273.1891	-61.037	508713.0736	1190650.58	310.734199	76.0389753	273.1441487	S zone
WKL0120	114.5	Vein	20	70	273.8939	-61.018	508709.4475	1190650.79	304.1722513	81.7473394	156.707552	S zone
WKL0120	114.5	Vein	42	170	273.8939	-61.018	508709.4475	1190650.79	304.1722513	19.9664931	251.3442988	S zone
WKL0120	114.5	S2	30	260	273.8939	-61.018	508709.4475	1190650.79	304.1722513	59.3181291	10.93954353	S zone
WKL0120	125.1	So	13	158	274.6029	-61.001	508704.3233	1190651.13	294.8995851	50.6060799	246.1737232	S zone
WKL0120	126.1	Vein	80	90	274.6029	-61.001	508703.84	1190651.17	294.0248926	30.5267868	114.3490417	S zone
WKL0120	126.1	So	18	58	274.6029	-61.001	508703.84	1190651.17	294.0248926	88.5095634	148.1442645	S zone
WKL0120	126.3	Vein	27	76	274.6029	-61.001	508703.7434	1190651.18	293.8499558	72.985283	159.0625041	S zone

DH_Hole	DH_Depth	Structure Type	Alpha	Beta	Azimut	Dip	DH_East	DH_North	DH_RL	Plot_Dip	Plot_DipDir	Domain
WKL0120	128	Vein	40	64	274.6029	-61.001	508702.9218	1190651.24	292.3630144	66.4552382	143.0390891	S zone
WKL0120	133.3	Vein	11	258	275.3126	-60.985	508700.3608	1190651.45	287.727527	74.5834366	359.645384	S zone
WKL0120	135.65	Vein	26	278	275.3126	-60.985	508699.2254	1190651.55	285.6722909	71.1735974	25.05588139	S zone
WKL0120	142.6	S_2	60	340	276.0231	-60.972	508695.8688	1190651.86	279.5944476	58.0369236	83.94316718	S zone
WKL0120	143.7	Vein	32	280	276.0231	-60.972	508695.3377	1190651.91	278.632543	66.9239977	30.36869841	S zone
WKL0120	143.7	Vein	32	350	276.0231	-60.972	508695.3377	1190651.91	278.632543	86.6609544	87.08916983	S zone
WKL0120	147	Intrusive contact	85	320	276.0231	-60.972	508693.7446	1190652.07	275.7469084	33.000359	90.07308322	S zone
WKL0120	148.5	Vein	20	90	276.0231	-60.972	508693.0206	1190652.14	274.4352944	72.5988975	175.9614809	S zone
WKL0120	149.2	Vein	35	100	276.0231	-60.972	508692.6828	1190652.18	273.8232158	55.2114158	175.1737498	S zone
WKL0120	149.2	Vein	55	280	276.0231	-60.972	508692.6828	1190652.18	273.8232158	48.0924761	46.60130398	S zone
WKL0120	156.27	Intrusive contact	35	254	276.7343	-60.96	508689.272	1190652.55	267.6415423	52.332533	12.25269339	S zone
WKL0120	156.4	Vein	8	170	276.7343	-60.96	508689.2093	1190652.55	267.527881	53.4880787	264.0284006	S zone
WKL0120	172.8	Vein	18	270	277.0717	-60.901	508681.2987	1190653.51	253.1935121	74.3348477	16.04720438	S zone
WKL0120	174	S_0	25	350	277.0717	-60.901	508680.7195	1190653.58	252.1449753	86.2862249	267.9940505	S zone
WKL0123	133.64	Vein	70	312	273.2	-63.083	508777.4675	1190649.38	291.720476	42.7525476	71.22302321	S zone
WKL0123	139.85	Vein	35	54	273.2	-63.083	508774.6606	1190649.53	286.1832325	72.9338608	137.0982509	S zone
WKL0123	139.85	S_0	60	62	273.2	-63.083	508774.6606	1190649.53	286.1832325	48.2452125	129.4955382	S zone
WKL0123	147.6	S_0	60	352	273.2	-63.083	508771.1577	1190649.73	279.2728239	56.7656969	88.43946239	S zone
WKL0123	148.9	S_0	60	340	273.2	-63.083	508770.5701	1190649.76	278.1136586	55.9779703	81.30434257	S zone
WKL0123	149	Vein	11	226	273.2	-63.083	508770.5249	1190649.77	278.024492	61.3912423	326.7566226	S zone
WKL0123	151.2	Vein	45	140	273.2	-63.083	508769.5305	1190649.82	276.0628277	28.8702228	202.9286197	S zone
WKL0123	157.1	S_0	31	230	273.2	-63.083	508766.8638	1190649.97	270.8020005	44.87362	341.7507778	S zone
WKL0123	157.1	Vein	26	176	273.2	-63.083	508766.8638	1190649.97	270.8020005	37.1776191	267.2563197	S zone
WKL0123	167.1	Vein	18	264	273.2	-63.083	508762.3439	1190650.22	261.8853443	71.3042009	6.312920249	S zone
WKL0123	167.5	Vein	24	268	273.2	-63.083	508762.1631	1190650.23	261.5286781	67.8454217	12.88954313	S zone
WKL0123	167.5	S_0	50	80	273.2	-63.083	508762.1631	1190650.23	261.5286781	50.7631107	148.0261433	S zone
WKL0123	168.9	Intrusive contact	45	268	273.2	-63.083	508761.5303	1190650.27	260.2803462	50.0831275	26.08307843	S zone
WKL0123	170.74	Vein	10	290	273.2	-63.083	508760.6987	1190650.32	258.6396814	89.8648241	25.48000283	S zone
WKL0123	174.4	Vein	22	240	273.2	-63.083	508759.0444	1190650.41	255.3761853	57.0512693	346.3227832	S zone
WKL0123	176.75	Vein	52	162	273.2	-63.083	508757.9822	1190650.47	253.2807711	14.6004566	224.2099574	S zone
WKL0123	195.3	Vein	32	253	273.2	-63.083	508749.5978	1190650.94	236.7403738	54.2143615	4.539953073	S zone
WKL0123	196	S_2	57	340	273.2	-63.083	508749.2814	1190650.95	236.1162079	58.9269047	80.65032129	S zone
WKL0123	196	Vein	30	72	273.2	-63.083	508749.2814	1190650.95	236.1162079	71.0534354	153.7655402	S zone
WKL0123	197	Vein	15	259	273.2	-63.083	508748.8294	1190650.98	235.2245423	71.6865824	0.363292803	S zone
WKL0123	200.9	Vein	30	250	273.2	-63.083	508747.0667	1190651.08	231.7470463	54.5550873	0.554703944	S zone
WKL0123	215.3	Vein	43	274	273.2	-63.083	508740.558	1190651.44	218.9070614	54.1955245	29.10930273	S zone
WKL0123	217.7	Vein	40	272	273.2	-63.083	508739.4733	1190651.5	216.7670639	55.8715321	25.56518941	S zone
WKL0123	218.5	Intrusive contact	80	298	273.2	-63.083	508739.1117	1190651.52	216.0537314	32.731203	76.73866039	S zone
WKL0123	218.5	S_0	80	290	273.2	-63.083	508739.1117	1190651.52	216.0537314	31.6537211	75.09581767	S zone
WKL0123	222.6	Vein	38	240	273.2	-63.083	508737.2585	1190651.63	212.3979024	43.3371457	357.1377155	S zone
WKL0123	230.8	Vein	26	82	273.2	-63.083	508733.5522	1190651.83	205.0862443	70.4727496	164.0095638	S zone
WKL0123	232.1	Vein	40	150	273.2	-63.083	508732.9646	1190651.87	203.927079	29.1350835	221.3332101	S zone
WKL0123	232.1	S_2	60	110	273.2	-63.083	508732.9646	1190651.87	203.927079	31.8294816	156.1962581	S zone
WKL0123	232.1	Vein	30	70	273.2	-63.083	508732.9646	1190651.87	203.927079	71.8354201	152.13532	S zone
WKL0123	241.7	Vein	30	276	273.2	-63.083	508728.6255	1190652.11	195.367089	66.1180062	22.83375776	S zone
WKL0123	282.2	S_1	8	258	273.2	-63.083	508710.32	1190653.13	159.2546314	77.4495082	356.1155797	S zone
WKL0123	290.9	S_0	40	160	273.2	-63.083	508706.3877	1190653.35	151.4971405	25.9703631	236.4628574	S zone
WKL0123	291.8	S_0	13	88	273.2	-63.083	508705.9809	1190653.37	150.6946414	79.3279188	175.4830641	S zone
WKL0123	294.67	Vein	70	130	273.2	-63.083	508704.6837	1190653.45	148.1355611	20.3779907	142.0123335	S zone